YEMATAW ADDIS ALEMU

SYNTHESIS, CHARACTERIZATION AND BIOLOGICAL EVALUATION OF ZINC(II) COMPLEXES WITH PHENANTHROLINE DERIVATIVES AND S-METHYL DITHIOCARBAZATE SCHIFF BASES

UNIVERSIDADE DO ALGARVE

FACULDADE DE CIÊNCIAS E TECNOLOGIA

2017

YEMATAW ADDIS ALEMU

SYNTHESIS, CHARACTERIZATION AND BIOLOGICAL EVALUATION OF ZINC(II) COMPLEXES WITH PHENANTHROLINE DERIVATIVES AND S-METHYL DITHIOCARBAZATE SCHIFF BASES

Erasmus Mundus MSc in Chemical Innovation and Regulation
Mestrado Erasmus Mundus em Inovação Química e Regulamentação

Trabalho efetuado sob a orientação de:

Work supervised by:

Dr. Isabel Correia (CQE, IST, Universidade de Lisboa)

Prof. Isabel Cavaco (Universidade do Algarve)

UNIVERSIDADE DO ALGARVE
FACULDADE DE CIÊNCIAS E TECNOLOGIA
2017

SYNTHESIS, CHARACTERIZATION AND BIOLOGICAL EVALUATION OF ZINC(II) COMPLEXES WITH PHENANTHROLINE DERIVATIVES AND S-METHYL DITHIOCARBAZATE SCHIFF BASES

Declaration of Authorship

I hereby declare that I am the author of this work, which is original and unpublished. Authors and works consulted are properly cited in the text and listed in the list of references included.

Yematawa Addis Alemu

Acknowledgements

First and foremost, I would like to thank the almighty God for giving me the strength to complete my study successfully. Without his blessings, this achievement would not have been possible.

Next, I would like to express my deepest sense of gratitude to my esteemed supervisor Dr. Isabel Correia. I would like to thank her for the constant and warm encouragement, thoughtful guidance, insightful decision, critical comments and patience in reviewing all the discussion of the obtained results and correction of the thesis. I would like to acknowledge her for giving me full freedom during my research work. I have to appreciate her stay with me in the laboratory for the first several weeks and giving me training on organic synthesis and analytical techniques starting from the scratch. Her support was not limited to academic affairs only. She has started helping me by finding my accommodation in Lisbon. We had also lots of funs during coffee breaks. I will consider her as one of very few persons who have contributed a lot in my life.

I am also thankful to Professor João Costa Pessoa for allowing me to do in his laboratory and giving me critical comments and suggestions on the obtained laboratory results in particular and on my thesis in general. I would like to offer my sincere thanks to Professor Isabel Cavaco from University of Algarve and Professor Emilio Tagliavini from University of Bologna for their all supports during my stay of this MSc study.

I am very grateful to Samuel Silvestre, from Universidade da Beira Interior and Fernanda Marques from Centro de Ciências e Tecnologias Nucleares for doing the cytotoxicity studies.

I would also like to acknowledge University of Algarve, Bologna University, Barcelona University, Heriot Watt University, Instituto Superior Técnico (IST) and CQE. European commission is also acknowledged for funding me.

My acknowledgement also goes to Nadia Ribeiro for her kind assistance during my laboratory works from the beginning to the end. I would like to appreciate her polite behaviour and sharing lot of funs that we had during our break times. My thanks extends to Patrique Nunes, Cristina Matos, Filipa Ramilo Gomes and other research group members of CQE-4 in IST who have been so helpful and cooperative in giving their support at all times to help me in different ways during my laboratory works.

Last, but by far not least, I would like to thank my mother Ayelech Kokeb (Emahoy) for her tremendous contributions in my life. Without her loving upbringing and nurturing, I would not have been where I am today and what I am today. I am also very thankful to my wife Genet Fentie and my lovely son Nahom Yemataw. My acknowledgement also extended to my all families and friends.

Finally, I would like to dedicate this work to my lovely son Nahom Yemataw. For good father, caring a son is very precious gift from God. But, I have lost this opportunity for the last two years since I have been far away from him. Dear my lovely son, I would also like to say sorry for the incident that happened on you!

Abstract

The discovery of novel active compounds with new mechanisms of action, higher efficacy and improved selectivity is a matter of urgency to multi drug resistance and toxicity problems associated with many therapeutic drugs. In the current work S-methyl dithiocarbazate Schiff base: SalSmdt, $Mp(Smdt)_2$, VanSmdt, PySmdt and their Zn(II) complexes: $Zn[(SalSmdt)(H_2O)]\bullet 0.5H_2O$, $Zn_2[(Mp(Smdt)_2)(CH_3COO)]$, $Zn[(VanSmdt)(H_2O)]$ and $Zn[(PySmdt)(CH_3COO)]\bullet 1.5H_2O$ were synthesized. The Schiff bases were obtained by condensation of S-methyl dithiocarbazate (smdt) with different aromatic aldehydes: salicylaldehyde (sal), *o*-vanillin (van), pyridoxal (py) and 2,6-diformyl-4-methylphenol (Mp). Additionally, $Zn[(phen)_2(NO_3)_2]\bullet 2H_2O$, $Zn[(aminophen)_2(NO_3)_2]\bullet 1.5H_2O$ and $Zn[(Mephen)_2(NO_3)_2]\bullet 3.5H_2O$ complexes were developed by reaction of Zn(II) with 1,10-phenanthroline (phen), 4,7-dimethyl-1,10-phenanthroline (Mephen) and 5-amino-1,10-phenanthroline (aminophen). All compounds were characterized by elemental analysis, FTIR, UV-Vis, NMR, MS and fluorescence spectroscopies. The characterization suggests that the Schiff base ligands coordinate the metal ion through the phenolate–O, the imine-N and the sulfur atom in the thiol form (except in $Zn[(PySmdt)(CH_3COO)]$ for which the thione is proposed). The stability of the compounds in buffered aqueous media (5 % DMSO and 95 % PBS, pH 7.4) was evaluated and all compounds are stable at least for three hours. The antioxidant potential was tested using the 2,2-diphenyl-1-picrylhydrazyl assay. All S-methyl dithiocarbazate Schiff bases showed moderate antioxidant activity but the Zn(II) complexes, with the exception of $Zn[(PySmdt)(CH_3COO)]$, are inactive. The Zn-phenanthroline complexes were tested for their DNA binding ability by fluorescence spectroscopy. The results indicate that there is interaction between the complexes and calf thymus DNA. Cytotoxicity studies with several tumor cell lines (PC-3, MCF-7 and CACO-2) are ongoing. The results obtained for the Schiff bases are promising since the IC_{50} values ranged from 4.41 to 28.99 μM. The phenanthroline ligands and their corresponding Zn complexes showed very high cytotoxicity towards A2780 ovarian cancer cells, with the Zn complexes showing slightly higher activity than the ligands.

Keywords: Schiff bases, phenanthroline, Zn(II) complexes, S-methyl dithiocarbazate, cytotoxicity

Resumo

A descoberta de novos fármacos, com mecanismos de acção alternativos, maior eficácia e selectividade é urgente para combater os problemas associados à resistência e à toxicidade dos fármacos correntes. Neste trabalho bases de Schiff derivadas do S-metil-ditiocarbazato: SalSmdt, $Mp(Smdt)_2$, VanSmdt, PySmdt e os seus complexos de zinco(II) foram sintetizados. As bases de Schiff foram obtidas através da condensação do S-metil-ditiocarbazato (smdt) com diferentes aldeídos aromáticos: salicilaldeído (Sal), *o*-vanilina (Van) pyridoxal (Py) e 2,6-diformil-4-metilfenol (Mp) em álcoois. Foram também sintetizados os complexos $Zn[(phen)_2(NO_3)_2]\bullet 2H_2O$, $Zn[(aminophen)_2(NO_3)_2]\bullet 1.5H_2O$ e $Zn[(Mephen)_2(NO_3)_2]\bullet 3.5H_2O$ por reacção do Zn(II) com 1,10-fenantrolina (phen), 4,7-dimetil-1,10-fenantrolina (Mephen) e 5-amino-1,10-fenantolina (aminophen), respectivamente. Todos os compostos foram caracterizados por análise elementar, espectroscopia de FTIR, UV-Vis, RMN, fluorescência e espectrometria de massa. A caracterização sugere que as bases de Schiff coordenam o ião metálico através do O-fenolato, o N-imina e o átomo de enxofre na forma tiol (excepto no $Zn[(PySmdt)(CH_3COO)]$ para o qual se propõe o ligando na forma tiona). A estabilidade dos compostos foi avaliada em meio aquoso tamponizado (5 % dmso e 95 % PBS, pH=7.4) tendo-se concluído que todos os compostos são estáveis durante pelo menos 3h. O potencial antioxidante dos compostos foi testado usando um ensaio com 2,2-difenil-1-picrilhidrazil. Todas as bases de Schiff possuem actividade antioxidante moderada, mas os complexos de Zn(II) (excepto o $Zn[(PySmdt)(CH_3COO)]$) são inactivos. Os complexos derivados das fenantrolinas foram testados quanto à sua capacidade para interagir com o ADN usando espectrofotometria de fluorescência e revelaram capacidade, sendo o Zn(aminophen) o mais activo. Encontram-se a decorrer estudos de citotoxidade com várias linhas celulares tumorais (PC-3, MCF-7 e CACO-2). Os resultados das bases de Schiff são promissores, uma vez que os IC_{50} são da ordem dos μM (entre 4.41 e 28.99). As fenantrolinas e seus correspondentes complexos de Zn(II) mostraram citotoxicidade muito elevada nas células tumorais A2780, com os complexos a revelarem actividade ligeiramente superior aos ligandos.

Table of contents

Index of Figures

Index of Tables

Index of Schemes

Symbols and Abbreviations

DNA → Deoxyribonucleic acid

(n→π*) → Electronic transition from the n orbital to the π* orbital

(π→π*) → Electronic transition from the π orbital to the π* orbital

^{13}C NMR → Carbon 13 nuclear magnetic resonance

^{1}H NMR → Proton nuclear magnetic resonance

aminophen → 5-amino-1,10-Phenanthroline

COSY → Homonuclear correlation spectroscopy

DEPT → Distortionless enhancement by polarization transfer

DMSO → Dimethyl sulfoxide

DPPH → 2,2-diphenyl-1-picrylhydrazyl

ESI-MS → Electrospray Ionization Mass Spectrometry

FTIR → Fourier Transform Infra-Red Spectroscopy

CtDNA → Calf thymus DNA

HMBC → Heteronuclear multiple-bond correlation spectroscopy

HPLC → High performance liquid chromatography

HSQC → Heteronuclear single-quantum correlation spectroscopy

IC_{50} → Half-inhibitory concentration

m /z → mass/ charge

MeOH → Methanol

Mephen → 4,7-dimethyl-1,10- phenanthroline

MilliQ → Double deionized water

PBS → Phosphate Buffered Saline

Phen → 1,10-Phenanthroline

PNPP → (4-nitrophenyl)-phosphate hexahydrate

PTFE → Polytetrafluoroethylene

py → pyridoxal

RP-HPLC → Reverse phase HPLC

Sal → Salicylaldehyde

Smdt → S-methyl dithiocarbazate

UV-Vis → Ultra-violet-Visible Spectroscopy

Van → *o*-vanillin

δ → chemical shift

ε → Molar extinction coefficient

λ_{em} → Fluorescence emission wavelength

λ_{ex} → excitation wavelength

λ_{max} → maximum wavelength

ν → vibration frequency

1. Introduction

The discovery of novel active compounds with new mechanisms of action, higher efficacy and improved selectivity is a matter of urgency to multi drug resistance and toxicity problems associated with many therapeutic drugs [**1**]**.** Great attention has been given to transition metal complexes and extensive biological effects have been found for many of them [**2**]. One of the first therapeutic metallodrugs was salvarsan (**-a**), an arsenic-based antimicrobial agent developed by Paul Ehrlich for the treatment of syphilis. With the addition of mercury and bismuth, salvarsan remained the standard remedy for syphilis until it was replaced by penicillin after World War II. Salvarsan is regarded as the birth of modern chemotherapy and often cited as the beginning of modern research and development of metallodrugs. In 1965, the star of the field, the anticancer agent cisplatin, was discovered by Barnett Rosenberg and Loretta VanCamp at Michigan State University [**3**]. This platinum-based (-**b**) anticancer drug has played a crucial role. Complexes with other metal ions like titanium and ruthenium are also being explored with some success but none is used in the clinic yet [**2**,**4**].

Despite the achievements in the metal based drugs, especially in platinum-based drugs, they are still associated with many drawbacks such as general toxicity, nonspecific targeting and acquired drug resistance, which has stimulated researchers to seek and develop more effective, less toxic, and target-specific metal-based drugs [**5**]. Complexes based on essential transition metals, such as Co(II), Ni(II), Cu(II) and Zn(II) have been found interesting recently. These metal ions are biocompatible, endogenous and they are present in biological systems [**4**,**5**]. They are nowadays present in several inorganic drugs used against a variety of diseases [**4**].

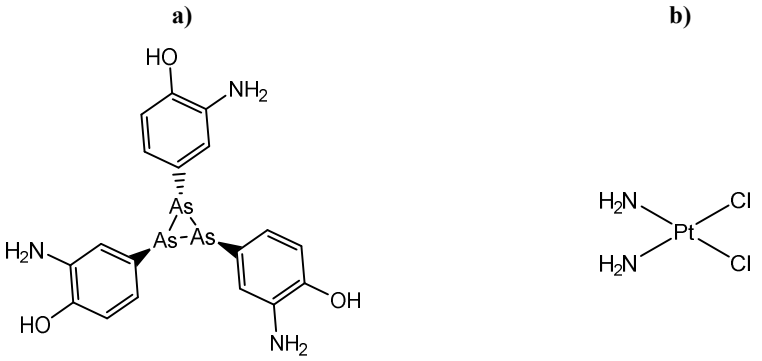

Figure 1 Salvarsan (a) and cisplatin (b) metallodrugs **[**3**]**

Transition metal complexes possess several advantages that make them attractive alternatives to organic small molecules for the development of therapeutic agents. They can adopt numerous geometries, including square-planar, square-pyramidal, trigonal-bipyramidal and octahedral, depending on the coordination number of the metal ion. Many of these geometries are unavailable to purely organic molecules, which are limited to linear, trigonal planar or tetrahedral shapes because carbon cannot exceed a coordination number of four. The diversity of molecular structures afforded by transition metal complexes may therefore allow them to sample regions of the chemical space that are inaccessible to organic molecules. Moreover, these metal complexes can undergo redox reactions and ligand-exchange reactions inside the body, allowing for unique mechanisms of action to take place [**6**]. In general, because of the intrinsic nature of their centers, characteristic coordination modes, accessible redox states and kinetic properties allow metal complexes to offer potential advantages over organic agents alone [**2**].

The role of the ligands in the metal complex is also very important. For example, they control the reactivity of the metal and determine the nature of interactions involved in the recognition of biological target sites such as deoxyribonucleic acid (DNA), enzymes and protein receptors. Therefore, the choice of ligands for the formation of essential metal -based drugs is crucial. As a result, a great expansion of research in the coordination chemistry of sulphur and nitrogen-containing ligands such as Schiff base and phenanthroline derivatives has taken place during recent years [**7**,**8**].

1,10-phenanthroline (phen) is a classic nitrogen heterocycle and chelating bidentate ligand for metal ions. It is a rigid planar, hydrophobic, electron-poor heteroaromatic system, whose

nitrogen atoms are placed in a good position to act cooperatively in cation binding [**4**]. Its rigid structure is imposed by the central ring. That means the two nitrogen atoms are always held in fixed positions. They do not have free rotation like the bipyridyl system (**Figure 2**) [**9**]. These structural features determine its coordination ability towards metal ions [**4**,**9**].

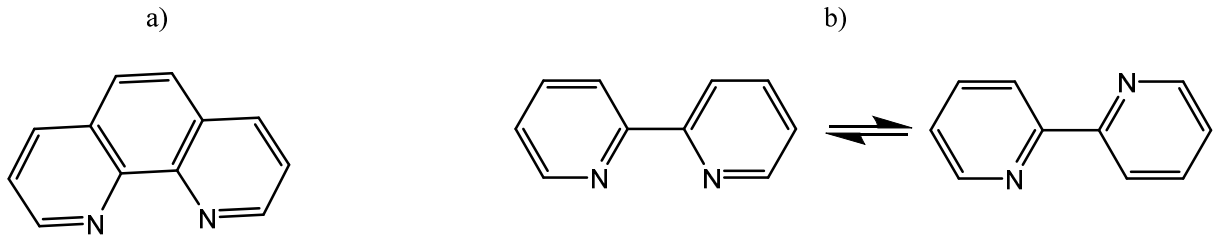

Figure 2 Structure of 1,10-Phenanthroline (a) and 2, 2'-dipyridine (b) [**9**]

Because of having excellent planar π systems, phenanthroline and its derivatives have often been involved in model compounds to mimic non-covalent interactions in biological processes [**10**,**11**]. 1,10–phenanthroline and its derivatives form very stable complexes with many first-row transition metals giving compounds with potential therapeutic applications. **Figure 3** shows examples of metal complexes with mixed-ligands containing 1,10-phenanthroline or its derivatives, which have different biological activities [**12**].

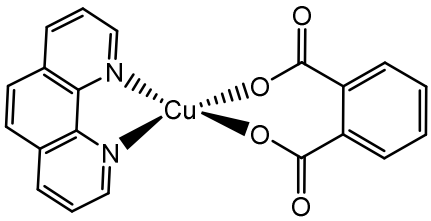

Anticancer [**12**]

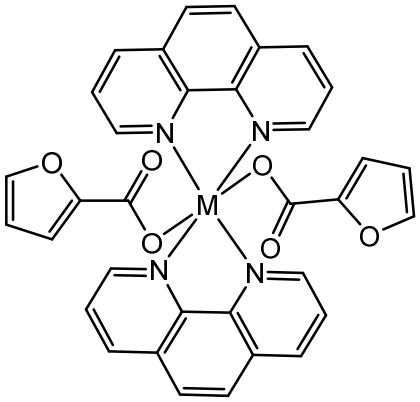

Where M = Mn (II), Co (II), Ni (II), Cu (II),

Zn (II), Cd (II) and Hg (II)

Antibacterial [**13**]

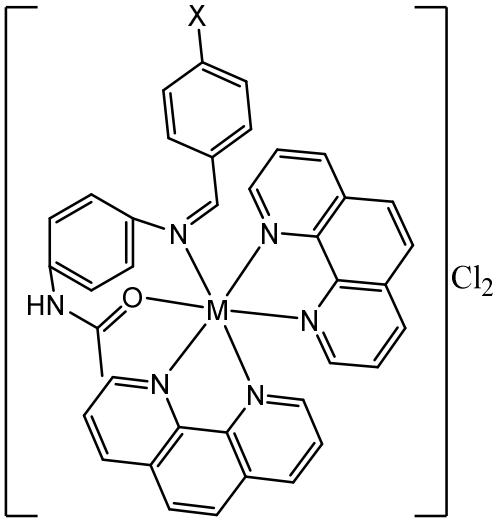

Where X= OH, Cl; M = Cu (II), Zn (II), Mn (II), Co (II), and Ni (II)

Antibacterial [**14**,**15**]

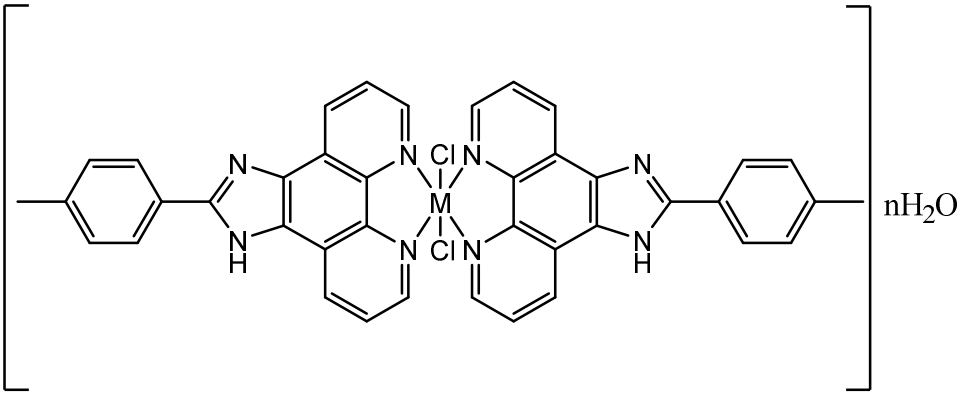

Where M = Co (II), n = 1; Ni (II), n= 2

Antibacterial [**16**]

Figure 3 Examples of metal complexes of mixed-ligands containing 1,10-phenanthroline derivatives, and its reported biological effects.

In general, phenanthroline derivatives and their metal complexes have a wide range of biological activities such as antibacterial [**17**], antifungal, antitumor and antiviral activities [**4**,**18**]. They

interact with DNA by aromatic π stacking between base pairs. This interaction results in the lengthening, stiffening, and unwinding of the helix [**18**].

Schiff bases are organic compounds formed by the condensation reaction of primary amines with aldehydes or ketones (**Figure 4**) under specific condition [**19**,**20**,**21**,**22**] and were first reported by Hugo Schiff in 1864 [**20**,**23**]. The common structural feature of Schiff bases (also known as imines or azomethines) is a nitrogen analogue of an aldehyde or ketone in which the carbonyl group (CO) has been replaced by an imine or azomethine group [**20**,**21**,**24**] and the general structural formula is shown in **Figure 4**.

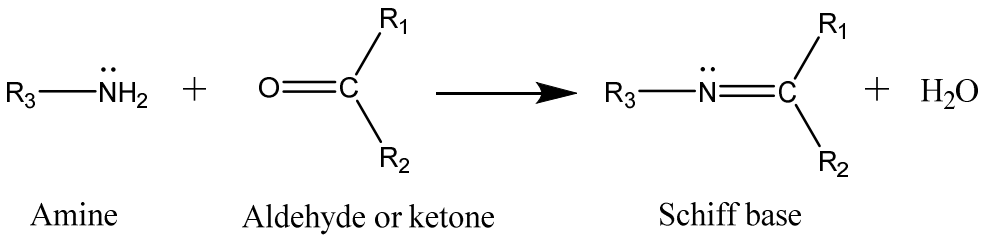

Figure 4 General scheme for the formation of Schiff bases **[**4**]**

Schiff bases are used as pigments and dyes, catalysts, intermediates in organic synthesis, and as polymer stabilizers [**21**]. They have also been shown to exhibit a broad range of biological activities, including antidiabetic [**25**], antibacterial, antifungal, anticancer, antioxidant, anti-inflammatory, antimalarial, antiviral [**24**], analgesic, antimicrobial, anticonvulsant, antitubercular [**26**], antiproliferative, antipyretic [**21**], and diuretic activities [**19**].

Besides the N-donor atom of the azomethine group, Schiff base ligands can possess other donor atoms such as O and S in its backbone [**27**]. The dithiocarbazate Schiff bases (NH_2NHCS_2R) have received considerable attention because they can provide an interesting series of Schiff bases whose properties can be significantly modified by introducing different organic substituents (R_1, R_2, R_3 in **Figure 5**) that impart a variety of donor properties [**28**]. Because of the presence of both hard nitrogen and soft sulfur donor atoms in the backbones of these ligands, they readily coordinate with a wide range of transition metal ions yielding stable metal complexes, some of which have been shown to exhibit interesting physical and chemical properties and potentially useful biological activities [**29**]. The biological activities of the metal complexes of these Schiff bases differ from those of either the ligand or the metal ion itself [**30**].

For example, Schiff bases derived from S-methyl or S-benzyl dithiocarbazates (**Table** 1) [**27**] show widely different biological activities, although they may vary only slightly in their molecular structure [**30**]. They can be coordinated to transition metal ions in various modes to form stable metal complexes [**4**,**20**].

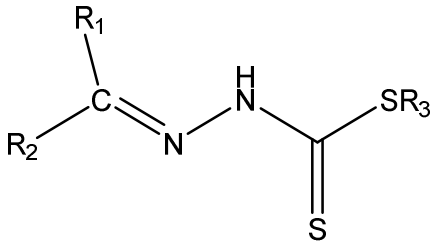

Figure 5 General structure of dithiocarbazate Schiff base derivatives **[**31**]**

Table 1 : List of some dithiocarbazate Schiff base derivatives and their metal complexes

Ligands (L)	Metal complexes	Ref.
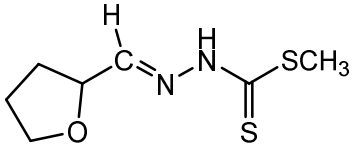 Antifungal	$Cu(L)_2$-Antibacterial and anticancer $Zn(L)_2$-Anticancer	[**32**]
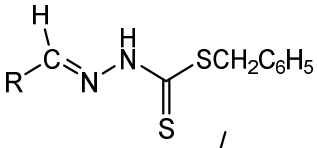 Where R=  , 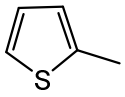 and  Antibacterial and antifungal	$[Sn(L)_2Ph_2]$ and $[Sn(L)Ph_2Cl]$ Antibacterial and antifungal	[**33**]
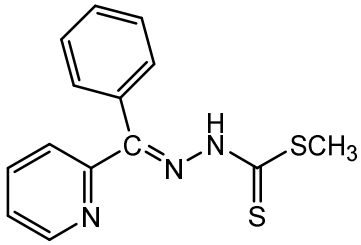 Antibacterial and antitumor activity	$[Cu_2(L)_2(CH_3COO)](ClO_4)$ and $[Zn_2(L)_2(ClO_4)_2]$ Antibacterial and antitumor activity	[**30**]

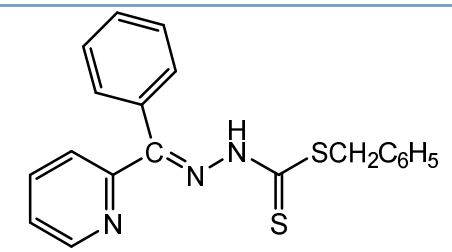 Antibacterial and antitumor activity	$[Zn(L)_2]$ Antibacterial and antitumor activity	[**30**]
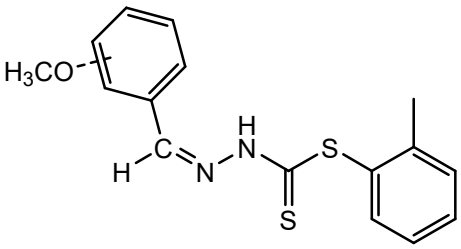 1= OCH_3 at ortho position 2= OCH_3 at meta position	$[M(L_1)_2]$ and $[M(L_2)_2]$ where M = Cu^{2+}, Ni^{2+}, and Zn^{2+} $Cu(L_1)_2$ and $Cu(L_2)_2$ showed anticancer activity	[**25**]

Zinc is an essential trace element in all living systems including animals and humans [**1**,**34**]. It is the second most prominent trace metal in the human body. Zinc is important for numerous cell processes and is a major regulatory ion in the metabolism of cells [**35**]. It is involved in a wide range of cellular processes, including cell proliferation, reproduction, immune function and defense against free radicals [**36**]. It is also required by all cells for activation of a large number of Zn-dependent enzymes, which have roles in normal metabolic processes involved in biochemical-mediated functions. In addition, Zn-dependent enzymes have many specific key roles in overcoming tissue injury or inflammatory disease states [**37**]. Therefore, developing zinc complexes as drugs is very important because it is endogenous and has minimal side effects. Many zinc complexes show different biological activities such as treatment of Alzheimer disease [**38**], antibacterial [**39**], anticonvulsant [**40**], antiproliferative–antitumor activity [**41**], antidiabetic [**34**] and anti-inflammatory; all reported in the literature [**35**].

Zinc can form complexes with different types of ligands. The properties of zinc complexes also depend on the nature of the ligands coordinated to it. The electron donor and electron acceptor properties of the ligand, structural functional groups and the position of the ligand in the coordination sphere determine the properties of the corresponding zinc complexes [**42**]. As it was

discussed before, phenanthroline and Schiff base derivatives either in the form of mixed-ligands or alone, have been used to form a lot of metal complexes. There are many zinc complexes with different phenanthroline and Schiff base derivatives synthesized and reported in the literature [**7**,**25**,**30**,**43**,**44**,**45**]. The phenanthroline and Schiff base derivatives coordinate to the zinc ion by the nitrogen of the azomethine groups. These zinc complexes of phenanthroline and Schiff bases have shown different biological activities. For example, Zn(II) complexes with phen imidazole derivatives (see **Figure 6**) showed antibacterial activity [**17**]. Similarly, the zinc complexes with mixed-ligands norfloxacin and 1,10-phenanthroline [**46**]; naproxen and 2,9-dimethyl-1,10-phenanthroline have shown very high antibacterial activities [**47**].

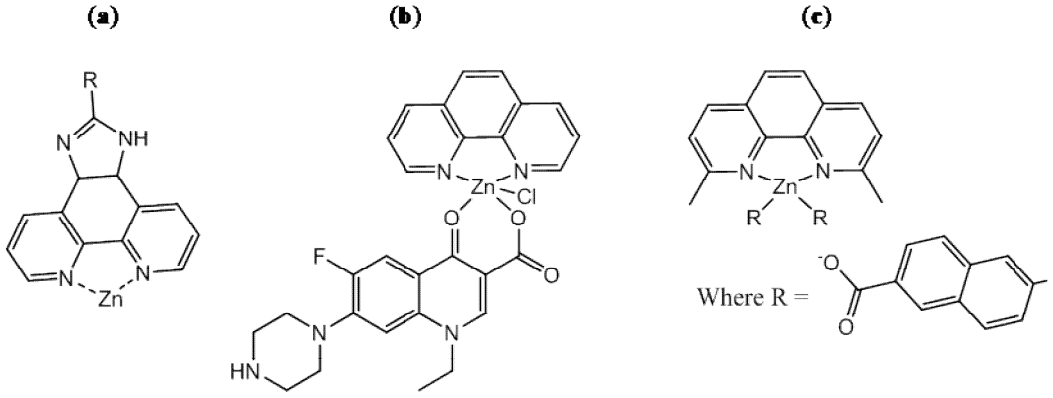

Figure 6 Zinc complex with phenanthroline imidazole derivatives (**a**), Zn(norfloxacin) (1,10-phen) (**b**) and [Zn(Naproxen)$_2$ -2,9-dimethyl-1,10-phen] (**c**).

In addition, zinc complexes with phenanthroline derivatives such as 1,10-phenanthroline-5,6-dione [**7**], diphenyl-1,10-phenanthroline, dimethyl-1,10-phenanthroline having different biological activities have also been reported [**48**].

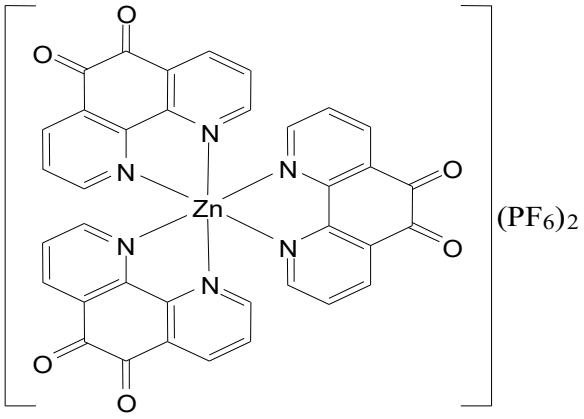

[**7**]

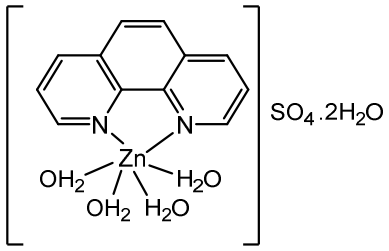

[**11**]

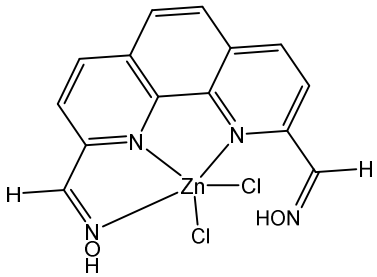

[**43**]

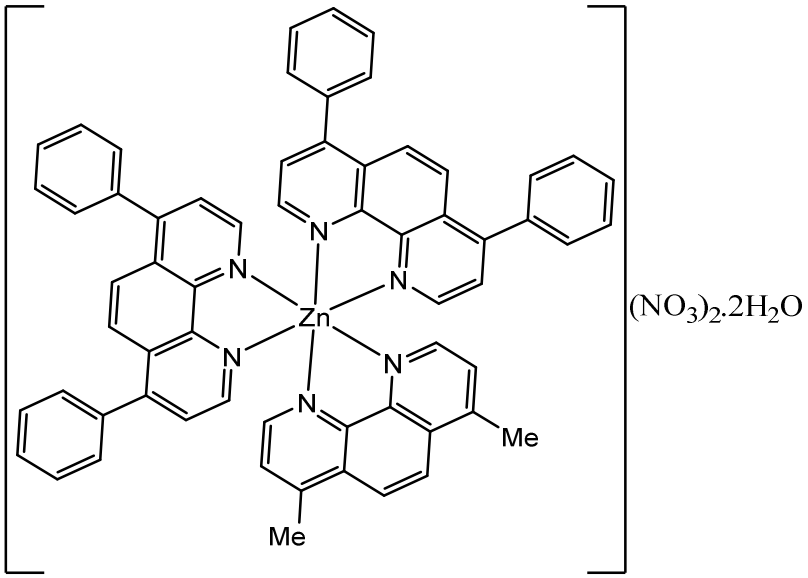

[**48**]

Figure 7 Zinc complexes with phenanthroline derivatives and mixed –ligand complexes

As described before in **Table 1** , zinc-Schiff base complexes also have been shown to exhibit interesting physical and chemical properties and potentially useful biological activities [**29**].

The physical and chemical properties of compounds determine their biological activities. For example, the rate of absorption, distribution, metabolism and excretion (ADME) of drugs are critical parameters in determining their pharmacokinetics properties. This means that the level of efficacy and toxicity of the drug depends on its concentration at the site of action [**49**,**50**]. This in turn depends on the solubility and stability of the drug in aqueous media. Therefore, the drug has to be soluble in appropriate solvents and it is very important that it does not precipitate in the aqueous environment (or at physiological conditions) and that it is stable (not degradable) in the timescale of the studies with biological molecules [**51**,**52**,**53**].

Upon entering the cell the drug needs to reach the target or interact / interfere with the relevant cellular processes. Radical and reactive oxygen species (ROS) are related with many diseases such as inflammation, hypertension, coronary heart disease, atherosclerosis, Alzheimer's disease, Parkinson's disease etc. [**54**]. These free radicals are produced under certain environmental conditions and during normal cellular functions in the body. So, antioxidants play an important role to protect the human body against damage by radicals [**55**]. Consequently, evaluation of antioxidant activity of new compounds is required.

Many biological targets including, membranes, proteins, DNA etc. have been used for evaluation of biological activities of compounds [**56**]. The anticancer activity of cisplatin is believed to result from its interaction with DNA. The drug reacts with nucleophilic sites in DNA forming monoadducts, as well as intra and interstrand crosslinks. This has been used as rationale to choose DNA as biological target to evaluate the anticancer activity of other metal complexes [**57**].

DNA regulates many biochemical processes that occur in the cellular system. The different loci present in the DNA are involved in various regulatory processes such as gene expression, gene transcription, mutagenesis, carcinogenesis, etc. Transition metal complexes can bind to DNA by both covalent and non-covalent interactions. Covalent binding involves the coordination of the nitrogenous base or the phosphate moiety of the DNA to the central metal ion. The non-covalent binding modes are intercalation, which involves the stacking of the molecule between the base pairs of DNA, groove binding, which comprises the insertion of the molecule into the major or minor grooves of DNA and electrostatic or external surface binding [**5**,**58**].

Among these, intercalation is one of the most important DNA binding modes. The DNA binding mode and strength of the affinity are affected by a number of factors, such as planarity of ligands, the coordination geometry, the ligand donor atom type, the metal ion type and its flexible valence [**5**,**58**,**59**].

The main objective of the current work is to develop anticancer drugs. Herein, we report the synthesis, characterization and solution behavior of zinc complexes with two classes of ligands: S-methyl dithiocarbazate Schiff bases and phenanthroline derived ligands. Stability in aqueous media and evaluation of antioxidant activity of the synthesised compounds are reported. The DNA binding ability of the zinc phenathroline complexes is also reported. The cytotoxicity of the S-methyl dithiocarbazate Schiff bases as well as that of the phenanthrolines and its Zn-complexes was evaluated against cancer cell lines and is reported.

2. Experimental Part

2.1. Chemicals and reagents

1,10-phenanthroline, 2,6-diformyl-4-methylphenol, pyridoxal hydrochloride, hydrazine hydrate (all from Sigma-Aldrich), 4,7-dimethyl-1,10-phenanthroline, 5-amino-1,10-phenanthroline (both from Alfa Aesar), salicylaldehyde (Acros Organics), methyl iodide, ortho-vanillin and carbon disulfide were used as received. The zinc metal salts $Zn(NO_3)_2 \bullet 4H_2O$ (Fluka Chemika) and $Zn(CH_3COO)_2 \bullet 2H_2O$ (Panreac) were used as supplied. KOH (Panreac), NaOH (Akzonobel), KH_2PO_4 and Na_2HPO_4 were used as received. Solvents such as toluene (CHEM-LAB), ethanol, methanol (both from Carlo Erba), isopropanol (Sigma-Aldrich), DMSO (Fisher Scientific), diethyl ether (Riedel-de-Häen), acetone-d_6, CD_3OD, D_2O, DMSO-d_6 (all from Euriso-top), petroleum ether and acetonitrile were used. Phosphate buffered saline (PBS) was purchased from Sigma-Aldrich as tablets readily soluble in water (deionized water) giving 0.01 M in phosphate (NaCl, 0.138 M; KCl, 0.0027 M), pH 7.4 at 25 ºC. 2,2-diphenyl-1-picrylhydrazyl(DPPH), disodium salt of (4-nitrophenyl)-phosphate hexahydrate (PNPP), calf thymus DNA (ctDNA) were purchased from Sigma-Aldrich. Millipore® water was used in the experiments with biological molecules. All other materials not mentioned here were either analytical or reagent grade.

2.2. Instrumentation

Elemental analysis for C, H, N and S were carried on a FISONS EA 1108 CHNS-O apparatus at Laboratório de Análises of Instituto Superior Técnico. The NMR spectra were recorded at ambient temperature on a Bruker Avance II + 300 (Ultra Shield TM Magnet) spectrometer operating at 300.13 MHz. The ^1H NMR chemical shifts are reported in ppm using tetramethylsilane as internal reference. The Infra-Red spectra were recorded on Alpha RT-DLaTGS HR 0.8 FTIR spectrometer and the UV-Visible absorption spectra were recorded on a Perkin Elmer Lambda 35 UV-Vis spectrophotometer with 10.0 mm optical path cuvettes. A 500-MS Varian Ion Trap Mass Spectrometer was used to measure ESI-MS spectra of methanolic solutions of the ligands and complexes in both positive and negative modes. Ultimate 3000 HPLC system (Dionex) equipped with C_{18} (12.5×0.4 cm, 5 μm particles) and connected to chromeleon software was used. Fluorescence measurements were carried out on a SPEX®

Fluorolog spectrofluorimeter (Horiba JobinYvon) in a FL3- 11 configuration, equipped with a Xenon lamp and in a 10.0 mm quartz cuvette. The instrumental response was corrected by means of a correction function provided by the manufacturer. The experiments were carried out at room temperature and are all steady-state measurements.

2.3. Phenanthroline derived zinc complexes

2.3.1. Synthesis

The zinc complexes with phenanthroline derivatives were synthesized following procedures reported in the literature for similar compounds [**10**,**60**,**61**].

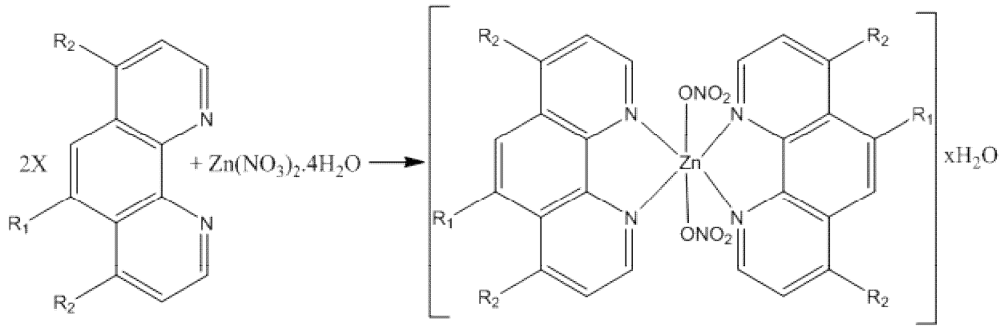

Where

$R_1 = R_2 = H$: $Zn[(phen)_2(NO_3)_2]\bullet 2H_2O$; $R_1 = H$, $R_2 = CH_3$: $Zn[(Mephen)_2(NO_3)_2]\bullet 3.5H_2O$;

$R_1 = NH_2$, $R_2 = H$: $Zn[(aminophen)_2(NO_3)_2]\bullet 1.5H_2O$

Scheme 1 Synthesis of the zinc(II) complexes with phenanthroline derived ligands

$Zn[(phen)_2(NO_3)_2]\bullet 2H_2O$: An ethanolic solution (1 ml) of 1,10-phenanthroline monohydrate (180 mg, 1 mmol) was added drop wise to a stirred ethanolic solution (1.5 ml) of zinc nitrate tetra hydrate ($Zn(NO_3)_2\bullet 4H_2O$) (130.7 mg, 0.5 mmol). A white precipitate was formed immediately. The mixture was stirred for 2 h at room temperature and left overnight at 4 ºC. The white solid was then collected by filtration, washed with a small amount of cold water, acetone and ethyl ether. Finally, the product was dried over silica gel under vacuum. (Yield: 176 mg, 64.0 %). ESI-MS (electro spray ionization mass spectra) (MeOH) *m/z* [Calculated (Found)]:

486.04 (486.04) (90 %) $[M(phen)_2(NO_3)]^+$; 212.3 (212.0) (14 %) $[M(phen)_2]^{2+}$. Elemental analysis for $C_{24}H_{16}N_6O_6Zn \bullet 2H_2O$: C, 48.90 %; H, 3.49 %; N, 14.26 %. Found: C, 48.9 %; H, 3.1 %; N, 14.1%. FTIR (KBr, cm^{-1}): 1620 (C=N), 1579 (C=C), 579 (Zn-N). ^1H NMR (300 MHz, DMSO-d6, δ (ppm)): 8.1-9.0 (aromatic-Hs). ^{13}C NMR (300 MHz, DMSO-d6, δ (ppm)): 126.3-149.3 (aromatic-Cs). UV-Vis [DMSO, λ_{max} / nm (ε / $M^{-1}cm^{-1}$)]: 325 (1.17×10^3), 294 (1.28×10^4), 272 (3.59×10^4), 267 (3.76×10^4).

$Zn[(Mephen)_2(NO_3)_2] \bullet 3.5H_2O$: An ethanolic solution (2 ml) of 4,7-dimethyl-1,10-phenanthroline (208 mg, 1 mmol) was added drop wise to a stirred ethanolic solution (1.5 ml) of zinc nitrate tetra hydrate ($Zn(NO_3)_2 \bullet 4H_2O$) (130.7 mg, 0.5 mmol). A light brown precipitate was formed immediately. The mixture was stirred for 2 h at room temperature and left overnight at 4 ºC. The solid was then collected by filtration, washed with a little amount of cold water, ethanol and ethyl ether. After drying over silica gel under vacuum, a beige solid product was obtained. (Yield: 239 mg, 78.9 %). ESI-MS (electro spray ionization mass spectra) (MeOH) *m/z* [Calculated (Found)]: 542.12 (542.0) (14 %) $[M(Mephen)_2(NO_3)]^+$; 240.1 (240.3) (100 %) $[M(Mephen)_2]^{2+}$. Elemental analysis for $C_{28}H_{24}N_6O_6Zn \bullet 3.5H_2O$: C, 50.60 %; H, 4.60 %; N, 12.60 %. Found: C, 50.6 %; H, 4.7 %; N, 12.5 %. FTIR (KBr, cm^{-1}): 1615 (C=N), 1576 (C=C), 639 (Zn-N). ^1H NMR (300 MHz, Methanol-d_4, δ (ppm)): 2.9-3.0 (aliphatic-Hs), 7.7-9.0 (aromatic -Hs). ^{13}C NMR (300 MHz,Methanol-d_4, δ (ppm)): 19.3 (aliphatic-C), 124.8-152.5 (aromatic-Cs). UV-Vis [DMSO, λ_{max} / nm (ε / M^{-1} cm^{-1})]: 327 (1.59×10^3), 305 (7.18×10^3), 274 (3.60×10^4), 268 (3.5×10^4).

$Zn[(aminophen)_2(NO_3)_2] \bullet 1.5H_2O$: Methanolic solution (4 ml) of 5-amine-1,10-phenanthroline (201.9 mg, 1 mmol) was added drop wise to a stirred ethanolic solution (1.5 ml) of zinc nitrate tetra hydrate ($Zn(NO_3)_2 \bullet 4H_2O$) (130.7 mg, 0.5 mmol). The yellow clear mixture was stirred at room temperature for 2 h and then refluxed at 70 ºC for more 3 h, after which an orange precipitate was formed. After cooling to room temperature the mixture was kept at 4 ºC overnight. The solid was then filtered under vacuum, washed with a little amount of cold water, acetone and ethyl ether. After drying over silica gel under vacuum, a yellow solid product was obtained. (Yield: 236 mg, 81.40 %). ESI-MS (electro spray ionization mass spectra) (MeOH) *m/z* [Calculated (Found)]: 516.10 (516.10) (10%) $[M(aminophen)_2(NO_3)]^+$; 227.00 (227.3) (100 %) $[M(aminophen)_2]^{2+}$. Elemental analysis for $C_{24}H_{18}N_8O_6Zn \bullet 1.5H_2O$: C, 47.50 %; H, 3.50 %; N,

18.50 %. Found: C, 47.5 %; H, 3.1 %; N, 18.4 %. FTIR (KBr, cm^{-1}): 1615 (C=N), 1593 (C=C), 513 (Zn-N). ^{1}H NMR (300 MHz, Methanol-d_4, δ (ppm)): 7.15-9.1 (aromatic -Hs). ^{13}C NMR (300 MHz, Methanol-d_4, δ (ppm)): 103.35-149.38 (aromatic-Cs). UV-Vis [DMSO, λ_{max} / nm (ε / M^{-1} cm^{-1})]: 363 (1.86×10^4), 298 (5.19×10^4), 268 (4.42×10^4).

From this point further the hydration water molecules included in the complex formulation will be omitted for simplicity, unless relevant. Also, sometimes the complexes will be referred to as $Zn(phen)_2$, $Zn(Mephen)_2$ and $Zn(aminophen)_2$.

2.3.2. Stability studies in aqueous medium

The stability of the Zn(II) complexes of phenanthroline derived ligands was evaluated using UV-Vis, fluorescence and NMR spectroscopies.

In the UV-Vis absorption study, 500 μM of $Zn[(Mephen)_2(NO_3)_2]$ and 1000 μM of $Zn[(phen)_2(NO_3)_2]$ or $Zn[(aminophen)_2(NO_3)_2]$ stock solutions of the complexes were prepared in DMSO. Then, further dilutions were done containing 125 μl of the stock solution and 2375 μl of PBS buffer (pH 7.4,10 mM), having the final concentrations 25 μM for $Zn[(Mephen)_2(NO_3)_2]$ and 50 μM for $Zn[(phen)_2(NO_3)_2]$ and $Zn[(aminophen)_2(NO_3)_2]$. UV-Visible absorption spectra (260-500 nm) were recorded and monitored for 24 h. Similarly, for the fluorescence studies stock solutions of the complexes with concentrations of 500 μM were prepared in DMSO. By dissolving 125 μl of the stock solutions in 2375 μl PBS, diluted solutions with a concentration of 25 μM were prepared. Then, the fluorescence emission spectra of $Zn[(phen)_2(NO_3)_2]$ (332-700 nm), $Zn[(Mephen)_2(NO_3)_2]$ (350-700 nm) and $Zn[(aminophen)_2(NO_3)_2]$ (455-700 nm) were recorded at 326, 345 and 450 nm excitation wavelengths, respectively. To evaluate the stability, the emission spectra were recorded at 3 h and 72 h.

The stability study by NMR was carried out for $Zn[(phen)_2(NO_3)_2]$ only. The reason is that this complex was found to be less stable when compared to $Zn[(Mephen)_2(NO_3)_2]$ and $Zn[(aminophen)_2(NO_3)_2]$, when evaluated by UV-Visible spectrophotometry.

A phosphate buffer solution with concentration 120 mM and pH of 7.54 was prepared by dissolving 2.4 mg KH_2PO_4 and 14.4 mg Na_2HPO_4 salts in 1 ml of D_2O. 12.5 mg of $Zn[(phen)_2(NO_3)_2]$ were dissolved in 250 μl of DMSO-d_6. Then, 20 μl of this solution were

mixed with 380 µl of the phosphate buffer giving 5 % DMSO and 95 % PBS. Finally, the stability of the compound was studied for 24 h by ^{1}H-NMR spectroscopy.

2.3.3. DNA binding ability study

Binding ability to DNA can be evaluated directly by titration of the complex (at constant concentration) with ctDNA and following spectroscopic absorption [**62**] or fluorescence emission spectra changes [**48**,**63**]. Alternatively, when the complex does not show fluorescence emission, the binding ability can be determined indirectly by a competition titration using a probe [ethidium bromide (EB) or thiazole orange (TO)] bound to ctDNA (at constant concentration) and following the quenching of the emission of fluorescence due to displacement of probe bound to ctDNA by the target compound [**64**,**65**].

The fluorescence quenching and enhancement can be evaluated by classical Stern–Volmer **Equation 1** [**65**] and **Equation** 2 [**48**] respectively.

$$I_o/I = 1 + K_Q[Q]$$

Equation 1

$$I_o/I = 1 – K_E[E]$$

Equation 2

Where I_o and I are the fluorescence intensity in the absence and presence of quencher / enhancer respectively. [Q] and [E] are the concentration of quencher and enhancer respectively. K_Q and K_E are the Stern–Volmer quenching and enhancement constants, respectively.

The binding assay was carried out based on reported procedures [**59**,**66**]. The stock solution of ctDNA was prepared by dissolving 1 mg into 1 ml PBS buffer (pH 7.4, 10 mM). The stock solution was kept at 4 ^{o}C for 2 days to allow dissolution of the DNA and used within 4 days. The DNA concentration of the stock solution was determined using the molar absorption coefficient 6600 $M^{-1}cm^{-1}$ at 260 nm. The UV absorbance ratio at 260 and 280 nm of ctDNA solution was determined and the values were found to be 1.84, which indicate that the ctDNA is sufficiently free from protein. 0.5 mM stock solutions of the metal complexes were prepared in DMSO. Several samples with different DNA:Zn complex molar ratios (*ca.* 0; 0.2; 0.4; 0.6; 0.8; 1.0; 2.0; 4.0) were prepared maintaining the concentration of the metal complex solutions at 25 µM (in 5

% DMSO and 95 % PBS) and gradually increasing the concentration of ctDNA. The Absorbance values at the emission and excitation wavelengths were kept below 0.2. The fluorescence emission spectra were measured with the following parameters: λ_{ex}= 326, 345 and 450 nm (for $Zn(phen)_2$, $Zn(Mephen)_2$ and $Zn(aminophen)_2$ respectively) and both slits were of 5 nm. All the experiments were carried out at 25 ^oC.

2.3.4. Evaluation of antioxidant activity

The DPPH (2,2-diphenyl-1-picrylhydrazyl) radical scavenging method has been widely used to evaluate the free radical scavenging activity of various antioxidant substances. It is a rapid technique for screening the radical scavenging activity of specific compounds and has been used by many researchers [**55**,**67**]. This assay is based on the measurement of the decrease in absorbance of DPPH at 516 nm after reaction with the test compound. The effect of antioxidants on DPPH radical scavenging is due to the hydrogen donating ability or radical scavenging activity of the samples [**55**].

The scavenging reaction between (DPPH) and an antioxidant (H-D) can be written as:

$$\underset{\text{(Purple)}}{\text{(DPPH)}} + \text{(H-D)} \rightarrow \underset{\text{(Yellow)}}{\text{DPPH-H}} + \text{(D)}$$

Antioxidants react with DPPH, a stable free radical that is thus reduced, and as a result the absorbance decreases due to the formation of the DPPH-H from the DPPH radical. The degree of discoloration also indicates the scavenging potential of the antioxidant compounds or samples in terms of hydrogen donating ability [**55**].

Stock solutions of complexes $Zn[(phen)_2(NO_3)_2]$ (0.86 mM), $Zn[(Mephen)_2(NO_3)_2]$ (0.86 mM), and $Zn[(aminophen)_2(NO_3)_2]$ (1.21 mM) were prepared in DMSO. By dissolving 2.4 mg of DPPH (2,2-diphenyl-1-picrylhydrazyl) in 50 ml of methanol, a DPPH stock solution with concentration 121.7 µM was prepared and kept in the dark during the entire experiment. Then, 5 samples having different n(compound) / n(DPPH) mole ratios and a final volume of 2500 µl were prepared by mixing 1500 µl of DPPH, and different volumes of the compounds' solutions and methanol. The samples were vigorously shaken and kept in the dark for 30 minutes. Finally, the spectra were recorded between 300 and 700 nm, so that the absorbance values at 516 nm

could be read. The antioxidant activity (% scavenging activity) was calculated using **Equation 3** [**55**] below.

$$\text{DPPH scavenging ability (\%)} = \frac{Abs_0 - Abs_1}{Abs_0} \times 100$$

Equation 3

Where Abs_0 = the absorbance of the control DPPH solution, and Abs_1 = the absorbance in the presence of sample solutions or standards for positive control. The value for IC_{50} was determined by a linear regression where the % of scavenging activity is 50 and compared with that of ascorbic acid, a standard which was used as positive control [**68**].

2.4. S-methyl dithiocarbazate derived Schiff bases and their zinc complexes

2.4.1. Synthesis

The S-methyl dithiocarbazate derived Schiff bases and their corresponding zinc(II) complexes were prepared following previously reported methods [**32**] with some modifications.

S-methyl dithiocarbazate (Smdt): Potassium hydroxide (1.14 g; 20 mmol) was dissolved in 9:1 ethanol-water mixture (7 ml) and cooled in ice. To the mixture, excess hydrazine hydrate (1 g; 0.98 ml; 30 mmol) was added slowly with stirring. The reason to add an excess of hydrazine hydrate was to compensate the loss due to its volatile nature. Carbon disulphide (1.52 g; 1.207 ml; 20 mmol) in ethanol (1.25 ml) was then added drop wise from a burette, with constant vigorous stirring over a period of 1 h. The temperature of the mixture was kept below 10 ^{o}C during the addition. A yellow oil was formed, separated with a funnel and dissolved in 2:3 ethanol-water mixture (5 ml) and the solution was cooled in ice. Methyl iodide (2.9 g; 1.272 ml; 20 mmol) was added slowly, with vigorous stirring. Ice-cold water (5 ml) was then added and the stirring was continued for another 10 minutes. The white solid product was separated by filtration, washed with water; and dried in air. The crude product was recrystallized from toluene (9 ml). Yield: 8.142 g (33.3 %); mp: 80 ºC. Elemental analysis for $C_2H_6N_2S_2$: C, 19.66 %; H, 4.95 %; N, 22.92 %; S, 52.47 %. Found: C, 19.5 %; H, 4.8 %; N, 23.0 %; S, 53.8 %.

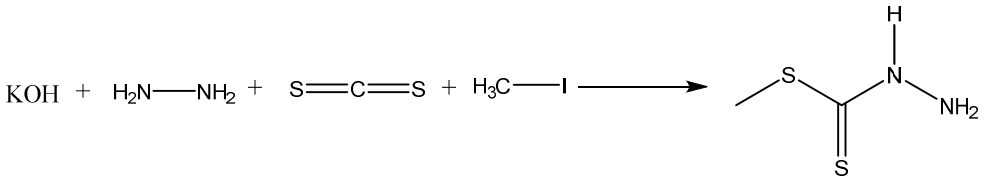

Scheme 2 Synthesis of Smdt ligand

Salicylaldehyde S-methyl dithiocarbazate Schiff base (SalSmdt): S-methyl dithiocarbazate (0.1515 g, 1.25 mmol) was dissolved in methanol (6 ml) and heated under stirring. Then, salicylaldehyde (133 µl, 1.25 mmol) was added. Additionally, 30 ml of methanol was added. The reaction mixture was refluxed for 3 h and the solution became colorless. After cooling, the white solid product was formed. The product was filtered, washed with 10 ml of cold MeOH and 30 ml of petroleum ether. Finally, it was dried under vaccum. (Yield: 0.206 g, 72.82 %). ESI-MS (electro spray ionization mass spectra) (MeOH) *m/z* [Calculated (Found)]: 227.03 (227.0) (18 %) $[L+H]^+$; 225.01 (225.3) (100 %) $[L-H]^-$. Elemental analysis for $C_9H_{10}N_2OS_2$: C, 47.77 %; H, 4.45 %; N, 12.38 %; S, 28.33 %. Found: C, 47.6 %; H, 4.3 %; N, 12.3 %; S, 28.8 %. FT-IR (KBr, cm^{-1}): 3435 (OH), 3111 (NH), 1616 (C=N), 967 (C=S). ^{1}H NMR (300 MHz, Acetone-d_6, δ (ppm)): 2.65 (s, 3H, C_{13}-H), 6.97 (d, 1H, C_2 -H), 6.99 (t, 1H, C_4 -H), 7.38 (t, 1H, C_3-H), 7.48 (d, 1H, C_5-H), 8.52 (s, 1H, C_7-H), 10.24 (s, 1H, O-H), 12.25 (s, 1H, N-H). ^{13}C NMR (300 MHz, Acetone-d_6, δ (ppm)): 17.52 (C_{13}), 117.60 (C_2), 118.17 (C_6), 120.57 (C_4), 132.38 (C_5), 133.20 (C_3), 149.36 (C_7), 156.72 (C_1) and 198.74 (C_{10}). UV-Vis [DMSO, λ_{max} / nm (ε / M^{-1} cm^{-1})]: 367 (2.68×10^4), 353 (3.32×10^4), 322 (1.63×10^4), 292 (8.84×10^3). RP-HPLC (50 % ACN: 50 % Water, R_T / min): 6.4.

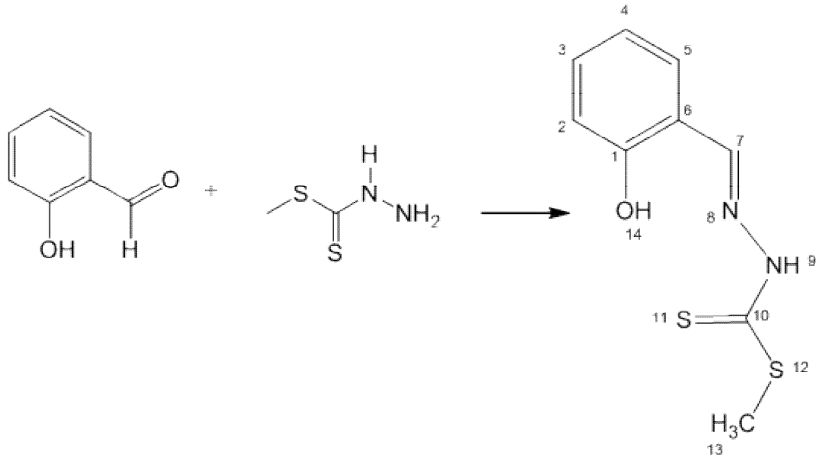

Scheme 3 Synthesis of SalSmdt ligand

Methyl-phenol-di-S-methyl dithiocarbazate Schiff base Mp(Smdt)$_2$: 0.2446 g (2.0 mmol) of S-methyl dithiocarbazate was dissolved in 5 ml of methanol. A solution of 2,6-diformyl-4-methylphenol was also prepared by dissolving 0.1640 g (1.0 mmol) in 15 ml of methanol. The two solutions were mixed and allowed to reflux for 4 h under stirring. A yellow precipitate was formed. After cooling, the solid was filtered, washed with methanol followed by petroleum ether and dried under vacuum. (Yield: 0.32 g, 85.9 %). ESI-MS (electrospray ionization mass spectra) (MeOH) *m/z* [Calculated (Found)]: 373.02 (372.9) (12 %) $[L+H]^+$; 371.01 (371.3) (83 %) $[L-H]^-$, 743.03 (742.7) (100 %) $[2L-H]^-$. Elemental analysis for $C_{13}H_{16}N_4OS_4$: Calculated: C, 41.91 %; H, 4.33 %; N, 15.04 %; S, 34.42 %. Found: C, 42.0 % ; H, 4.4 %; N, 14.7 %; S, 34.2 %. FT-IR (KBr, cm^{-1}): 3433 (OH), 3103 (NH), 1617 (C=N), 1039 (C=S). ^{1}H NMR (300 MHz, DMSO-d_6, δ (ppm)): 2.30 (s, 3H, C_7-H), 2.57 (s, 6H, C_{14} & $_{18}$-H), 7.57 (s, 2H, C_3 & $_5$ -H), 8.52 (s, 2H, C_8 & $_{16}$-H), 10.81 (s, 1H, O-H), 13.51 (s, 2H, N-H). ^{13}C NMR (300 MHz, DMSO-d_6, δ(ppm)): 16.80 (C_{14} & $_{18}$), 19.79 (C_7), 119.64 (C_2 & $_6$), 129.61 (C_4), 131.30 (C_3 & $_5$), 144.75 (C_8 & $_{16}$), 154.55 (C_1), 197.45 (C_{11} & $_{20}$). UV-Vis [DMSO, λ_{max} / nm (ε / M^{-1} cm^{-1})]: 394 (2.41×10^4), 383 (2.61×10^4), 344 (3.83×10^4), 330 (3.64×10^4). RP-HPLC(50 % ACN:50 % Water, R_T / min): 8.8.

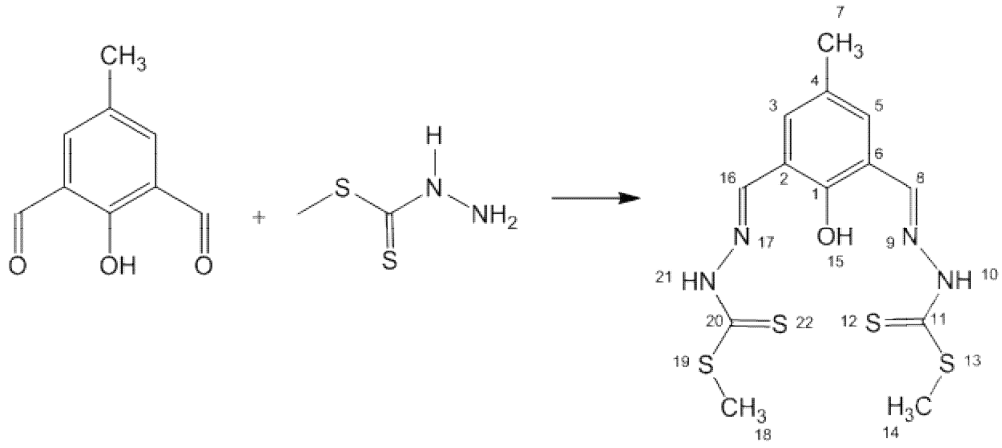

Scheme 4 Synthesis of Mp(Smdt)$_2$ ligand

***o*-Vanillin S-methyl dithiocarbazate Schiff base (VanSmdt):** S-methyl dithiocarbazate (0.1515 g, 1.25 mmol) was dissolved in 20 ml isopropanol. *o*-Vanillin (0.198 g, 1.25 mmol) was added under stirring. The reaction mixture was refluxed for 3 h and the white solid product was formed. After cooling, the product was filtered, washed with 10 ml of cold isopropanol and 30 ml of petroleum ether. Finally, it was allowed to dry under vacuum. (Yield: 0.1846 g, 57.6 %).

ESI-MS (electro spray ionization mass spectra) (MeOH) *m/z* [Calculated (Found)]: 257.04 (257.04) (25 %) $[L+H]^+$; 255.02 (255.14) (100 %) $(L-H)^-$. Elemenal analysis for $C_{10}H_{12}N_2O_2S_2$: Calculated: C, 46.86 %; H, 4.72 %; N, 10.93 %; S, 25.01 % . Found: C, 46.7 %; H, 4.7 %; N, 10.9 %; S, 25.6 %. FT-IR (KBr, cm^{-1}): 3416 (O-H), 3178 (N-H), 1616 (C=N), 1073 (C=S). ^1H NMR (300 MHz, Acetone-d_6, δ (ppm)): 2.63 (s, 3H, C_{13}-H), 3.87 (s, 3H, C_{15} -H), 6.90 (t, 1H, C_4-H), 7.06 (d, 1H, C_3-H), 7.18 (d, 1H, C_5-H), 8.56 (s, 1H, C_7-H), 9.65 (s, 1H, O-H), 13.34 (s, 1H, N-H). ^{13}C NMR (300 MHz, Acetone-d_6, δ (ppm)): 17.18 (C_{13}), 56.49 (C_{15}), 114.86 (C_3), 119.06 (C_6), 120.32 (C_4), 121.98 (C_5), 146.74 (C_2), 148.74 (C_7), 149.19 (C_1), 199.10 (C_{10}). UV-Vis [DMSO, λ_{max} / nm (ε / M^{-1} cm^{-1})]: 367 (1.92×10^4), 363 (2.04×10^4), 339 (2.53×10^4), 292 (6.79×10^3). RP-HPLC (50 % ACN:50 % Water, R_T / min): 4.5.

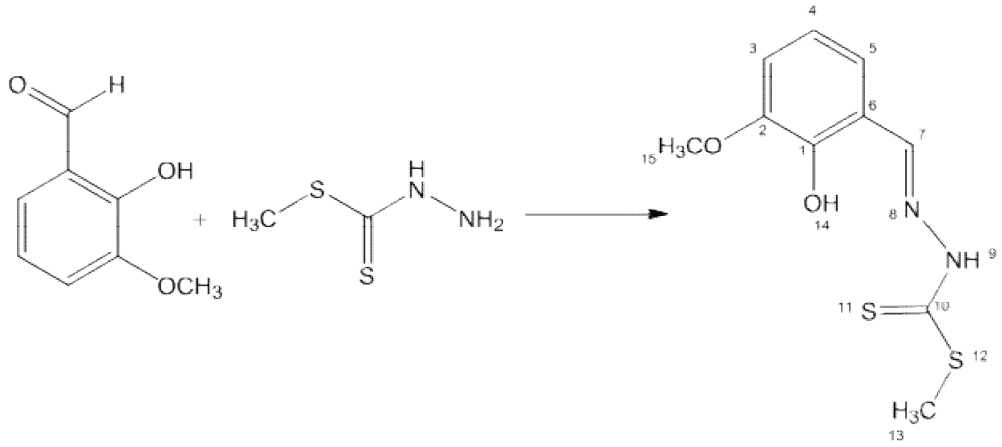

Scheme 5 Synthesis of VanSmdt ligand

Pyridoxal S-methyl dithiocarbazate Schiff base (PySmdt): S-methyl dithiocarbazate (0.3055 g, 2.5 mmol) was dissolved in 40 ml methanol and NaOH (0.100 g; 2.5 mmol) was added. Then, pyridoxal hydrochloride (0.5091 g, 2.5 mmol) was slowly added and the mixture was stirred for 15 min at room temperature. The reaction mixture was refluxed for 3 h and the white solid product was formed. The mixture was cooled, filtered, and washed with 50 ml water and 50 ml petroleum ether. Finally, the product was dried under vacuum. (Yield: 0.5674 g, 86.64 %). ESI-MS (electro spray ionization mass spectra) (MeOH) *m/z* [Calculated (Found)]: 272.05 (272.04) (100 %) $[L+H]^+$; 270.03 (270.18) (100 %) $[L-H]^-$; 541.07 (540.73) (49 %) $[2L-H]^-$. Elemental analysis for $C_{10}H_{13}N_3O_2S_2$: C, 44.26 %; H, 4.83 %; N, 15.49 %; S, 23.63 %. Found: C, 44.0 %; H, 4.8 %; N,15.4 %; S, 24.3 %. FT-IR (KBr, cm^{-1}): 2930-3357 (br, OH & NH), 1612 (C=N),

1047 (C=S). ^{1}H NMR (300 MHz, DMSO-d_6, δ (ppm)): 2.42 (s, 3H, C_{15}-H), 2.61 (s, 3H, C_{13}-H), 4.63 (s, 2H, C_{16} -H), 5.34 (s, 1H, 17–OH), 8.04 (s, 1H, C_7-H), 8.81 (s, 1H, C_4-H), 10.61 (s, 1H, 14-OH), 13.74 (s, 1H, NH). ^{13}C NMR (300 MHz, DMSO-d_6, δ (ppm)): 17.12 (C_{13}), 19.18 (C_{15}), 59.21 (C_{16}), 120.20 (C_5), 133.31 (C_6), 138.73 (C_7), 145.79 (C_4), 147.13 (C_2), 150.03 (C_1), 197.52 (C_{10}). UV-Vis [DMSO, λ_{max}/nm (ε / M^{-1} cm^{-1})]: 351 (1.83×10^4), 339 (2.05×10^4), 298 (6.849×10^3). RP-HPLC (50 % ACN:50 %Water, R_T / min): 2.78.

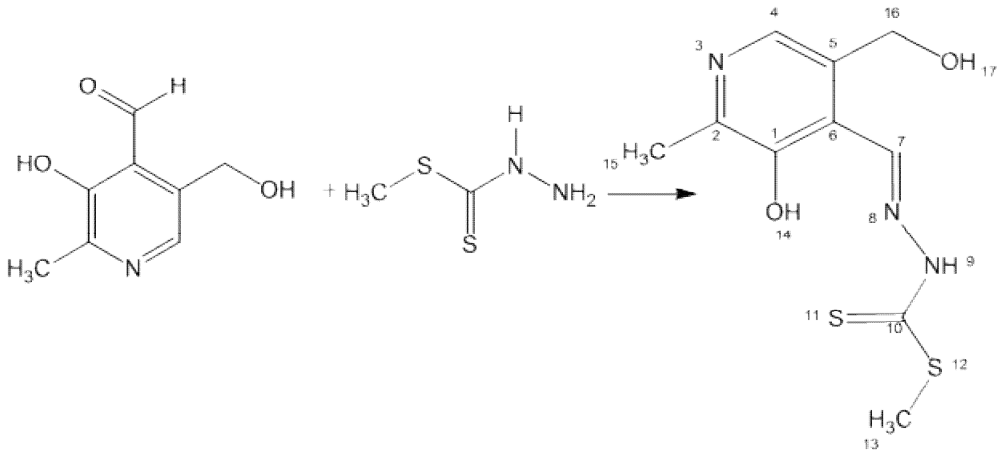

Scheme 6 Synthesis of PySmdt ligand

Zn[(SalSmdt)(H_2O)]•0.5H_2O: 194 mg (8.84×10^{-4} mol) of zinc acetate ($Zn(CH_3COO)_2$•$2H_2O$) was added to an ethanolic solution (25 ml) of SalSmdt (0.100 g; 4.42×10^{-4} mol) with constant stirring for 15 min at room temperature. Then, the mixture was refluxed for 2 h under stirring. Finally, the solid was filtered, washed with 30 ml of water and dried in vacuum. (Yield: 0.1184 g, 83.6 %). ESI-MS (electro spray ionization mass spectra) (MeOH) *m/z* [Calculated (Found)]: 353.00 (352.5) (100 %) $[ML+2CH_3OH-H_2O+H]^+$, 610.89 (611.1) (100 %) $[2ML-H]^{-\cdot}$ Elemental analysis for $ZnC_9H_{10}N_2O_2S_2$•$0.5H_2O$: Calculated: C, 33.75 %; H, 3.59 %; N, 8.75 %; S, 20.02 %. Found: C, 34.0 %; H, 3.0 %; N,8.4 %; S, 19.6. FTIR (KBr, cm^{-1}): 3315-3667 (br, OH (from H_2O)), 1593 (C=N), 952 (C-S). ^{1}H NMR (300 MHz, Acetone-d_6, δ (ppm)): 2.44 (s, 3H, C_9-H), 6.8 (t, 1H, C_6-H), 7.00 (d, 1H, C_2 -H), 7.25 (t, 1H, C_1 -H), 7.39 (d, 1H, C_5-H), 8.73 (s, 1H, C_7-H). ^{13}C NMR (300 MHz, Acetone-d_6, δ (ppm)): 14.46 (C_9), 118.25 (C_6), 120.56 (C_2), 122.65 (C_4), 133.50 (C_1), 135.38 (C_5), 161.29 (C_7), 165.10 (C_3). UV-Vis [DMSO, λ_{max} / nm (ε / M^{-1} cm^{-1})]: 400 (1.197×10^4), 319 (8.412×10^3), 291 (8.767×10^3). RP-HPLC (50 % ACN:50 % Water, R_T / min): 6.3.

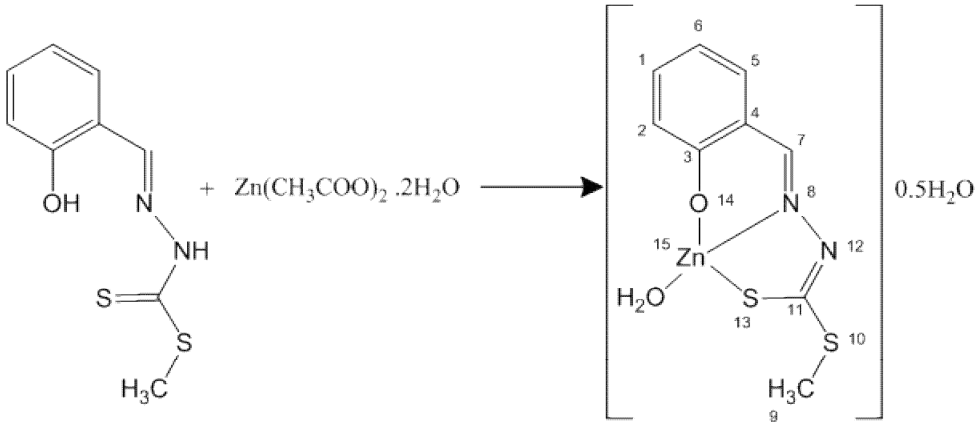

Scheme 7 Synthesis of Zn[(SalSmdt)(H_2O)]•0.5H_2O complex

Zn_2[(Mp(Smdt)$_2$)(CH_3COO)]: 117.8 mg (5.367×10^{-4} mol) of $Zn(CH_3COO)_2$•$2H_2O$) was added to an ethanolic solution (25 ml) of $MP(Smdt)_2$ (100 mg; 2.68×10^{-4} mol) with constant stirring for the first hour at room temperature. Then, the reaction was kept under stirring for extra 2 h at reflux temperature and a yellow product was formed. The mixture was cooled, the product filtered and washed with ethanol (30 ml) and dried under vacuum. (Yield: 0.0619 g; 41.29 %). ESI-MS (electro spray ionization mass spectra) (MeOH) *m/z* [Calculated (Found)]: 587.87(588.0) (60 %) $[ML+CH_3OH]^-$. Elemental analysis for $C_{15}H_{16}N_4O_3S_4Zn_2$: Calculated: C, 32.21 %; H, 2.88 % ;N, 10.02 % ; S, 22.93 %. Found: C, 32.2 % ; H, 3.3 %; N, 9.9 %; S, 21.7 % . FT-IR (KBr, cm^{-1}): 1613 (C=N), 1460 $(COO)_{asy}$, 1375 $(COO)_{sym}$, 1000 (C-S). ^{1}H NMR (300 MHz, DMSO-d6, δ (ppm)): 1.05 (s, 3H, C_{28}-H), 2.24 (s, 3H, C_7-H), 2.43 (s, 6H, C_{12} & $_{17}$-H), 7.41 (s, 2H, C_1 & $_5$ -H), 8.69 (s, 2H, C_8 & $_9$ -H). ^{13}C NMR (300 MHz, DMSO-d6, δ (ppm)): 13.95 (C_{12} & $_{17}$), 19.36 (C_7), 138.88 (C_1 & $_5$), 159.64 (C_8 & $_9$). UV-Vis [DMSO, λ_{max} / nm (ε / $M^{-1}cm^{-1}$)]: 432 (1.176×10^4), 349 (1.558×10^4), 310 (1.547×10^4). RP-HPLC (50 % ACN:50 % Water, R_T / min): 6.1.

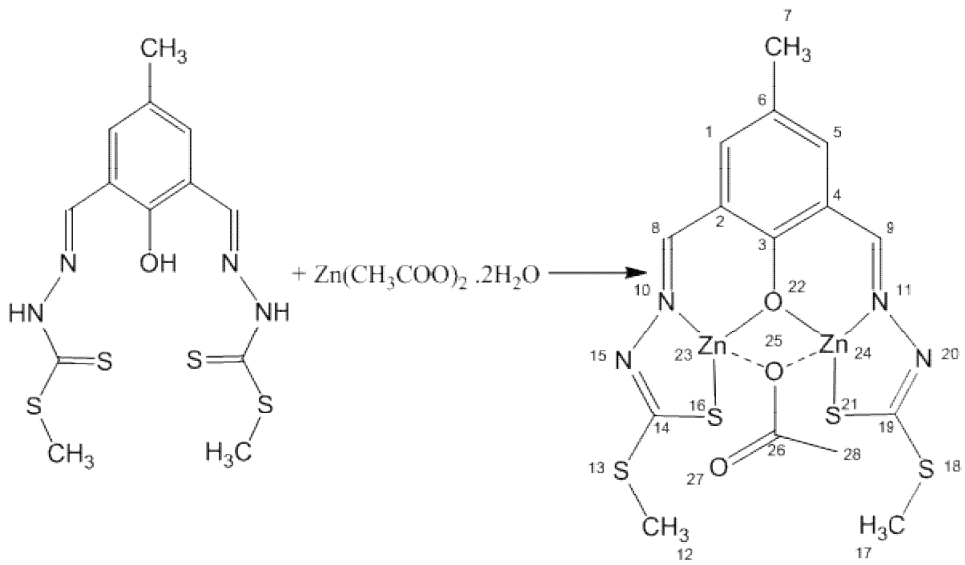

Scheme 8 Synthesis of $Zn_2[(Mp(Smdt)_2)(CH_3COO)]$ complex

Zn[(VanSmdt)(H_2O)]: 68.5 mg (3.12×10^{-4} mol) zinc acetate ($Zn(CH_3COO)_2\bullet2H_2O$) was added to an ethanolic solution (25 ml) of VanSmdt (0.080 g; 3.12×10^{-4} mol) with constant stirring for the first 30 min, at room temperature. Then the reaction was refluxed at 80 ^{o}C for 2 h under stirring. A light yellow solid product was formed and cooled. The product was filtered, washed with 30 ml ethanol and dried under vacuum. (Yield: 0.0493 g, 46.79 %). ESI-MS (electro spray ionization mass spectra) (MeOH) *m/z* [Calculated (Found)]: 670.91(670.85) (100 %) $(2ML+H_2O-H)^-$. Elemental analysis for $C_{10}H_{12}N_2O_3S_2Zn$: Calculated: C, 35.56 %; H, 3.58 %; N, 8.29 %; S, 18.99 %. Found: C, 35.2 %; H, 2.5 %; N,7.7 %; S, 19.4 %. FTIR (KBr, cm^{-1}): 3427(OH from H_2O), 1597 (C=N), 1034 (C-S). ^{1}H NMR (300 MHz, DMSO-d_6, δ (ppm)): 2.41(s, 3H, C_{11}-H), 3.72 (s, 3H, C_7-H), 6.39 (m, 1H, C_6 -H), 6.82 (m, 2H, C_1&$_5$ -H), 8.55 (s, 1H, C_9 -H). ^{13}C NMR (300 MHz, DMSO-d_6, δ (ppm)): 14.17 (C_{11}), 55.65 (C_7), 113.17 (C_6), 126.43 (C_5), 152.09 (C_2) and 159.84 (C_9). UV-Vis [DMSO, λ_{max} / nm (ε / M^{-1} cm^{-1})]: 406 (7.69×10^3), 328 (8.90×10^3), 292 (6.86×10^3). RP-HPLC (50 % ACN:50 % Water, R_T / min): 4.67.

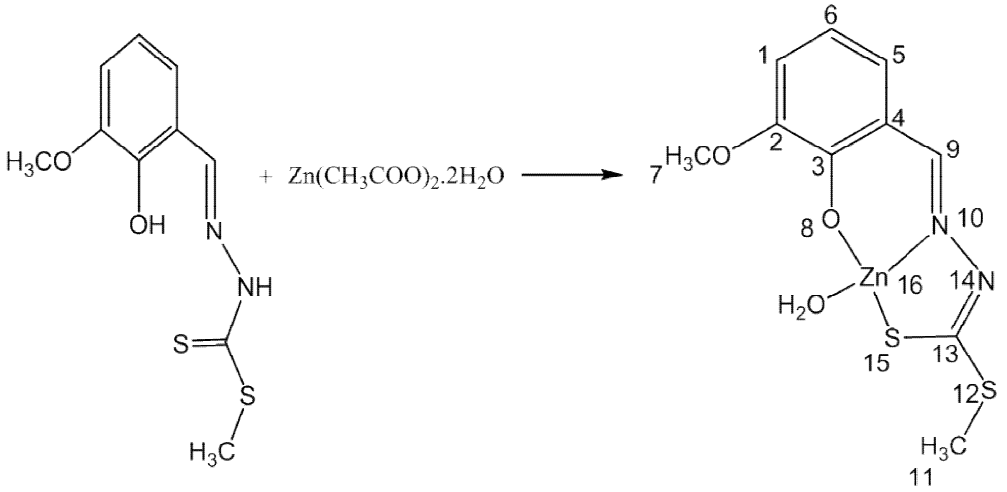

Scheme 9 Synthesis of Zn[(VanSmdt)(H_2O)] complex

Zn[(PySmdt)(CH_3COO)]•1.5H_2O: 271 mg (1.00×10^{-3} mol) of PySmdt was dissolved in 20 ml of methanol and stirred for 20 min at room temperature. 220 mg (1.00×10^{-3} mol) zinc acetate ($Zn(CH_3COO)_2$•$2H_2O$) was also added and stirred at room temperature for extra 20 min. The mixture was refluxed for 2 h at refluxing temperature under constant stirring. After 2 h reflux, the solution became orange but there was no formation of precipitate. The solution was concentrated under reduced pressure. Then, the product was precipitated by adding diethyl ether and allowed to cool. Finally, the product was filtered, washed by diethyl ether (30 ml) and dried under vacuum. (Yield: 250 mg, 59.75 %). ESI-MS (electro spray ionization mass spectra) (MeOH) *m/z* [Calculated (Found)]: 333.97 (334.1) (100 %) $(ML\text{-}CH_3COO)^+$; 412.00 (411.6) (80 %) $(ML+H_2O+H)^+$; 392.00 (392.21) (13 %) $(ML\text{-}H)^-$. Elemental analysis for $C_{12}H_{15}N_3O_4S_2Zn$•$1.5H_2O$: Calculated: C, 34.45 %; H, 4.24 %; N, 10.04 %; S, 15.33 %. Found: C, 34.9 %; H, 4.0 %; N, 9.4 %; S, 14.6 %. FT-IR (KBr, cm^{-1}): 3417 (OH from H_2O), 1597 (C=N), 1493 $(COO)_{asy}$, 1304 $(COO)_{sym}$, 1022 (C-S). ^1H NMR (300 MHz, DMSO-d_6, δ (ppm)): 2.39 (s, 3H, C_{12}-H), 2.44 (s, 3H, C_{13}-H), 4.51 (s, 2H, C_7 -H), 5.18 (s, 1H, 8-OH), 7.43 (s, 1H, C_6 -H), 8.92 (s, 1H, C_9-H), 11.97 (s, 1H, NH). ^{13}C NMR (300 MHz, DMSO-d_6, δ (ppm)): 14.13 (C_{13}), 21.35 (C_{12}), 59.51 (C_7), 131.40 (C_6), 133.45 (C_4), 153.78 (C_2), 155.82 (C_9), 161.71 (C_3) and 178.43 (C_{20}). UV-Vis [DMSO, λ_{max} / nm (ε / M^{-1} cm^{-1})]: 420 (7.160×10^3), 338 (8.094×10^3), 298 (6.849×10^3). RP-HPLC (50 % ACN:50 % Water, R_T / min): 4.71.

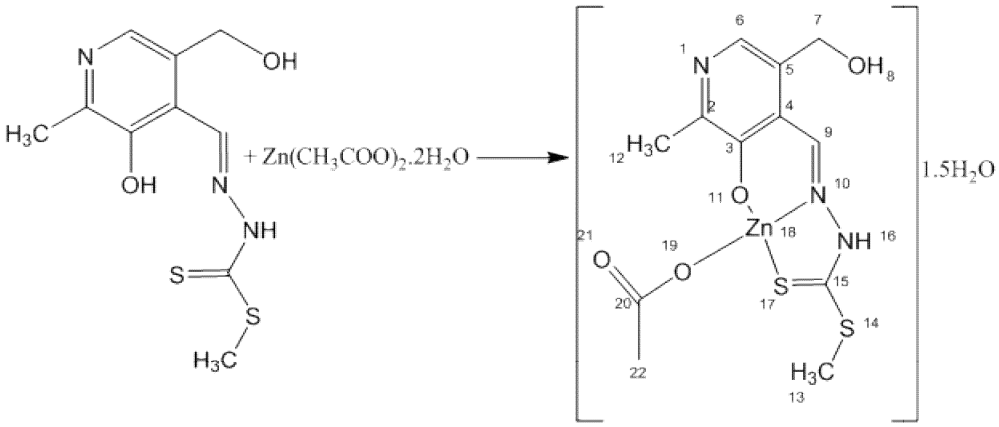

Scheme 10 Synthesis of Zn[(PySmdt)(CH_3COO)]•1.5H_2O complex

2.4.2. Stability studies in aqueous medium

The stability of the ligands and their corresponding Zn(II) complexes was evaluated by UV-Visible spectroscopy, following the procedure described below.

Stock solutions of both ligands and complexes were prepared in DMSO with a concentration of 2000 µM for Smdt, VanSmdt and Zn[(PySmdt)(CH_3COO)]; 500 µM for complexes Zn[(SalSmdt)(H_2O)], Zn_2[(Mp($Smdt)_2$)(CH_3COO)] and Zn[(VanSmdt)(H_2O)]; and 250 µM for the ligands Mp($smdt)_2$, SalSmdt and PySmdt. Then, further dilutions were prepared containing 125 µl of the stock solution and 2375 µl of PBS buffer (pH 7.4, 10 mM), having the final concentrations of 100 µM for Smdt, VanSmdt and Zn[(PySmdt)(CH_3COO)]; 25 µM for complexes Zn[(SalSmdt)(H_2O)] and Zn[(VanSmdt)(H_2O)]; 12.5 µM for the ligands Mp($smdt)_2$, SalSmdt and PySmdt in 5 % DMSO and 95 % PBS. For Zn_2[(Mp($Smdt)_2$)(CH_3COO)] instead of PBS, 125 µl of the complex stock solution was diluted in 2375 µl DMSO to prepare 25 µM final concentration. UV-Visible absorption spectra (260-500 nm) were recorded and monitored for 24 h for ligands and 48 h for complexes.

The stability of these compounds was also evaluated by RP-HPLC. The RP-HPLC analysis was carried out using the following procedure. The acetonitrile and MilliQ water used to prepare the eluent were filtered and degassed by sonication. Individual sample solutions of Schiff base ligands and zinc complexes with concentrations of 1 mM were prepared in 50 % acetonitrile and 50 % water solvent mixture. Then, the solutions were filtered using 0.2 µm PTFE. Finally, the

sample solutions were eluted on a C_{18}-column (12.5×0.4 cm, 5 µm particles) with an isocratic eluent composed of acetonitrile and water (50 % CH_3CN:50 % H_2O) over 20 min. The injection volume and flow rate was 20 µl and 1 ml / min, respectively. The chromatograms were recorded at 260, 330, 350 and 375 nm and the stability of the compounds was evaluated based on the analysis of the chromatogram.

2.4.3. Evaluation of antioxidant activity

The evaluation of the antioxidant activity was done with DPPH as reported in section 2.1.4.

2.4.4. Phosphatase activity

Phosphatase activity is one of the important functions among the wide range of enzymatic roles of divalent zinc ions that has been used as basis for extensive studies of various functional mimics of phosphoesterases. Over the years Zn(II) complexes have been studied as phosphate ester models taking into account their extraordinary Lewis acidity, redox rigidity, nucleophile generation, leaving group stabilization and physiological relevance [**69**]**.** Therefore, the aim of this experiment is to evaluate if the synthesized Zn(II) complexes are capable of promoting the hydrolysis of phosphate monoesters.

The phosphatase activity of the zinc complexes was carried out using the disodium salt of (4-nitrophenyl) phosphate hexahydrate (PNPP) as monophosphate ester substrate based on reported procedures [**70**]. 500 µM stock solutions of the complexes were prepared in DMSO. The stock solution of PNPP (20 mg / 1 tab) with concentration 2.69 mM was prepared by dissolving 1 tablet in 20 ml PBS. Then, three samples: diluted complex solution without PNPP, diluted PNPP solution without complex and the mixture of complex and PNPP at fixed C(compound) / C(PNPP) concentration ratio in a final volume of 3 ml were prepared. PBS was used for the dilution. Finally, the UV-Visible absorption spectra were recorded between 260 and 600 nm at 25 ^{o}C and 37 ^{o}C for all samples. The absorption spectra were recorded at least for 1 h with 20 min interval and the absorbance changes between 400-430 nm were evaluated.

2.5. Cytotoxicity study

The cytotoxicity effect of the synthesized compounds against cancer cells was carried out either at Universidade da Beira Interior by Samuel Silvestre (the dithiocarbazate compounds) or at Centre for Nuclear Sciences and Technologies by Fernanda Marques (the phenanthroline compounds). For the Schiff bases, the procedure was the following: The tumor cell lines PC-3 (prostate), MCF-7 (breast) and CACO-2 (intestinal) were cultured at 37 °C in a humidified air incubator with 5 % CO_2. PC-3 cells were cultured in RPMI 1640 medium with 10 % fetal bovine serum and 1 % of the antibiotic mixture of 10,000 U/ml penicillin G and 100 mg / ml of streptomycin. The high-glucose Dulbecco´s modified Eagle medium (DMEM) supplemented with 10 % fetal bovine serum and 1 % antibiotic / antimycotic (10,000 U/ml penicillin G, 100 mg / ml streptomycin and 25 µg /ml anfothericin B) was used to culture MCF-7 cells. CACO-2 cells were also cultured in DMEM medium supplemented with 10 % FBS and 1 % of the antibiotic mixture of 10,000 U/ml penicillin G and 100 mg /ml of streptomycin.

The in vitro antiproliferative effects were evaluated by the MTT ([3-(4,5-dimethylthiazol-2-yl)-2,5-diphenyl tetrazolium bromide]) assay. Cells were tripsinized and counted by the trypan-blue exclusion assay and then 100 µl of cell suspension / well with an initial density of 2×10^4 cells/ml was seeded in 96-well culture plates and left to adhere for 48 h. After the cells adherence, the medium was replaced by several solutions of the compounds in study (30 µM for screening assay and 0.01, 0.1, 1, 10, 50 and 100 µM for concentration-response studies) in the appropriate medium for approximately 48 h. The percentage of DMSO in cell culture medium did not exceed 1%. 5-fluorouracil (5-FU) was used as positive control and untreated cells were used as the negative control. Each experiment was performed in quadruplicate and independently repeated at least two times. After the incubation period, the medium was removed and 100 µl of phosphate buffer saline (NaCl 137 mM; KCl 2.7 mM, Na_2HPO_4 10 mM and KH_2PO_4 1.8 mM in deionized water and pH adjusted to 7.4) were used to wash the cells. Then 100 µl of the MTT solution (5 mg/ml) was prepared in the appropriate serum-free medium and was added to each well, followed by incubation for 4 h at 37 °C. Then after, the MTT containing medium was removed and the formazan crystals were dissolved in DMSO. Then the absorbance was measured at 570 nm using a microplate reader. Cell viability values were expressed as percentages relative to the absorbance determined in the cells used as negative controls.

Cytotoxicity effects of the Zn(II)(Rphen) complexes on A2780 (ovarian) cancer cell line were also evaluated by MTT assay using 96-well plates. The cell line was cultured at 37 °C in a humidified air incubator with 5 % CO_2. The compounds were first dissolved in DMSO and then in medium through serial dilutions ranging from 0.01 μM to 100 μM. The final DMSO concentration did not exceed 1% (v/v) in either control or treated cells and under these conditions it had no effect on the cellular activity. After treatment with the complexes for different time periods, the cell medium was replaced by 200 μl (0.5 mg/ml) of a MTT solution in PBS and further incubated for 3 h at 37°C. The resulting purple formazan from tetrazolium reduction were solubilized in DMSO and gently dissolved. Finally, the absorbance of control and treated cells was measured at 575 nm using a microplate reader. The cytotoxicity of the complexes was expressed as the IC_{50} calculated from dose-response curves using the GraphPad Prism software.

3. Results and discussion

Two families of zinc complexes were synthesized. Reaction of zinc nitrate tetra hydrate, $Zn(NO_3)_2 \bullet 4H_2O$, with commercially available phenanthroline derived ligands at room temperature in methanol yielded $Zn(Rphen)_2$ type complexes (R= H, NH_2 or CH_3). Additionally, the Schiff base ligands were synthesized by the condensation reaction of aromatic aldehydes and S-methyl dithiocarbazate in methanol / isopropanol at refluxing temperature for 3-4 h. Similarly, zinc complexes were prepared from the reaction of zinc acetate dihydrate, $Zn(CH_3COO)_2 \bullet 2H_2O$, with the Schiff base ligands in methanol / ethanol at room temperature for the first 20-60 min and then at refluxing temperature for 1-2 h. The solid products were filtered, washed and dried under vacuum. All the synthesized compounds are soluble in DMSO except $Zn[(VanSmdt)(H_2O)]$, which is only sparingly soluble. The reaction's percentage yields ranged from 64.0 to 81.4 for the zinc complexes with phenanthroline derivatives; 33.3 to 86.6 for the Schiff base ligands; and 41.3 to 83.6 for the zinc complexes with the Smdt Schiff base ligands. The elemental analysis and spectroscopic characterization results are discussed in the following sections.

3.1. Zinc complexes with phenanthroline derivatives

3.1.1. Characterization

Results of elemental analysis data are given in **Table 2**. The percentage of carbon, hydrogen and nitrogen in all the zinc complexes were in good agreement with the calculated values for the proposed structures. All complexes contain water molecules.

Table 2: Analytical data for the zinc complexes with phenanthroline derivatives

Compound	Elemental analysis calculated (found) (%)		
	C	H	N
$Zn[(phen)_2(NO_3)_2] \bullet 2H_2O$	48.90 (48.9)	3.49 (3.1)	14.26 (14.1)
$Zn[(aminophen)_2(NO_3)_2] \bullet 1.5H_2O$	47.50 (47.5)	3.50 (3.1)	18.50 (18.4)
$Zn[(Mephen)_2(NO_3)_2] \bullet 3.5H_2O$	50.60 (50.6)	4.60 (4.7)	12.60 (12.5)

The UV-Vis absorption spectra measured for the phenanthroline derivative ligands and their corresponding zinc complexes in DMSO at room temperature are depicted in **Figure 8**. Zn(II)

has d^{10} closed-shell electronic configuration. Therefore, d–d transitions are not expected in the spectra of zinc complexes [**71**].

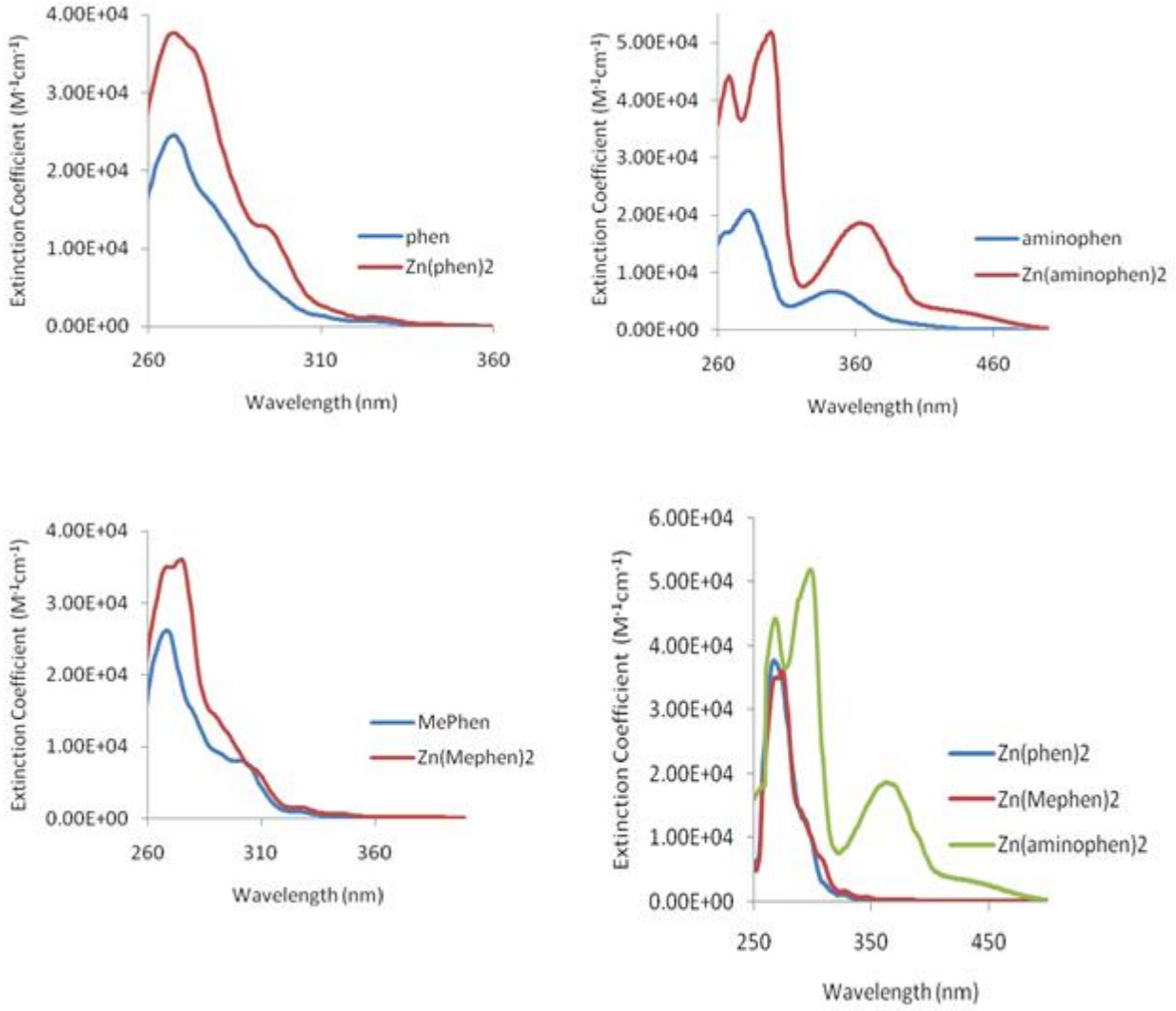

.

Figure 8 UV-Visible absorption spectra for phenanthroline derivative ligands and their zinc(II) complexes in DMSO at room temperature

The absorption bands at 274, 282 and 268 nm of phen, aminophen and Mephen ligands, respectively, may be attributed to π→π* transitions of the azomethine chromophore (C=N) group [**48**,**72**,**73**]. These bands were observed at higher wavelengths (bathochromic shift): 294, 298 and 274 nm in the absorption spectra of $Zn[(phen)_2(NO_3)_2]$, $Zn[(aminophen)_2(NO_3)_2]$ and $Zn[(Mephen)_2(NO_3)_2]$ complexes, respectively. These bathochromic shifts imply that the ligands have formed complexes with the zinc ion through their azomethine group [**37**]. In addition,

spectral bands observed at 268, 264, and 268 nm may be assigned to π→π* transitions of 'C=C' group of phen, aminophen and Mephen ligands, respectively. These spectral bands are observed at 267, 268 and 268 nm for $Zn[(phen)_2(NO_3)_2$, $Zn[(aminophen)_2(NO_3)_2]$ and $Zn[(Mephen)_2(NO_3)_2]$ complexes, respectively, which shows that there are no significant shifts indicating that there is no participation of this group in the coordination. Weak bands at 324, 345 and 326 nm for phen, aminophen and Mephen, respectively, may also be attributed to n→π* transitions in the phenanthroline. In the case of their corresponding zinc complexes, there is no wavelength shifts except for $Zn[(aminophen)_2(NO_3)_2]$ to 363 nm. In general, the bathochromic shift for the azomethine group and higher extinction coefficients (higher absorption intensity) confirm that there is formation of complexes [**74**,**75**].

Fluorescence emission spectra of the zinc complexes with phenanthroline derivatives were taken in DMSO with excitation wavelengths of 326, 450 and 345 nm for $Zn(phen)_2$, $Zn(aminophen)_2$ and $Zn(Mephen)_2$, respectively, at room temperature. The spectra are depicted in **Figure 9** and show emission maxima at 489 and 470 nm for $Zn(aminophen)_2$ and $Zn(Mephen)_2$, respectively. The emission spectrum for $Zn(phen)_2$ is very weak and is not presented. The emission bands may be attributed to the intraligand emission (π→ π*) from their corresponding ligands. The complexes' fluorescence intensity enhancement, when compared to the free ligands may be due to coordination to Zn(II), reducing the non-radiative decay of the intraligand excited state [**72**], due to increased rigidity in the coordinated ligands.

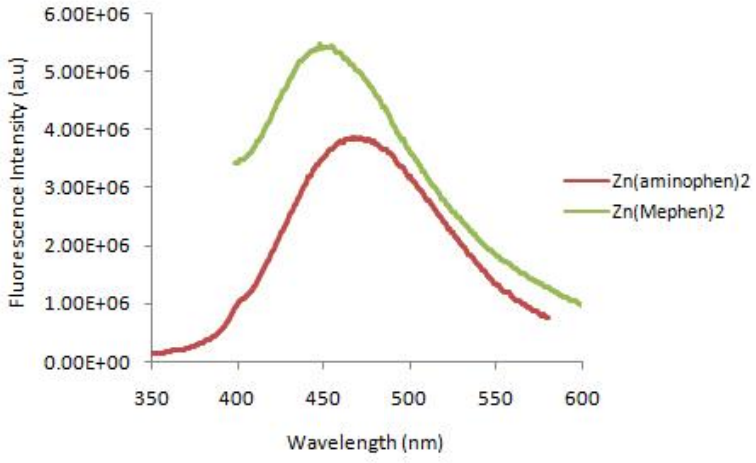

Figure 9 Fluorescence emission spectra of complexes of zinc with phenanthroline derivatives at room temperature in DMSO.

The complexes were also characterized by ESI-MS in the positive and negative modes and for all complexes it was possible to assign molecular peaks. The spectra showed peaks at m/z 212.02 , 227.29 and 240.33 that are due to the $[Zn(phen)_2]^{2+}$, $[Zn(aminophen)_2]^{2+}$ and $[Zn(Mephen)_2]^{2+}$ species, respectively. The assignments for these and other peaks corresponding to different species are presented in **Table 3.**

Table 3: Assignment of ESI-MS peaks of the $Zn(Rphen)_2(NO_3)_2$ complexes. L stands for the phenanthroline derivative.

Compound	Peak assignment	m/z (mass %)	
		Theoretical	Found
$Zn[(phen)_2(NO_3)_2]$	$ML_2(NO_3)^+$	486.04	486.06 (90%)
	ML_2^{2+}	212.26	212.02 (14%)
$Zn[(aminophen)_2(NO_3)_2]$	$ML_2(NO_3)^+$	516.10	515.96 (10%)
	ML_2^{2+}	227.00	227.29 (100%)
$Zn[(Mephen)_2(NO_3)_2]$	$ML_2(NO_3)^+$	542.12	541.96 (14%)
	ML_2^{2+}	240.10	240.33 (100%)

The IR spectra of the free phenanthroline ligands were also compared with that of their corresponding zinc complexes to determine the changes that have taken place during complexation. The infrared bands of the characteristic groups of the ligands and their complexes, together with their assignments are listed in **Table 4**. The assignments were done based on the information obtained from previous works reported in the literature for similar compounds [**13**,**14**,**15**,**17**].

The IR spectra of the phen, Mephen and aminophen ligands show characteristic bands at 1636, 1628 and 1667 cm^{-1}, respectively, due to the stretching of the (C=N) functional group. Bands at 1622, 1611 and 1568 cm^{-1} were also found, due to C=C stretching vibrations. In the IR spectra of the corresponding complexes, there were shifts in wave numbers for both groups. The IR spectral band values of (C-H) of the aromatic rings are observed at around 838-856 cm^{-1} and 729-743 cm^{-1} in the free ligands. These were red shifted to 821-858 cm^{-1} and 725-727 cm^{-1}, respectively, in their corresponding complexes. All these shifts can be explained by the fact that each nitrogen atom of the heterocycle donates a pair of electrons to the central zinc metal

forming a dative bond [**14**,**15**]. The IR spectra of all the complexes show new bands of Zn-N appearing at 579, 513, and 639 cm^{-1} for $Zn[(phen)_2(NO_3)_2]$, $Zn[(aminophen)_2(NO_3)_2]$ and $Zn[(Mephen)_2(NO_3)_2]$, respectively which are not observed in the corresponding free ligands [**13**,**14**].

Table 4: IR spectral assignments (cm^{-1}) of phenanthroline derivative ligands and their corresponding zinc complexes

Compound	C=C	C=N	C-H	Zn-N
$Zn[(phen)_2(NO_3)_2]\bullet 2H_2O$	1579	1620	850 725	579
Phen	1622	1636	856 743	----
$Zn[(aminophen)_2(NO_3)_2]\bullet 1.5H_2O$	1593	1615	821 727	513
Aminophen	1611	1667	838 735	----
$Zn[(Mephen)_2(NO_3)_2]\bullet 3.5H_2O$	1576	1615	858 727	639
Mephen	1568	1628	852 729	----

NMR spectroscopy is very important to identify the groups through which the ligands form their corresponding metal complexes and confirm the proposed structures. ^1D (^1H and ^{13}C) and ^2D (DEPT, COSY, HSQC and HMBC) NMR experiments were done for all ligands and zinc complexes. The ^1H NMR and ^{13}C NMR spectra of phen and $Zn(phen)_2$, recorded at room temperature in DMSO-d_6 and the chemical shifts are given in **Table 5** and **Table 6** respectively. In the ^1H NMR spectra of phen, it was possible to observe four types of aromatic protons appearing in the range of 7.7-9.1 ppm. In its corresponding $Zn(phen)_2$ complex, these protons are shifted downfield, appearing in the range of 8.1 - 9.0 ppm. In the ^{13}C NMR spectra, the chemical shift of the aromatic carbons of phen appear in the range of 123.5 - 150.1 ppm, but in its zinc complex the carbon peaks appear in the range 126.3-149.3 ppm, of which the majority show a

downfield shift. The downfield shift in both ^{1}H and ^{13}C NMR peaks of the zinc complexes confirms the complex formation of phen with Zn(II) ion through the aromatic ring nitrogen atoms, since coordination removes electron density from the ligand, and consequently, a deshielding effect [**37**].

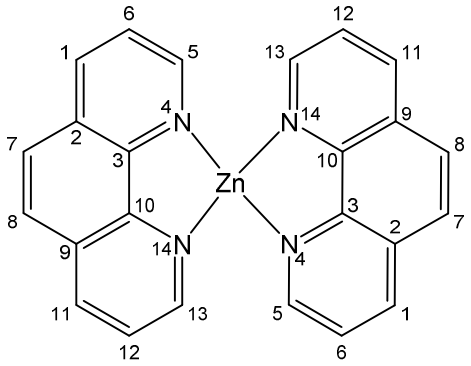

Scheme 11 $Zn(phen)_2$ complex

Table 5: ^{1}H NMR chemical shifts (δ / ppm) for phen ligand and $Zn(phen)_2$ complex in DMSO-d_6 solvent.

Compound	δ / (multiplicity, number of protons)			
	H_1 & H_{11}	H_5 & H_{13}	H_7 & H_8	H_6 & H_{12}
$Zn(phen)_2$	8.97 (d,4H)	8.75 (s,4H, br)	8.36 (s,4H)	8.08 (s,4H, br)
phen	9.10 (d,1H)	8.46 (d,1H)	7.94 (s,1H)	7.74 (m,1H)

s – singlet, d - doublet, t - triplet, m – multiplet, br-broad

Table 6: ^{13}C chemical shifts (δ / ppm) for phen ligand and $Zn(phen)_2$ complex using 300 MHz in DMSO-d6 solvent

Compound	δ / ppm of ^{13}C					
	C_1 & C_{11}	C_2 & C_9	C_3 & C_{10}	C_5 & C_{13}	C_6 & C_{12}	C_7 & C_8
$Zn(phen)_2$	140.6	129.2	139.7	149.3	126.3	127.6
phen	145.8	128.6	136.4	150.1	123.5	126.9

The ^{1}H and ^{13}C NMR characterization was also done for the aminophen ligand and its complex $Zn(aminophen)_2$ in CD_3OD at room temperature, as it is depicted in **Figure 10** and **Figure 11**.

The aromatic protons and carbons of aminophen in the ^{1}H and ^{13}C NMR spectra appear in the range of 6.99-9.07 ppm and 104.63-150.41 ppm, respectively. In the Zn(aminophen)$_2$ complex these are shifted to 7.15- 9.06 ppm and 103.35-149.38 ppm, respectively.

a)

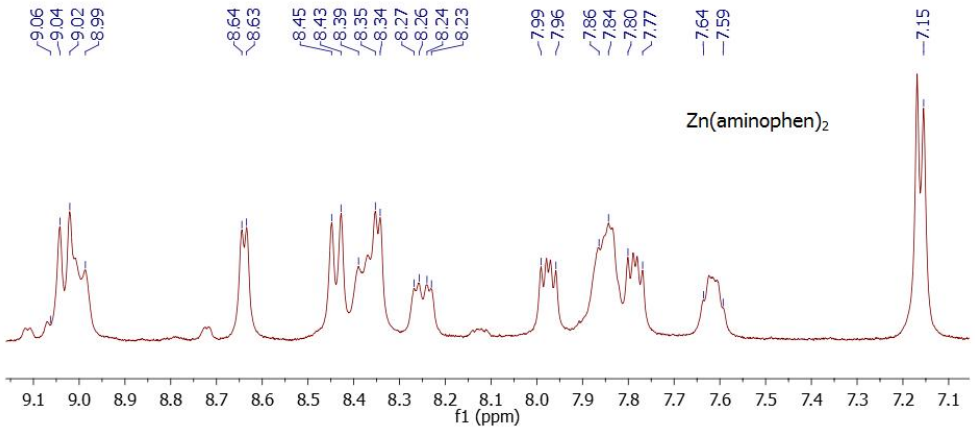

b)

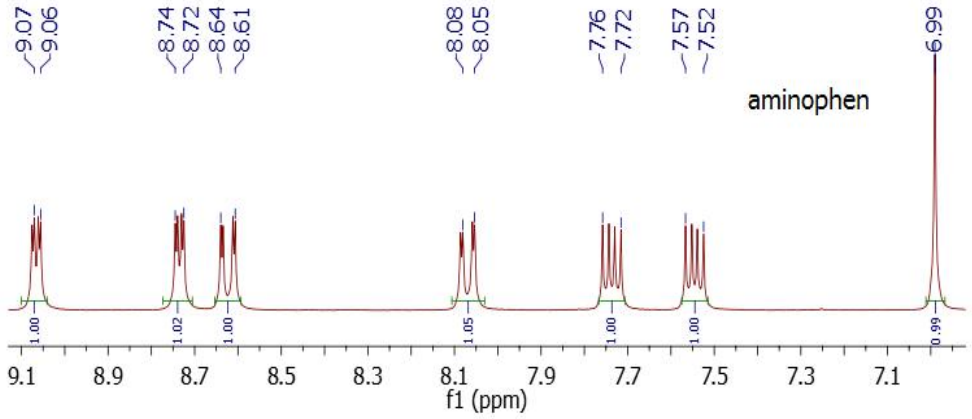

Figure 10 ^{1}H NMR spectra of Zn(aminophen)$_2$(**a**) and aminophen (**b**) in CD_3OD at room temperature

a)

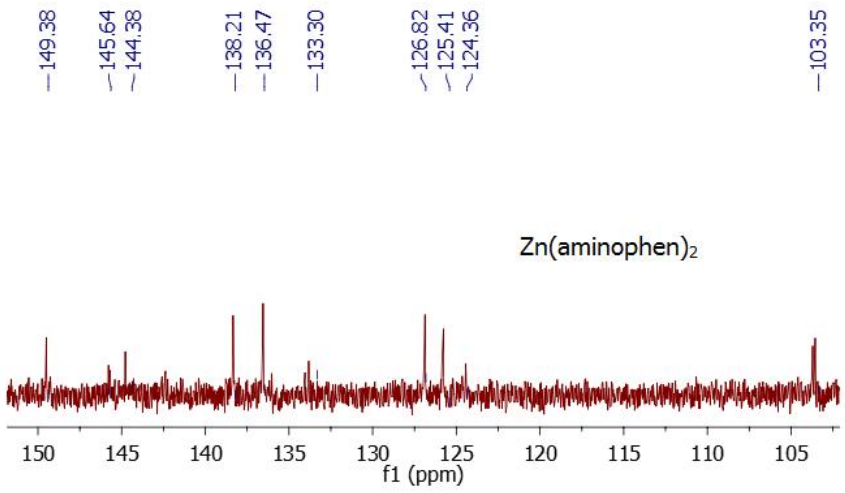

b)

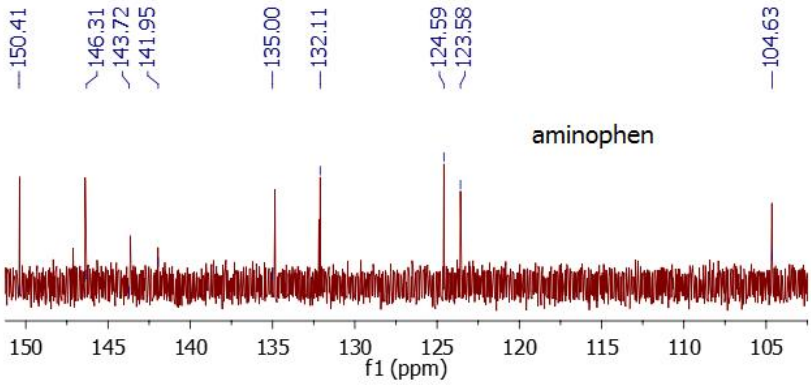

Figure 11 ^{13}C NMR spectra of Zn(aminophen)$_2$ (**a**) and aminophen (**b**) in CD_3OD at room temperature

As it can be seen from the ^{1}H and ^{13}C NMR spectra of the complex, there are extra proton and carbon peaks, which suggests that more than one species is formed in solution. To help the assignment a titration of Zn(aminophen)$_2$ with increasing amounts of aminophen ligand was carried out. Therefore, solutions with different molar ratios of Zn:L were prepared to see trends in the intensity of each peak of the ^{1}H NMR spectra, which in turn enabled to understand the behavior of complexation in solution (**Figure 12**). It is expected that the addition of free ligand will favor the formation of 1:3 species:

Zn(aminophen)$_2$ + aminophen ←> Zn(aminophen)$_3$.

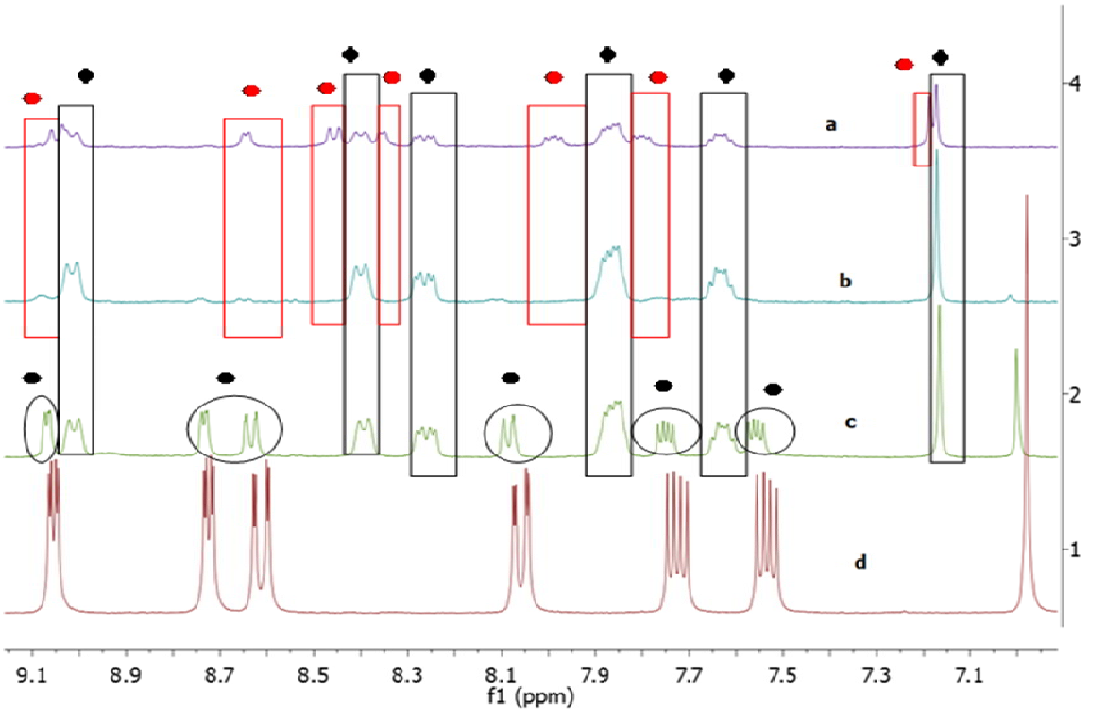

Figure 12 ^{1}H NMR titration of Zn(aminophen)$_2$ with aminophen in CD_3OD at room temperature. Where : **a**=500µl complex + 0 µl ligand; **b** = 500µl complex + 20 µl ligand; **c** = 500µl complex + 100µl ligand; **d** = 0µl complex + 500 µl ligand and ● standing for Zn:L = 1:2 Zn(aminophen)$_2$, ♦ Zn: L = 1:3 Zn(aminophen)$_3$ and ● aminophen ligand.

We propose that the following equilibrium takes place in solution, upon dissolution of the Zn(aminophen)$_2$(NO$_3$)$_2$:

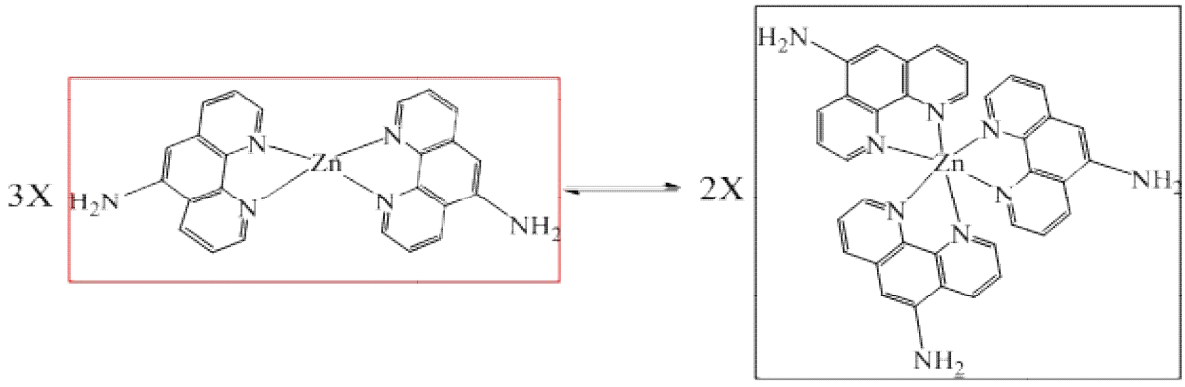

Scheme 12 Chemical equilibrium of Zn(aminophen)$_2$ (1:2) in solution with another 1:3 species in CD_3OD solution at room temperature

The ^{1}H and ^{13}C NMR spectra of Mephen ligand and $Zn(Mephen)_2$ complex were also measured in CD_3OD at room temperature (see **Figure 13** and **Figure 14**). The ^{1}H NMR spectrum of Mephen ligand showed aromatic proton peaks in the range 7.53- 8.87 ppm and aliphatic ones at 2.27 ppm. The ^{13}C NMR spectra of this ligand also showed aromatic carbon peaks in the range of 123.28-150.32 ppm and aliphatic carbons at 18.91 ppm. On the other hand, the ^{1}H NMR spectra of $Zn(Mephen)_2$ showed aromatic proton peaks in the range 7.70- 8.97 ppm and aliphatic ones in the range 2.92-2.97 ppm. And also, the ^{13}C NMR spectra of this complex showed aromatic and aliphatic carbon peaks in the range of 124.83-152.46 and 19.26 ppm, respectively. Again, downfield shifts are observed for both the protons and carbons' chemical shift of the Mephen moiety in the ^{1}H and ^{13}C NMR spectra of the $Zn(Mephen)_2$ complex, indicating the formation of a complex of Mephen with Zn (II) ion through the aromatic ring nitrogen atoms.

a)

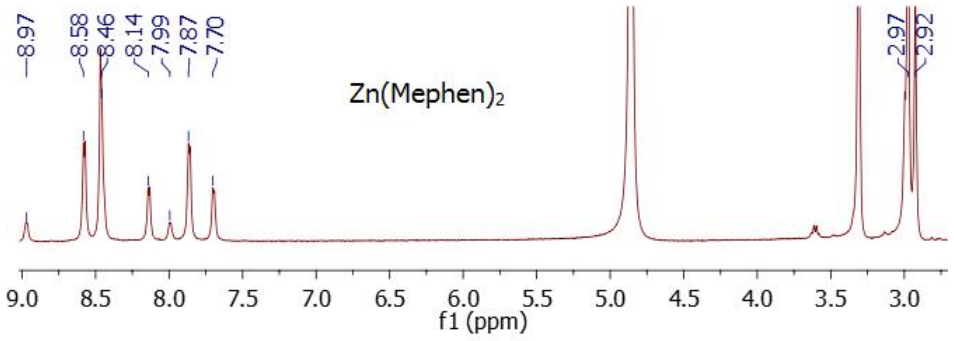

b)

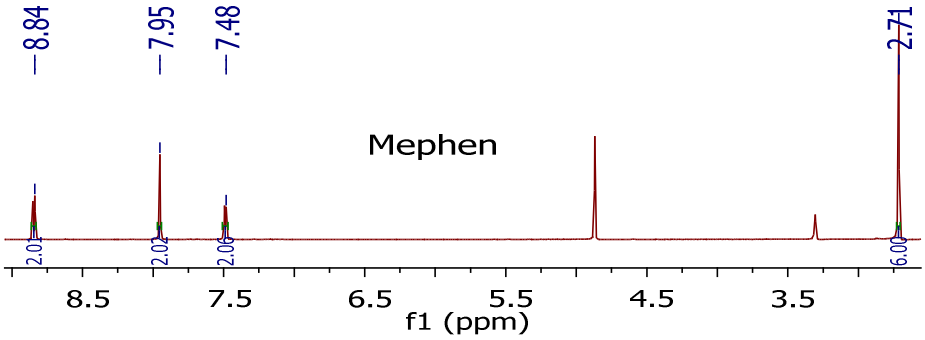

Figure 13 The ^{1}H NMR spectra of $Zn(Mephen)_2$ (**a**) and Mephen (**b**) in CD_3OD at room temperature

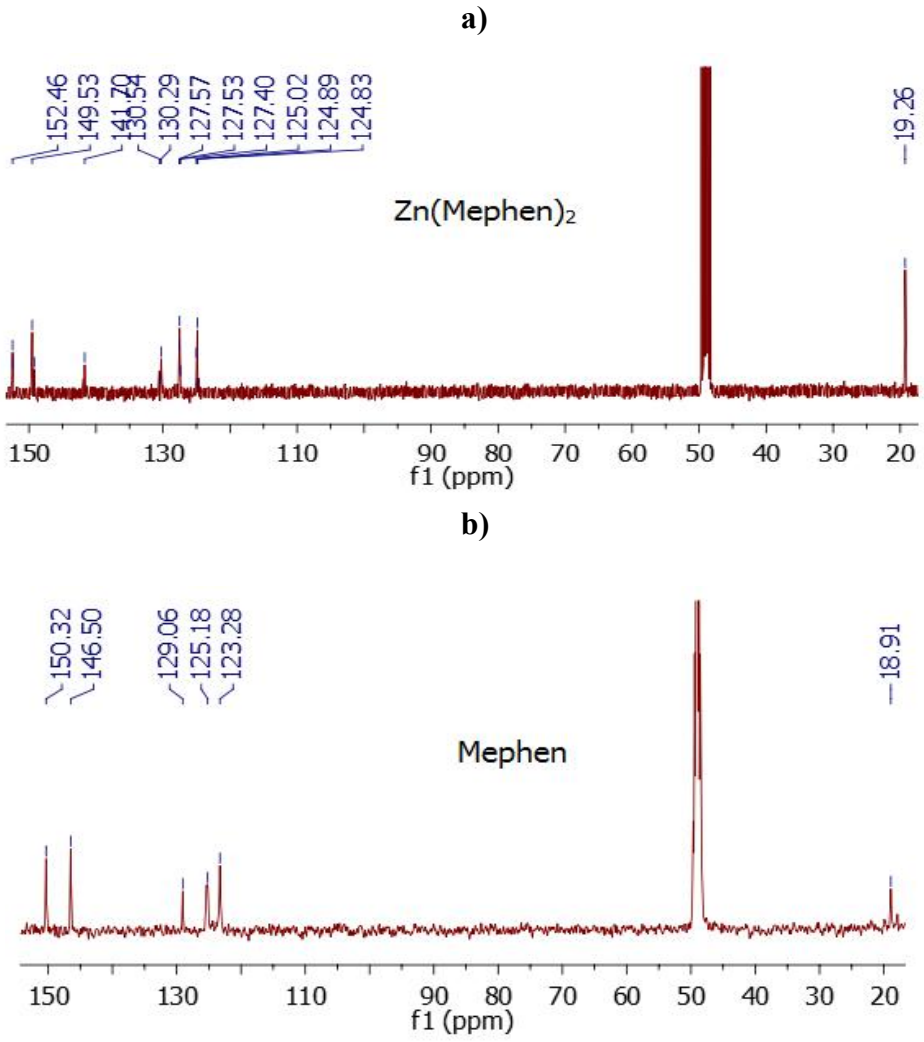

Figure 14 The ^{13}C NMR spectra of $Zn(Mephen)_2$ (**a**) and MePhen (**b**) in CD_3OD at room temperature

Again, due to formation of more than one species in solution, probably involving ligand exchange, additional proton and carbon peaks appeared in the NMR spectra of the complex. For this reason, it was difficult to make the assignment and ^1H NMR titration of $Zn(NO_3)_2 \bullet 4H_2O$ with Mephen was performed to get insight into the complexation behavior.

A75 mM solution of $Zn(NO_3)_2 \bullet 4H_2O$ in 0.7 ml CD_3OD was prepared. 20.4 µl of TMS (internal reference) and 31.24 mg of Mephen were mixed and dissolved in 2 ml of CD_3OD to prepare a solution with the same concentration (75 mM) of each compound. Then, the ^1H NMR spectra of the mixtures of $Zn(NO_3)_2$ and Mephen at different Zn to Mephen mole ratios: 0:1 (0:500 µl); 1:1 (250:250 µl); 1:2 (200:400 µl); 1:3 (120:370 µl) and 1:4 (100:400 µl) were recorded (see **Figure**

15). The ^{1}H NMR spectroscopic titration of the zinc ion with Mephen proved the assumption that there was formation of species with different stoichiometries in solution.

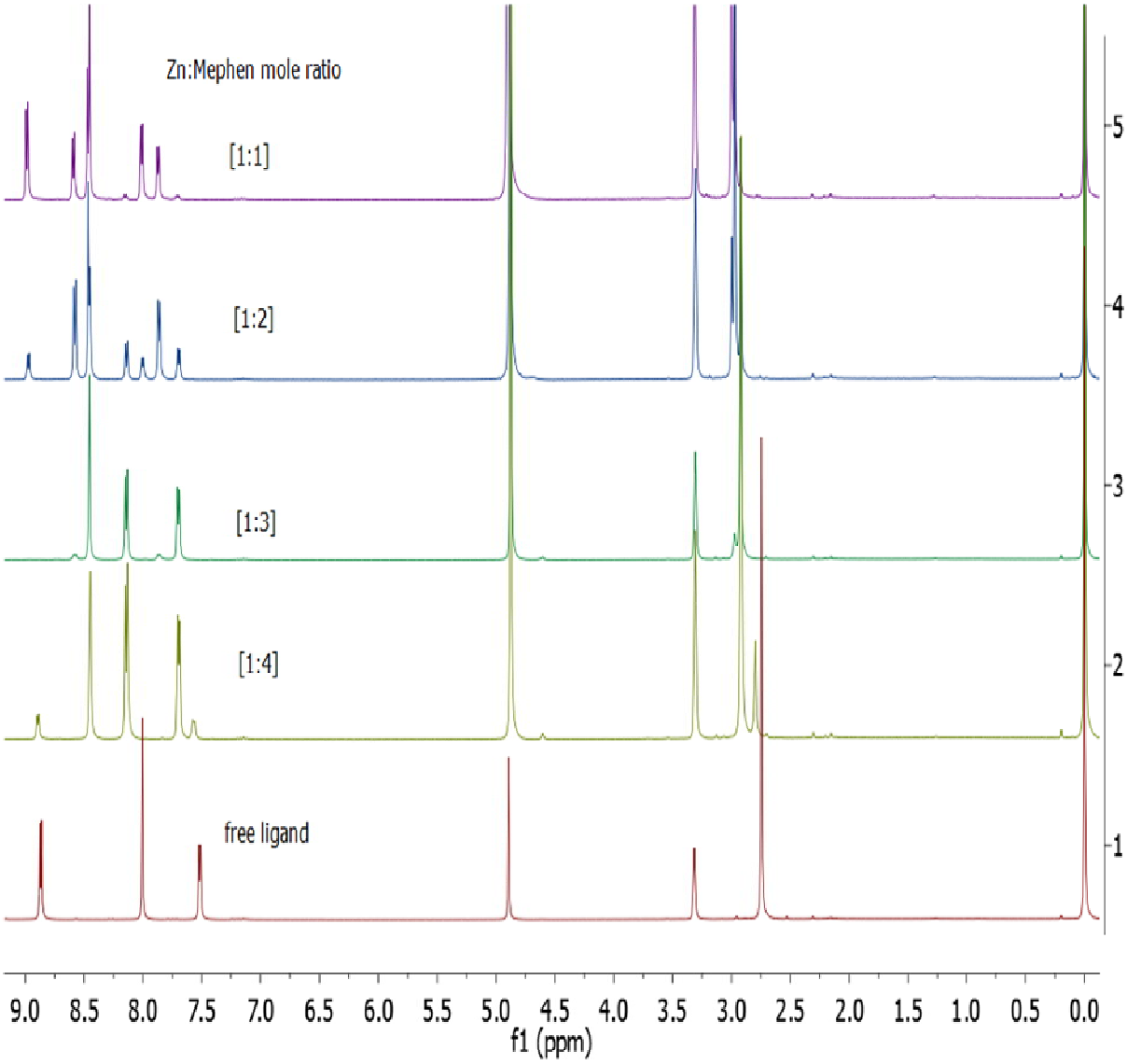

Figure 15 ^{1}H NMR spectra of the reaction mixture of $Zn(NO_3)_2 \bullet 4H_2O$ and Mephen solution at different Zn to Mephen mole ratios in CD_3OD at room temperature

a)

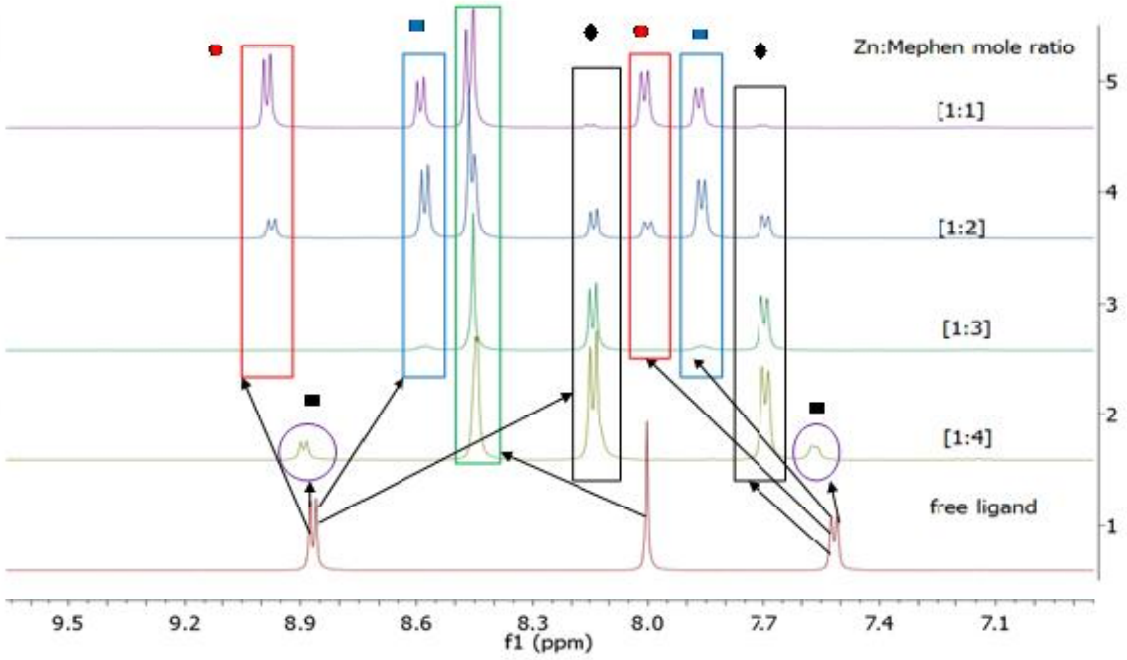

b)

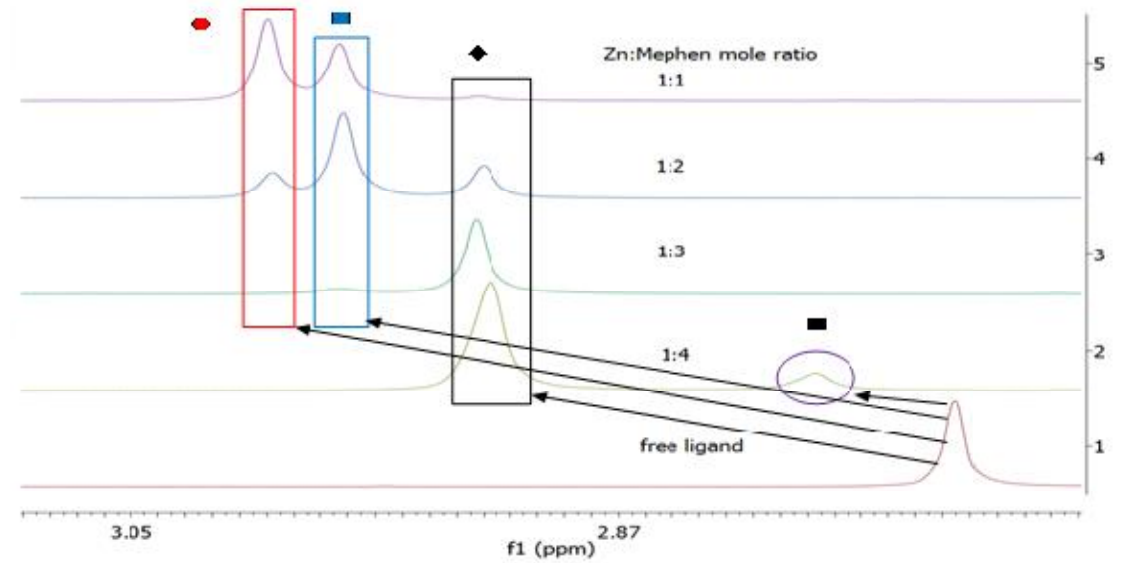

Figure 16 ^{1}H NMR spectra of aromatic (a) and aliphatic (b) regions of the reaction mixture of $Zn(NO_3)$•$4H_2O$ and Mephen at different mole ratios in CD_3OD at room temperature where ● stands for Zn:L=1:1 Zn(Mephen), ■Zn:L = 1:2 $Zn(Mephen)_2$, ♦ Zn:L =1:3 $Zn(Mephen)_3$ and ■ free Mephen ligand.

As can be seen from observation of the spectra in **Figure 16**, upon addition of Mephen ligand the intensity of the initial aromatic and aliphatic proton peaks decreases whereas new peaks are formed. The intensity of the newly formed peaks increases as the amount of added ligand increases. This indicates that the trend of species formation is 1:1→1:2 →1:3 upon the addition of Mephen ligand, as is expected. Therefore, it can be understood that the Zn $(Mephen)_2$ complex will give another 1:1 and 1:3 species in solution and the equilibrium is described as follows.

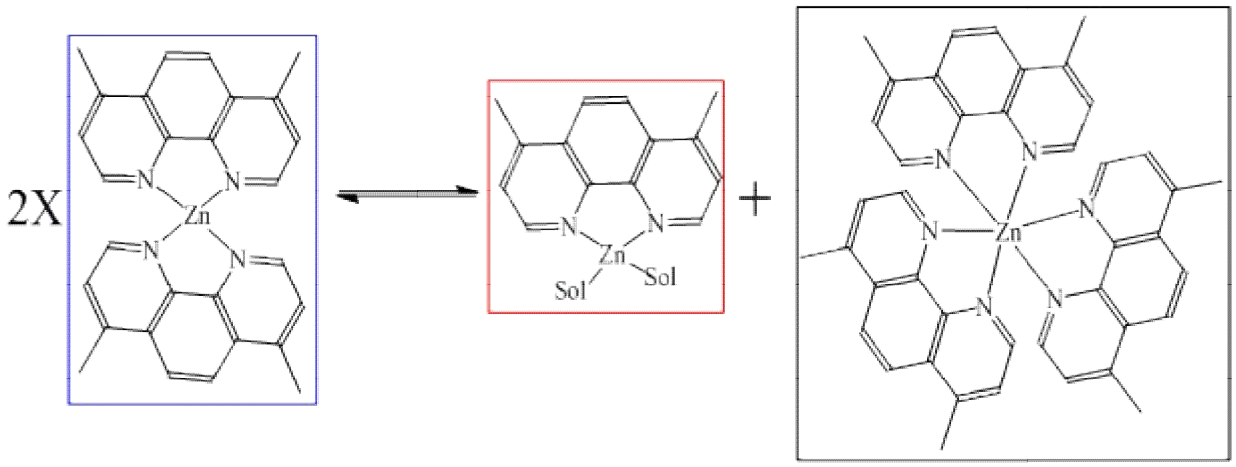

Scheme 13 Chemical equilibrium of Zn $(Mephen)_2$ with two other species (1:1 and 1:3 species) in CD_3OD at room temperature. Sol = solvent molecule

Therefore we can conclude that upon dissolution of the solid complex three species are present in solution corresponding to Zn:L molar ratios of 1:1, 1:2 and 1:3.

3.1.2. Stability

Analysis of biological systems requires work under aqueous conditions. Thus, knowing the complexes' speciation and their characteristics in aqueous solution is very important. It is necessary to ensure that the complexes do not precipitate in the aqueous environment (at physiological pH), and that they are stable (not hydrolyzed) in the timescale of the studies [**66**,**76**].

The stability of $Zn(phen)_2$, $Zn(aminophen)_2$ and $Zn(Mephen)_2$ complexes was evaluated with UV-Vis, fluorescence and NMR spectroscopies in PBS buffered solutions (at physiological pH) containing 5 % of DMSO, which is essential to solubilize the metal complexes. Phosphate

buffer saline (PBS) was chosen due to its composition, since the ion concentrations of the solution match those of the human body.

As it can be seen in **Figure 17**, the UV-Vis absorption intensity and shape of the spectra of the zinc complexes in 5 % DMSO and 95 % PBS did not show significant changes for 24 h, except a slight increase in the absorption intensity for $Zn(phen)_2$ and $Zn(Mephen)_2$. Therefore, it can be assumed that the zinc complexes are stable enough in the physiological environment to undergo the necessary reactions required for bioactivity.

a)

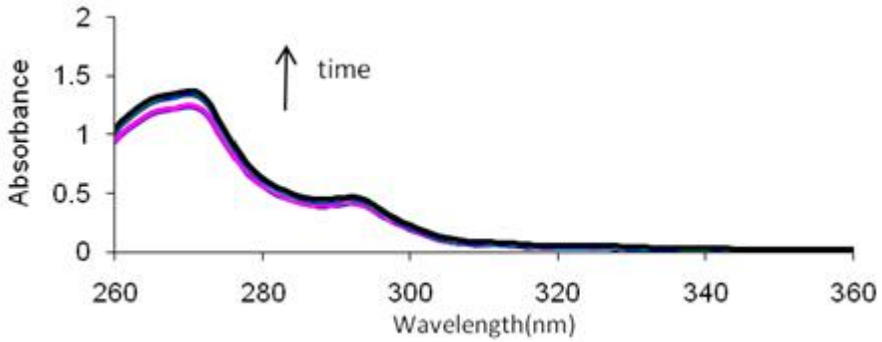

b)

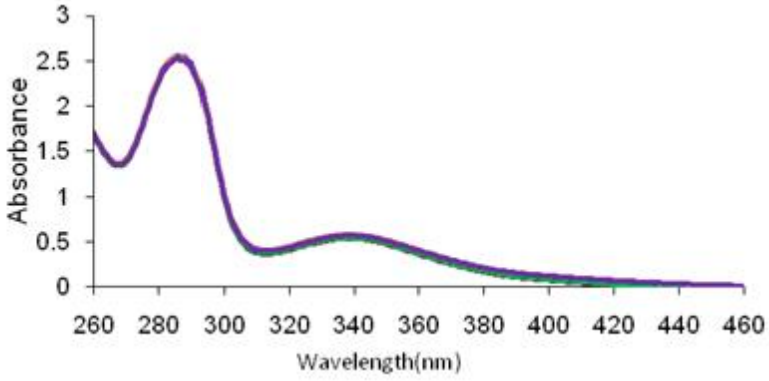

c)

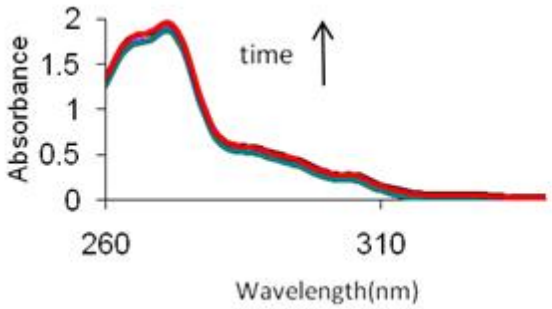

Figure 17 UV-Vis absorption spectra of 50 µM $Zn(phen)_2$ (**a**), 50 µM $Zn(aminophen)_2$ (**b**) and 25 µM $Zn(Mephen)_2$ (**c**) with increasing time (t_0, 5 min, 10 min, 20 min, 30 min, 1 h, 2 h; 3 h, 4 h and 24 h) in 5 % DMSO and 95 % PBS.

The stability of the complexes was also evaluated by fluorescence spectroscopy and the emission spectra are depicted in **Figure 18**. The emission intensity of $Zn(phen)_2$ slightly increased at 3 h. On the other hand, the emission intensity of $Zn(aminophen)_2$ and $Zn(Mephen)_2$ showed a slight decrease through time. However, the shape of the emission spectra for all of complexes did not show any changes. Once again the stability of the complexes is corroborated.

a)

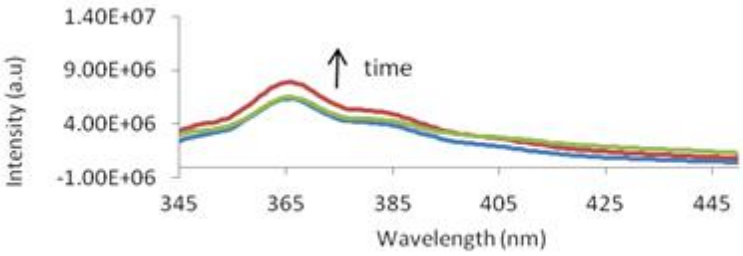

b)

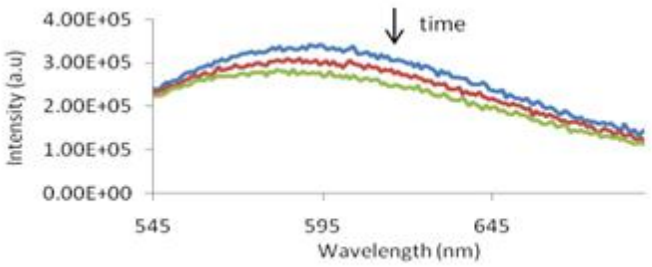

c)

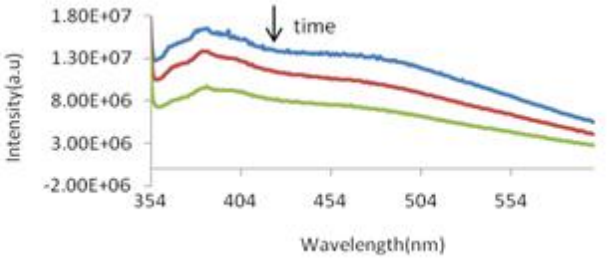

Figure 18 Fluorescence emission spectra of 25 µM $Zn(phen)_2$ (a), $Zn(aminophen)_2$ (b) and $Zn(Mephen)_2$ (c) with increasing time (t_0 , 3 h, 72 h) in 5 % DMSO and 95 % PBS.

The stability study by NMR was also carried out for $Zn[(phen)_2(NO_3)_2]\bullet 2H_2O$ only. A phosphate buffer solution with pH 7.54 was prepared in 1 ml of D_2O. 12.5 mg $Zn(aminophen)_2$ was dissolved in 250 µl of DMSO-d_6. Then, 20 µl of the $Zn(aminophen)_2$ DMSO-d_6 solution was mixed with 380 µl of the phosphate buffer solution which contain 5 % DMSO and 95 % PBS. Then, the stability of the compound was studied for 24 h by monitoring the ^{1}H NMR spectra.

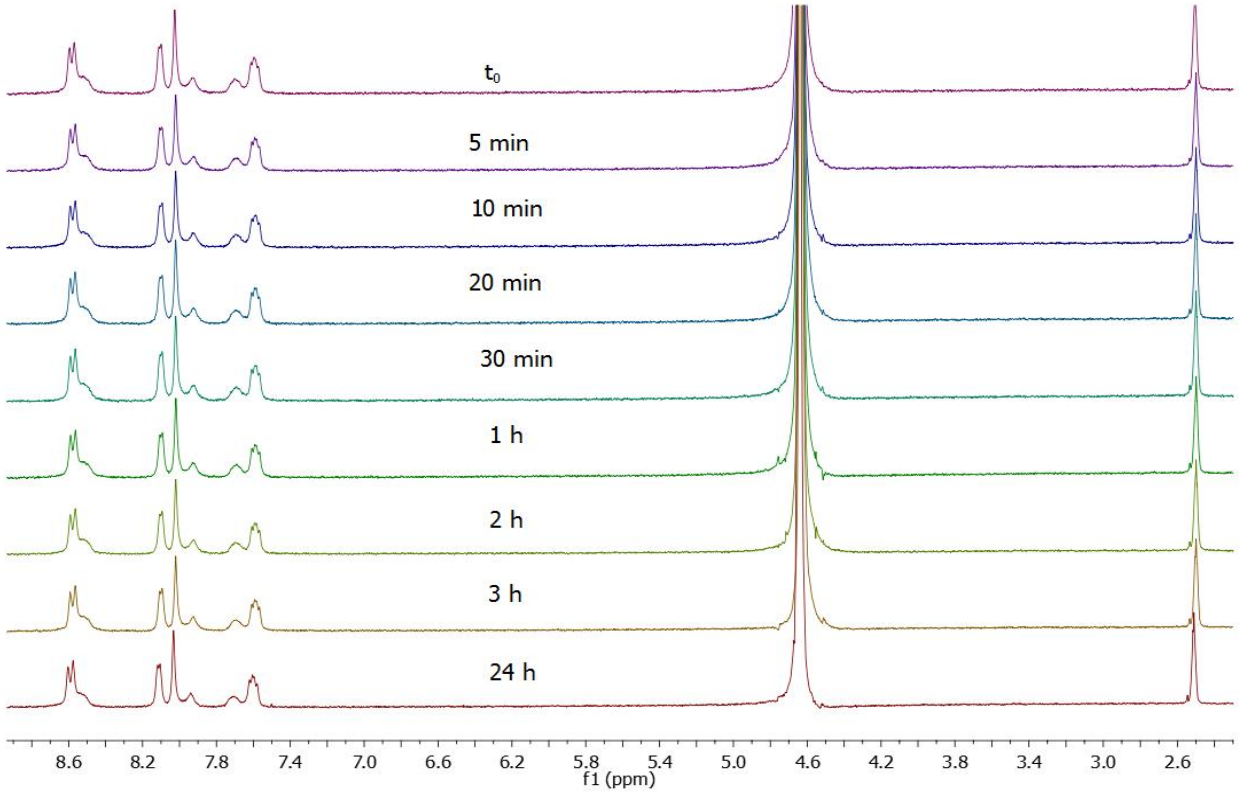

Figure 19 ^{1}H NMR spectra of $Zn[(phen)_2$in DMSO-d_6 : D_2O (5%:95 %) over 24 h.

The ^{1}H NMR spectra of $Zn(phen)_2$ show that the compound is stable in solution, with no hydrolysis and no precipitate formation observed over a period of 24 h.

3.1.3. Antioxidant activity

As it is described in the experimental section, radical and reactive oxygen species (ROS) are related with many diseases [**54**]. Thus, evaluating the antioxidant activity of the compounds is very important, since it may be a key to understanding their biological activity. The antioxidant activities of the $Zn(Rphen)_2$ complexes was evaluated with a widely used free radical scavenging method which uses DPPH (2,2-diphenyl-1-picrylhydrazyl) [**55**,**67**].

The detailed procedure followed is described in the experimental section. The absorption spectra of the mixture of the test compounds and DPPH in different mole ratios were scanned between 300 and 700 nm. Then, by following the intensity trend at 516 nm, it was possible to evaluate the free radical scavenging ability of the tested compounds. None of the compounds showed antioxidant activity as it can be seen in **Figure 20** for $Zn(phen)_2$, as an example.

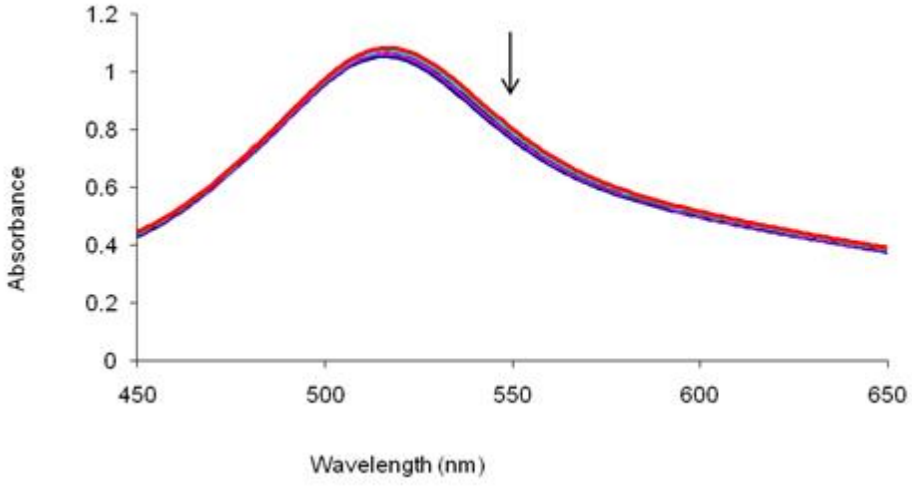

Figure 20 UV-Vis absorption spectra measured for solutions containing DPPH (73 μM in MeOH) and different % (n / n) of $Zn(phen)_2$. (↓) indicates decreasing intensity with increasing nCompound / nDPPH mole ratio (0.00 %, 25.81 %, 49.27 %, 75.07 %, 100.88 %).

3.1.4. DNA binding ability

The DNA binding ability of the compounds was also evaluated. DNA is an important drug target because it regulates many biochemical processes that occur in the cellular system [**5**,**58**]. Thus, since the Zn-phenanthroline complexes contain large aromatic systems that can potentially bind DNA through intercalation, their binding ability was evaluated. The studied complexes are fluorescent and, thus a direct fluorescence method was used. That means that titration of the complex (at constant concentration) with ctDNA was carried out.

The fluorescence emission spectra intensity increased for $Zn(aminophen)_2$ and slightly decreased for $Zn(phen)_2$ and $Zn(Mephen)_2$ as the concentration of ctDNA increased (**Figure 21**). This confirms that there is an interaction between the test compounds and DNA, which should involve different mechanisms for the aminophen complex and the other two [**48**,**63**].

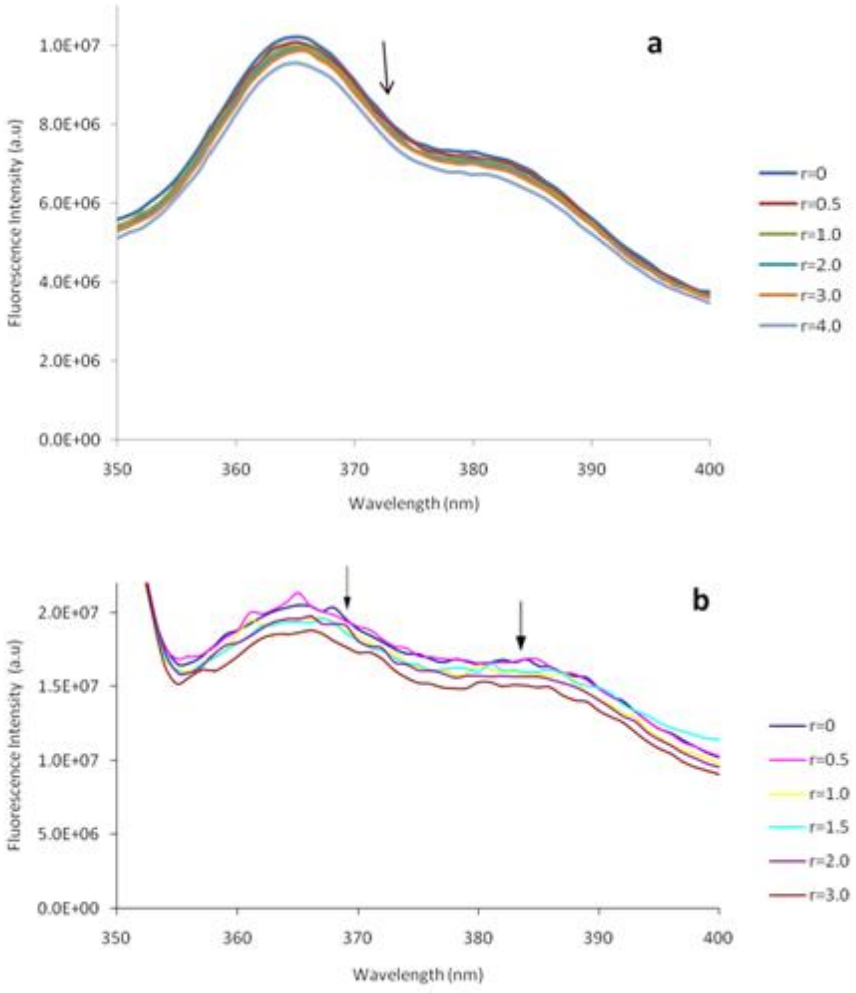

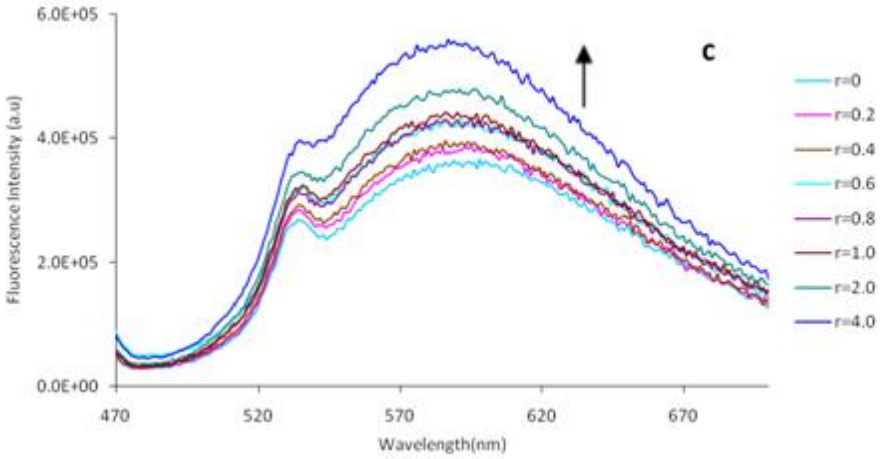

Figure 21 Fluorescence spectral changes of 25 μM $Zn(phen)_2$ (**a**), $Zn(Mephen)_2$ (**b**) and $Zn(aminophen)_2$ (**c**) on the titration of increasing amounts of ctDNA (r= [DNA] / [Complex]) in 5 % DMSO and 95 % PBS (λex (nm) = 326 (**a**), 345 (**b**), 450 (**c**)):Arrows (↓) and (↑), refers decreasing and increasing of the fluorescence intensity respectively.

The fluorescence quenching and enhancing ability of the compounds can be evaluated by classical Stern–Volmer equation 1 [**65**] and equation 2 [**48**] respectively. The Stern Volmer plot obtained for $Zn(aminophen)_2$ is included in **Figure 22**. The Stern-Volmer enhancement constant obtained is 8.1×10^3 M^{-1}. The fluorescence enhancement suggests that upon interaction of the complex with DNA the complex becomes more protected from deactivation by the polar water molecules. Several mechanisms may be involved but the differences found for the three complexes suggest that intercalation in between the base pairs should not be acting. This would surely lead to fluorescence enhancement, which does not happen with two of the studied complexes. So we propose a nonintercalative docking of the complexes within the minor/major groove. Additionally, the amino group might be involved in hydrogen bonds with the phosphate groups. Further studies should be done to better understand the mechanisms involved and the differences found for the 3 complexes.

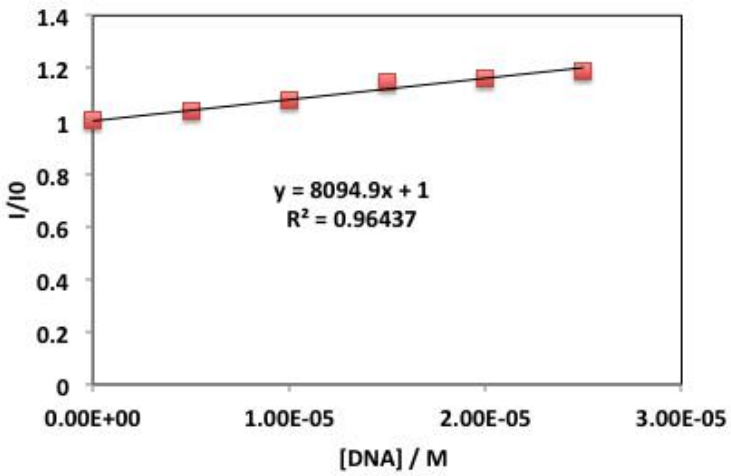

Figure 22 Stern – Volmer plot for Zn(aminophen)$_2$. λ_{em} = 589 nm

3.2. S-methyl dithiocarbazate derived Schiff base ligands and their corresponding zinc complexes

3.2.1. Characterization

The analytical data for the percentage of carbon, hydrogen, nitrogen and sulfur in all the studied S-methyl dithiocarbazate Schiff base ligands and their zinc complexes were in a good agreement with that of the calculated values for the proposed structures (**Table 7**). We propose that the Zn(II) ion is tetra coordinated with the ligands coordinated to the metal ion through the phenolate oxygen, the imine nitrogen and the sulfur atom from the dithiocarbazate, and either a water molecule or an acetate ion occupies the 4th position of the tetrahedron.

The S-methyl dithiocarbazate Schiff base ligands can be involved in tautomeric equilibrium between the thiol and the thione forms (see **Scheme 14**). The analysis suggest that in the solid state the ligands are in the thione form and in most complexes (except Zn(PySmdt)) the ligands are coordinated with the sulphur in the thiol form (see also the FTIR section).

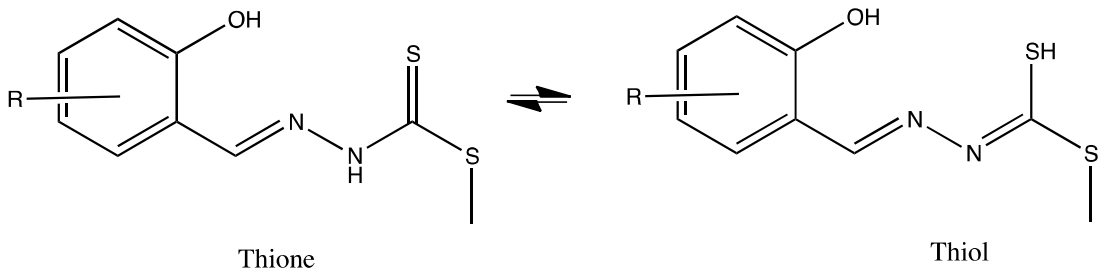

Scheme 14 The tautomeric equilibrium of the S-methyl thiocarabazate Schiff bases

Table 7: The elemental data of S-methyl dithiocarbazate derived Schiff base ligands and their zinc(II) complexes

Compound	Elemental analysis calculated (found) (%)			
	C	H	N	S
SalSmdt	47.77 (47.6)	4.45 (4.3)	12.38 (12.3)	28.33 (28.8)
$Mp(Smdt)_2$	41.91 (42.0)	4.33 (4.4)	15.04 (14.7)	34.42 (34.2)
VanSmdt	46.53 (46.1)	4.76 (4.5)	10.85 (10.8)	24.84 (25.4)
PySmdt	44.26 (44.0)	4.83 (4.8)	15.49 (15.4)	23.63 (24.3)
$Zn[(SalSmdt)(H_2O)]\bullet 0.5H_2O$	33.75 (34.0)	3.59 (3.0)	8.75 (8.4)	20.02 (19.6)
$Zn_2[(Mp(Smdt)_2)(CH_3COO)]$	32.21 (32.2)	2.88 (3.3)	10.02 (9.9)	22.93 (21.7)
$Zn[(VanSmdt)(H_2O)]$	35.56 (35.2)	3.58 (2.5)	8.29 (7.7)	18.99 (19.4)
$Zn[(PySmdt)(CH_3COO)]\bullet 1.5H_2O$	34.45 (34.9)	4.24 (4.0)	10.04 (9.4)	15.33 (14.6)

The studied compounds were characterized by UV-Vis absorption spectroscopy and their electronic spectra in DMSO at room temperature are depicted in **Figure 23**. The electronic spectrum of $Mp(Smdt)_2$ shows absorption bands at 310 and 330 nm which may be attributed to $\pi\rightarrow\pi^*$ transitions of the aromatic ring; 344 nm assigned to $\pi\rightarrow\pi^*$ transition of azomethine moiety and 383 nm with 394 nm (shoulder) attributed to $n\rightarrow\pi^*$ of groups containing lone pair of electrons. In the spectrum of the $Zn_2[(Mp(Smdt)_2)(CH_3COO)]$ complex, the absorption band of

the azomethine group shifted to 349 nm and the bands due to groups with lone pair of electrons disappeared. Whereas, a new band at 432 nm appeared which is due to ligand to metal charge transfer (LMCT) from the phenolate to the Zn ion. Similarly, in all other zinc(II) complexes the LMCT band is present at ca. 430 nm, and the intraligand bands are less intense and blue shifted. This might be due to increased planarity of the ligand upon coordination to the metal ion, which might increase the overall conjugation of the ligand system.

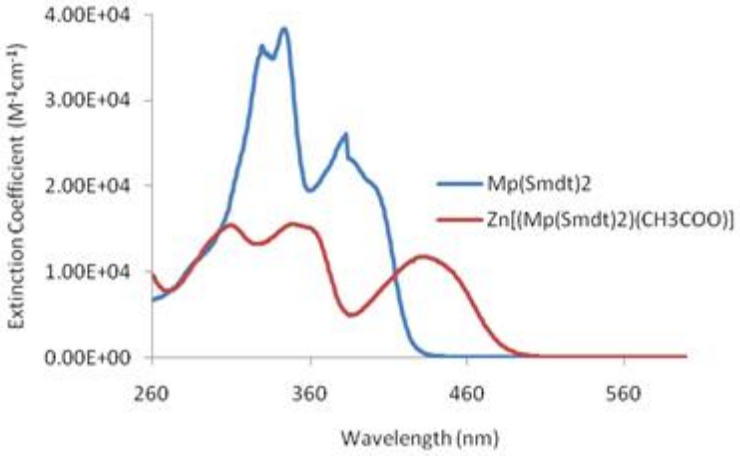

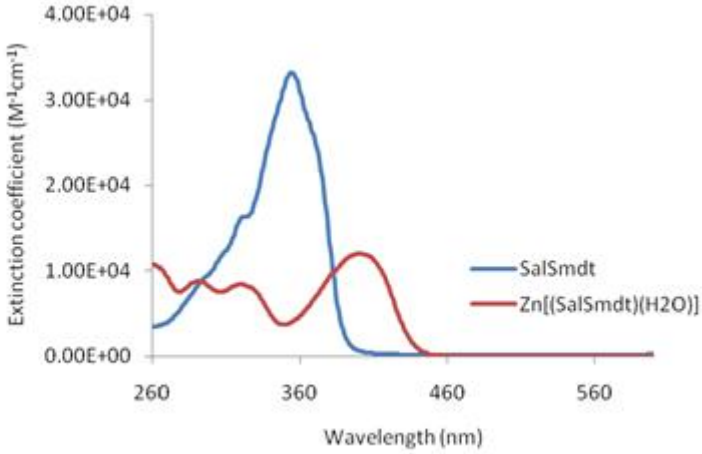

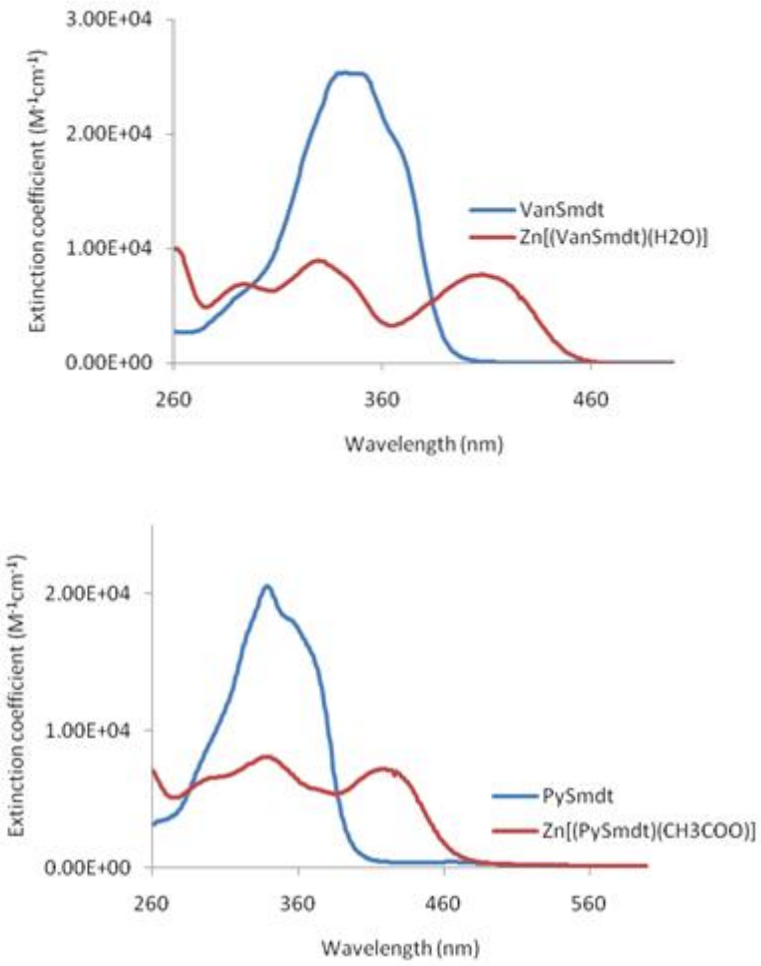

Figure 23 UV-Visible absorption spectra for S-methyl dithiocarbazate derived Schiff base ligands and their zinc(II) complexes in DMSO at room temperature

The compounds were also characterized by ESI-MS and the data is included in Table 8. The molecular peaks of all ligands were identified in both positive and negative mode ESI-MS spectra. Moreover, other peaks of both the ligands and complexes were detected in the spectra which all are supporting evidence for the proposed structures of compounds.

Table 8: Assignment of ESI-MS peaks for S-methyl dithiocarbazate derived Schiff base ligands and their zinc(II) complexes

Compound	Species	m/z	
		Theoretical	Found
SalSmdt	$(L+H)^+$	227.03	227.0 (18%)
	$(L-H)^-$	225.01	225.3 (100%)

$Mp(Smdt)_2$	$(L+H)^+$	373.02	372.9 (12%)
	$(L-H)^-$	371.01	371.3 (83%)
	$(2L-H)^-$	743.03	742.7 (100%)
VanSmdt	$(L+H)^+$	257.04	257.0 (25%)
	$(L-H)^-$	255.02	255.1 (100%)
PySmdt	$(L+H)^+$	272.05	272.0 (100%)
	$(L-H)^-$	270.03	270.2 (100%)
	$(2L-H)^-$	541.07	540.7 (49%)
$Zn[(SalSmdt)(H_2O)]$	$(ML+2CH_3OH-H_2O+H)^+$	353.00	352.5 (100%)
	$(2ML-H)^-$	610.89	611.1 (100%)
$Zn_2[(Mp(Smdt)_2)(CH_3COO)]$	$(ML+CH_3OH)^-$	587.87	588.0 (60%)
$Zn[(VanSmdt)(H_2O)]$	$(2ML + H_2O-H)^-$	670.91	670.85 (100%)
$Zn[(PySmdt)(CH_3COO)]$	$(ML-CH_3COO)^+$	333.97	334.1 (100%)
	$(ML+H_2O+H)^+$	412.00	411.6 (80%)
	$(ML-H)^-$	392.00	392.21 (13%)

The IR analysis result of the S-methyl dithiocarbazate derived Schiff base ligands were also compared with that of their corresponding zinc complexes which is used as supporting evidence for the formation of the complexes. The infrared bands of the characteristic groups of the ligands and their complexes together with their assignments are listed in **Table 9** [**77**]. The assignments were done based on reported values [**25**,**30**,**32**]. The IR spectra of the Schiff base ligands show bands of NH and OH in the range of 3357-2435 and 3103-3178 cm^{-1} respectively. The bands for azomethine group (C=N) and C=S appeared in the range of 1612-1617 and 967-1073 cm^{-1} respectively. None of the compounds exhibited any band at ca. 2700 due to S-H, so all data corroborate that all ligands are in the thione form in the solid state. On the other hand, the bands for OH group in the complexes appear in the range of 3315-3427 cm^{-1}, due to coordinated water molecules. The NH and C=S bands are absent in the spectra of all the complexes due to the coordination of the ligands to the metal ion through the azomethine and thiol groups respectively.

In the IR spectra of the complexes, bands appearing between 1593-1613 cm^{-1} are assigned to stretching vibration of the C=N moiety, showing shifts when compared to that of the corresponding ligands. The new C-S bands appearing at 952-1034 cm^{-1} can be used as evidence for the formation of the complexes, and coordination of the ligand as the thiol tautomer. Other new bands appeared at1460 cm^{-1} and 1375 cm^{-1} in the $Zn_2[(Mp(Smdt)_2)(CH_3COO)]$ spectra and at 1493 cm^{-1} and 1304 cm^{-1} in the $Zn[(PySmdt)(CH_3COO)]\bullet 1.5H_2O$ spectra, corresponding to asymmetric (COO)asy and symmetric $(COO)_{sym}$, which confirm coordination of the acetate ion [**77**].

Table 9: IR spectral assignments (cm^{-1}) of S-methyl dithiocarbazate derived Schiff base ligands and their corresponding zinc(II) complexes

Compound	V(cm^{-1})						
	O-H	N-H	C=N	C=S	C-S	$(COO)_{asy}$	$(COO)_{sym}$
SalSmdt	3435	3111	1616	967	-	-	-
$Mp(Smdt)_2$	3433	3103	1617	1039	-	-	-
VanSmdt	3416	3178	1616	1073	-	-	-
PySmdt	2930-3357		1612	1047	-	-	-
$Zn[(SalSmdt)(H_2O)]\bullet 0.5H_2O$	3315 - 3667	-	1593	-	952	-	-
$Zn_2[(Mp(Smdt)_2)(CH_3COO)]$	-	-	1613	-	1000	1460	1375
$Zn[(VanSmdt)(H_2O)]$	3427	-	1597	-	1034	-	-
$Zn[(PySmdt)(CH_3COO)]\bullet 1.5H_2O$	3417	-	-	1597	1022	1493	1304

The compounds were also characterized by NMR spectroscopy. The spectra of ligands and their corresponding zinc complexes were recorded at room temperature in acetone-d6 (SalSmdt, VanSmdt and their complexes) and in DMSO-d_6 ($Mp(Smdt)_2$, PySmdt and their complexes). The chemical shift of protons and carbons for both ligands and complexes are described in detail in the experimental part. In this section, only the ^1H and ^{13}C NMR spectral data of selected groups are presented in **Table 10.** The aromatic protons and carbons of the ligands were observed in the range 6.90-8.81 ppm and 114.86-156.72 ppm, respectively. In their zinc

complexes, the chemical shift of these protons and carbons were found between 6.39-7.43 ppm and 113.17-165.1 ppm, respectively. $Mp(Smdt)_2$ and PySmdt showed characteristic proton signals at 2.30 and 2.42 ppm, respectively, attributed to the methyl (CH_3) moiety (a substituent on the aromatic group). In their corresponding complexes, these protons were observed at 2.24 ppm ($Zn_2[(Mp(Smdt)_2)(CH_3COO)]$) and 2.39 ppm ($Zn[(PySmdt)(CH_3COO)]$). The carbon signals of this group were found at 19.79 ppm ($Mp(Smdt)_2$) and 19.18 ppm (PySmdt). In the spectra of their complexes, the carbon signals of this methyl group appeared at 19.36 ppm ($Zn_2[(Mp(Smdt)_2)(CH_3COO)]$) and 21.35 ppm ($Zn[(PySmdt)(CH_3COO)]$). The proton signals observed at 3.87 ppm in VanSmdt and 3.72 ppm in $Zn[(VanSmdt)(H_2O)]$ are attributed to the methoxy (OCH_3) group. The carbon signals of this methoxy group were displayed at 56.49 ppm and 55.65 ppm for VanSmdt and $Zn[(VanSmdt)(H_2O)]$, respectively. The proton and carbon signals of Ar-CH_2 in PySmdt were observed at 4.63 ppm and 59.21 ppm, respectively. In its corresponding complex ($Zn[(PySmdt)(CH_3COO)]$) the proton and carbon signals of this group were found at 4.51 ppm and 59.51 ppm respectively.

The ligands showed proton and carbon signals between 2.57-2.65 ppm and 16.80-17.52 ppm, respectively, which are attributed to S-CH_3. The proton and carbon signals of this group in the complexes shift upfield to 2.41-2.44 ppm and 14.13-14.46 ppm, respectively. This indicates that the sulfur atom of the thione group is coordinated to the metal ion. Other distinctive signals appeared between 8.04-8.56 ppm in the ligands, attributed to -CH=N group and shifted downfield to 8.55-8.92 ppm in their corresponding zinc complexes. The signals of the carbon of this group also shifted downfield from 138.73-149.36 ppm in the ligands to 155.82-161.29ppm, in the complexes. In addition, proton signals appearing in the ligands between 12.25-13.74 ppm which are attributed to NH (from the dithiocarbazate) group, disappeared in their corresponding complexes except in $Zn[(PySmdt)(CH_3COO)]$, where it appears at 11.97 ppm. Besides this, in this complex there are other evidences that coordination is through NH-C=S (the thione tautomer), instead of $N=C-S^-$ (the thiol tautomer, see p.e. the elemental analysis and FTIR). Proton signals appearing in the ligand's spectra between 9.65-10.81 ppm are attributed to OH (Ar-OH) group, and disappear in their corresponding zinc complexes, indicating that the ligands are coordinated to the metal ion through the phenolate group. In general, the chemical shift values and type of coordination are in agreement with that of previously reported values for similar compounds [**25**,**30**,**32**,**78**].

Table 10: Selected ^{1}H and ^{13}C NMR spectral data for ligands and complexes

Compound	^{1}H NMR chemical shift, δ (ppm)				^{13}C NMR chemical shift, δ (ppm)	
	SCH_3	HC=N	NH	Ar-OH	SCH_3	HC=N
SalSmdt	2.65	8.52	12.25	10.24	17.52	149.36
$Mp(Smdt)_2$	2.57	8.52	13.51	10.81	16.80	144.75
VanSmdt	2.63	8.56	13.34	9.65	17.18	148.74
PySmdt	2.61	8.04	13.74	10.61	17.12	138.73
$Zn[(SalSmdt)(H_2O)]$	2.44	8.73	-	-	14.46	161.29
$Zn_2[(Mp(Smdt)_2)(CH_3COO)]$	2.43	8.69	-	-	13.95	159.64
$Zn[(VanSmdt)(H_2O)]$	2.41	8.55	-	-	14.17	159.84
$Zn[(PySmdt)(CH_3COO)]$	2.44	8.92	11.97	-	14.13	155.82

3.2.2. Stability

Evaluation of the stability of all S-methyl dithiocarbazate derived Schiff base ligands and their zinc(II) complexes under investigation was carried out using UV-Visible spectrophotometry in aqueous solution (5 % DMSO and 95 % PBS), except for $Zn_2[(Mp(Smdt)_2)(CH_3COO)]$ which was done only in DMSO (because of solubility problem) at room temperature. The UV-Visible absorption spectra (260-500 nm) were recorded and monitored for 24 h for ligands and 48 h for complexes of which the detailed procedure is described in the experimental part. The shape of the spectra of the ligands and zinc complexes did not show any change as it is depicted in **Figure 24.** The UV-Vis absorption intensity of these compounds also did not show significant changes in the first 3 h. Only small intensity changes were observed for longer periods, probably due to precipitation (not detected by visual inspection). Therefore, it can be concluded that the Schiff base ligands and their zinc(II) complexes are reasonably stable in aqueous physiological conditions.

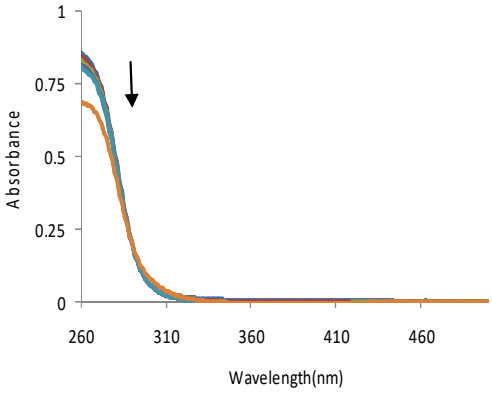
Absorbance
1
0.75
0.5
0.25
0
260
310
360
410
460
Wavelength(nm)

(a)

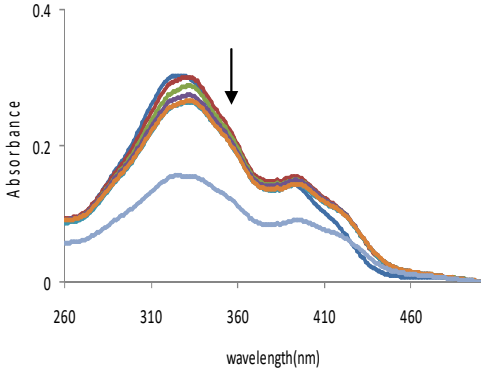
Absorbance
0.4
0.2
0
260
310
360
410
460
wavelength(nm)

(b)

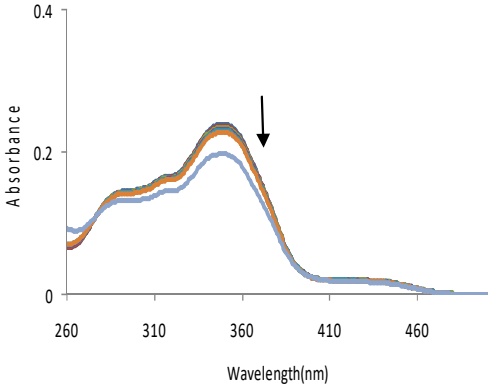
Absorbance
0.4
0.2
0
260
310
360
410
460
Wavelength(nm)

(c)

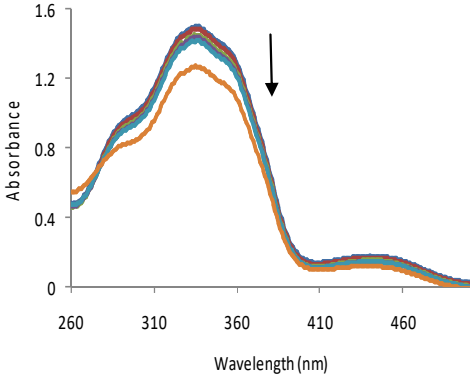
Absorbance
1.6
1.2
0.8
0.4
0
260
310
360
410
460
Wavelength (nm)

(d)

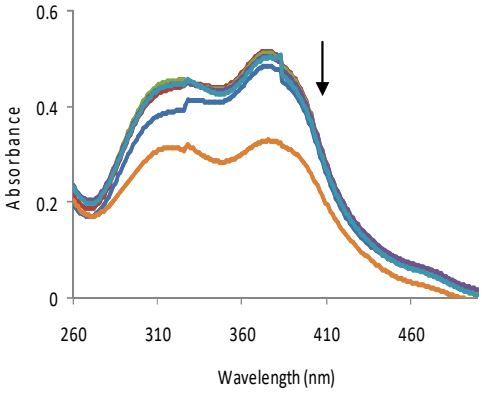
Absorbance
0.6
0.4
0.2
0
260
310
360
410
460
Wavelength (nm)

(e)

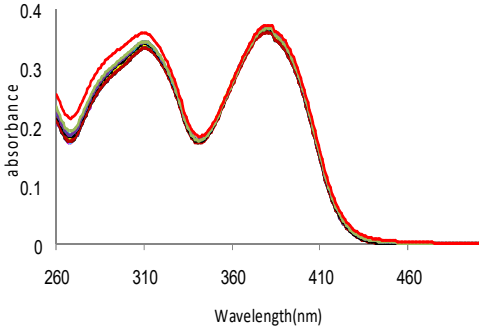
absorbance
0.4
0.3
0.2
0.1
0
260
310
360
410
460
Wavelength(nm)

(f)

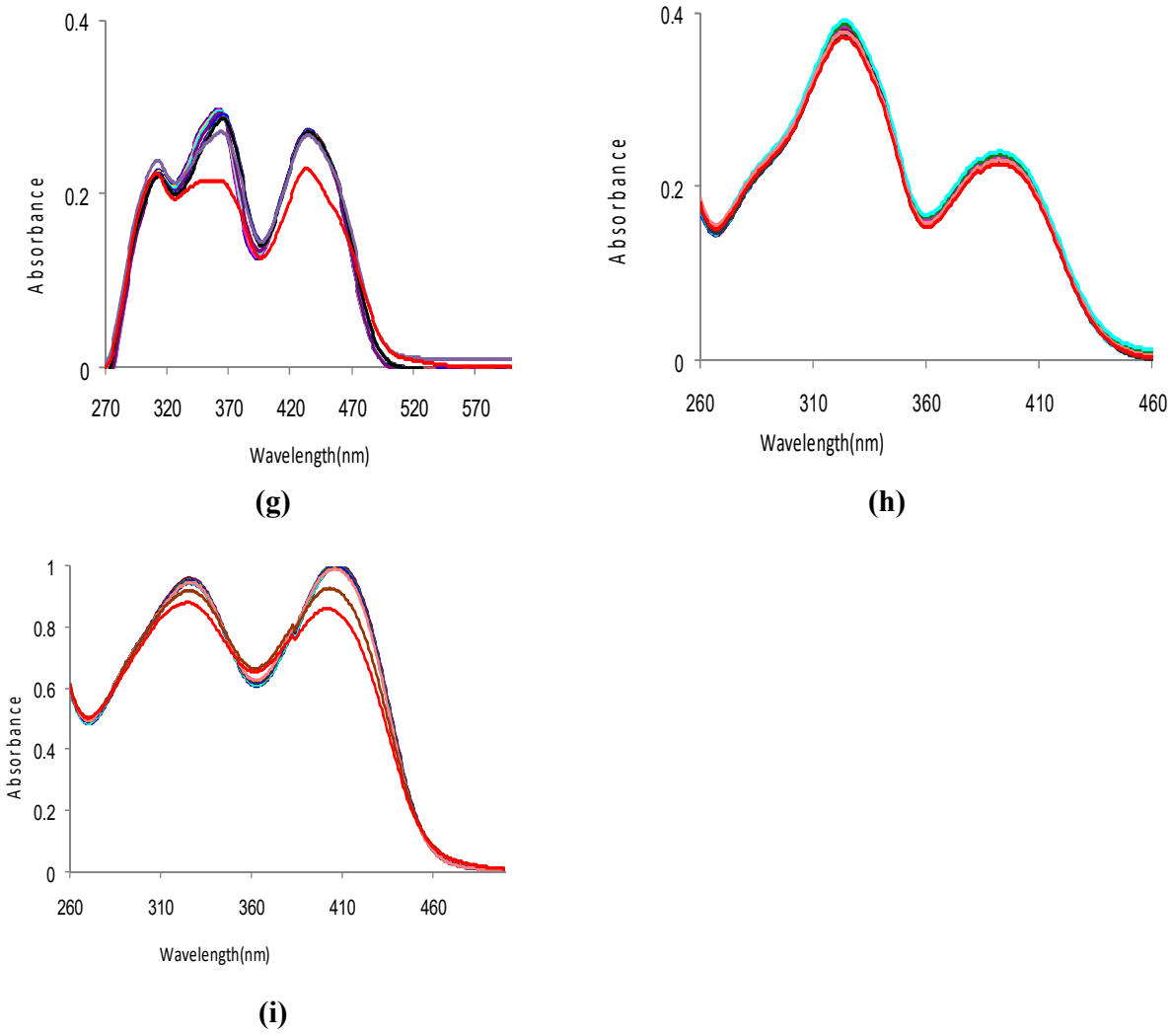

Figure 24 UV-Vis absorption spectra of solutions containing 100 µM Smdt (**a**), 12.5 µM $Mp(Smdt)_2$ (**b**), 12.5 µM SalSmdt (**c**), 100 µM VanSmdt (**d**), 12.5 µM PySmdt (**e**) 25 µM $Zn[(SalSmdt)(H_2O)]$ (f), 25 µM $Zn_2[(Mp(Smdt)_2)(CH_3COO)]$ (**g**), 25 µM $Zn[(VanSmdt)(H_2O)]$ (**h**) and 100 µM $Zn[(PySmdt)(CH_3COO)]$ (**i**) with increasing time (t_0, 30 min, 2 h, 3 h, 4 h and 24 h for ligands; and t_0, 5 min, 10 min, 20 min, 30 min, 1 h, 2 h; 3 h, 4 h , 24 h and 48 h for complexes) in 5% DMSO and 95 % PBS but (g) in DMSO only.

The stability of the S-methyl dithiocarbazate derived Schiff base ligands and their corresponding zinc complexes was further evaluated using RP-HPLC at room temperature. The RP-HPLC analysis was carried out using the procedure described in the experimental section in detail. The

chromatograms of SalSmdt and VanSmdt showed only a single peak corresponding to the Schiff base ligands no peaks corresponding to hydrolysis products being observed (p.e. salicylaldehyde and smdt, or *o*-vanillin and smdt, respectively). The Zn[(SalSmdt)(H_2O)] and Zn[(VanSmdt)(H_2O)] also showed a single peak corresponding to the zinc complexes as it is depicted in **Figure 25**. The retention times for the ligands and complexes are similar and therefore determined by the ligand interactions with the stationary and mobile phases. The chromatogram of Mp($Smdt)_2$ showed three peaks, which may be attributed to the starting compound Smdt, the expected ligand itself and other hydrolyzed species, possibly the "mono" Schiff base. In the chromatogram of PySmdt, two peaks were observed corresponding to the starting compound Smdt and the ligand itself. The chromatograms of the Zn_2[(Mp($Smdt)_2$)(CH_3COO)] and Zn[(PySmdt)(CH_3COO)] showed two peaks each corresponding to the complex and other dissociated species. In conclusion, the appearance of one single peak indicates that the compounds are stable but those, which showed two or three peaks are not stable under these chromatographic conditions.

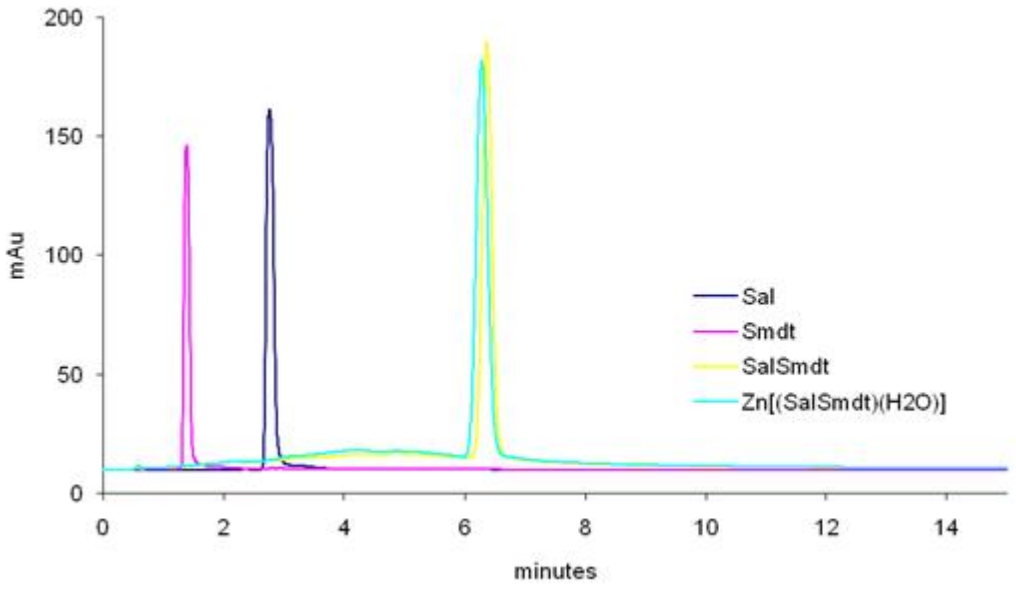

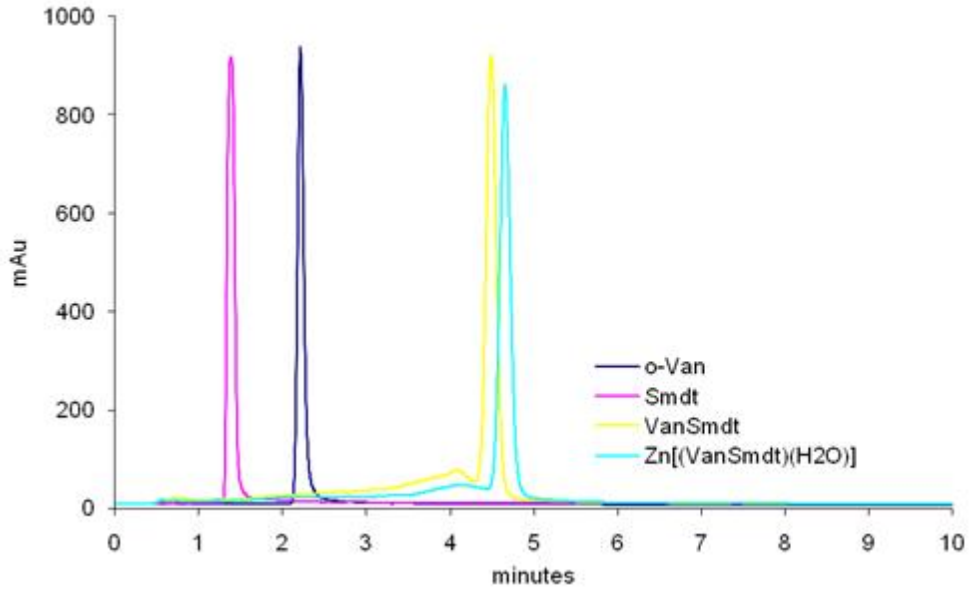

Figure 25 RP-HPLC chromatograms of reagents, S-methyl dithiocarbazate derived Schiff base ligands and their zinc complexes, eluted with 50% CH_3CN: 50% H_2O at a flow rate of 1 ml / min.

3.2.3. Antioxidant activity

The antioxidant activity of the S-methyl dithiocarbazate derived Schiff base ligands and their corresponding zinc complexes were also evaluated by the DPPH scavenging assay, following the procedure described in the experimental section. The absorption spectra of the mixtures of the test compounds and DPPH in different molar ratios were scanned between 300 and 700 nm. Then, by following the absorption intensity trend at 516 nm, it was possible to evaluate the free radical scavenging ability of the test compounds using **Equation 3**. Moreover, the values for IC_{50} were determined by a linear regression where the % of scavenging activity is 50 and compared with the IC_{50} value of ascorbic acid (the positive control).

All the spectra measured with solutions containing the studied Schiff base ligands showed a decrease in the absorption intensity at 516 nm **(Figure 26)** but their corresponding zinc complexes, except Zn[(PySmdt)(CH_3COO)], do not show any significant decrease. The IC_{50} values of the Schiff base ligands and their corresponding zinc complexes, along with ascorbic acid are presented in **Table 11**.

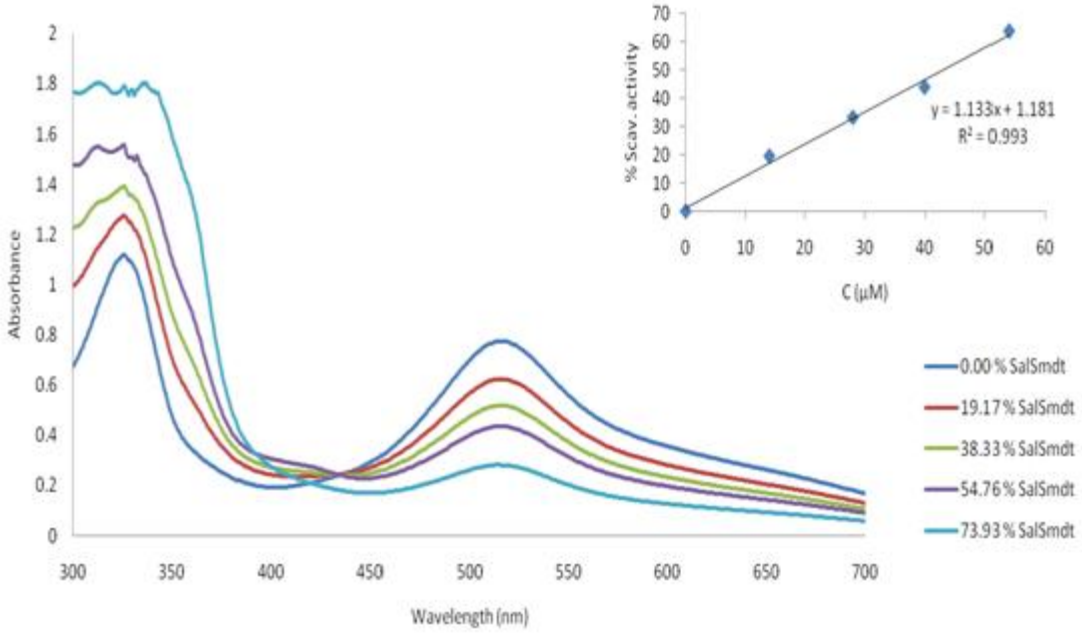
Absorbance
Wavelength (nm)
% Scav. activity
C (µM)
y = 1.133x + 1.181
R² = 0.993
0.00 % SalSmdt
19.17 % SalSmdt
38.33 % SalSmdt
54.76 % SalSmdt
73.93 % SalSmdt

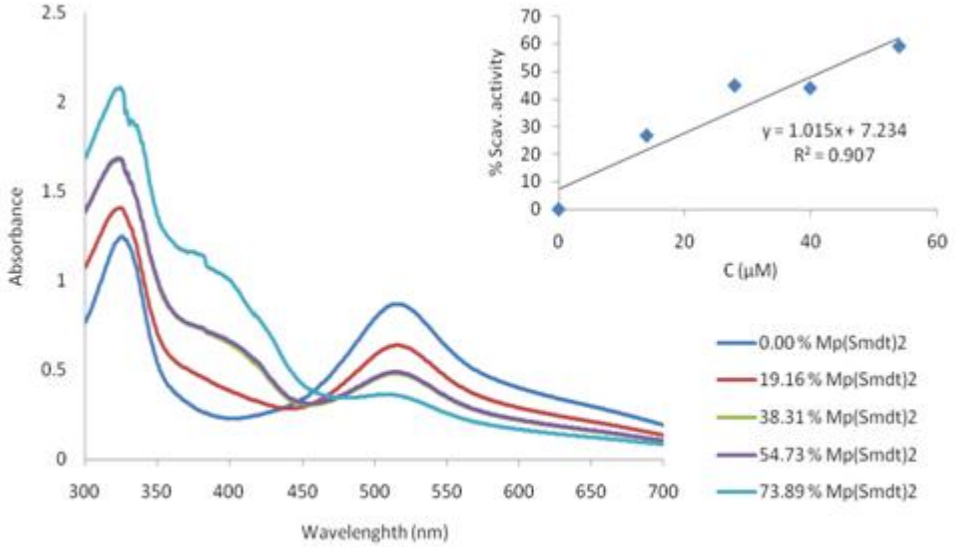
Absorbance
Wavelenghth (nm)
% Scav. activity
C (µM)
y = 1.015x + 7.234
R² = 0.907
0.00 % Mp(Smdt)2
19.16 % Mp(Smdt)2
38.31 % Mp(Smdt)2
54.73 % Mp(Smdt)2
73.89 % Mp(Smdt)2

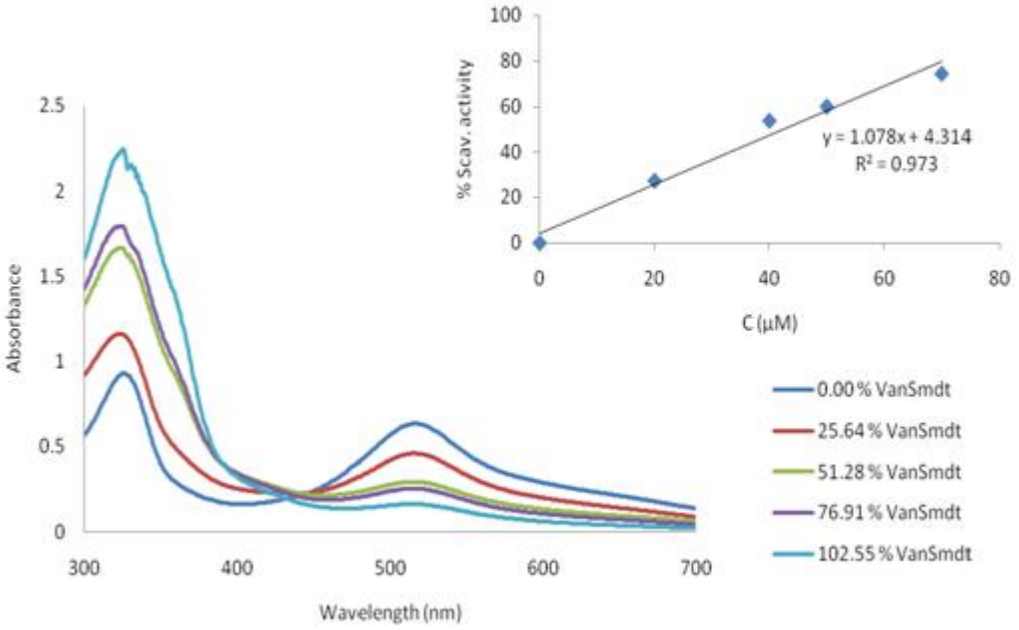
Absorbance
Wavelength (nm)
% Scav. activity
C (μM)
y = 1.078x + 4.314
R² = 0.973
0.00 % VanSmdt
25.64 % VanSmdt
51.28 % VanSmdt
76.91 % VanSmdt
102.55 % VanSmdt

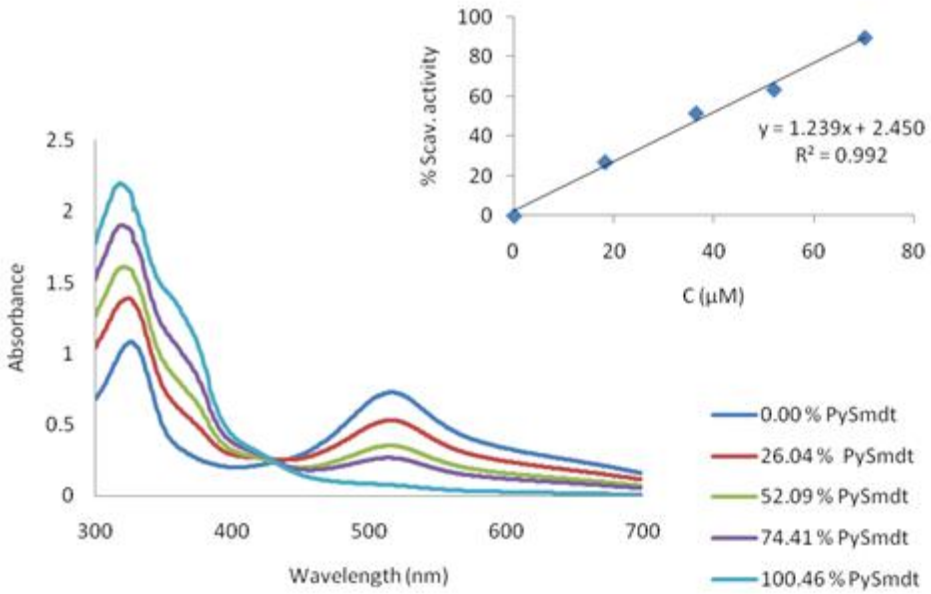
Absorbance
Wavelength (nm)
% Scav. activity
C (μM)
y = 1.239x + 2.450
R² = 0.992
0.00 % PySmdt
26.04 % PySmdt
52.09 % PySmdt
74.41 % PySmdt
100.46 % PySmdt

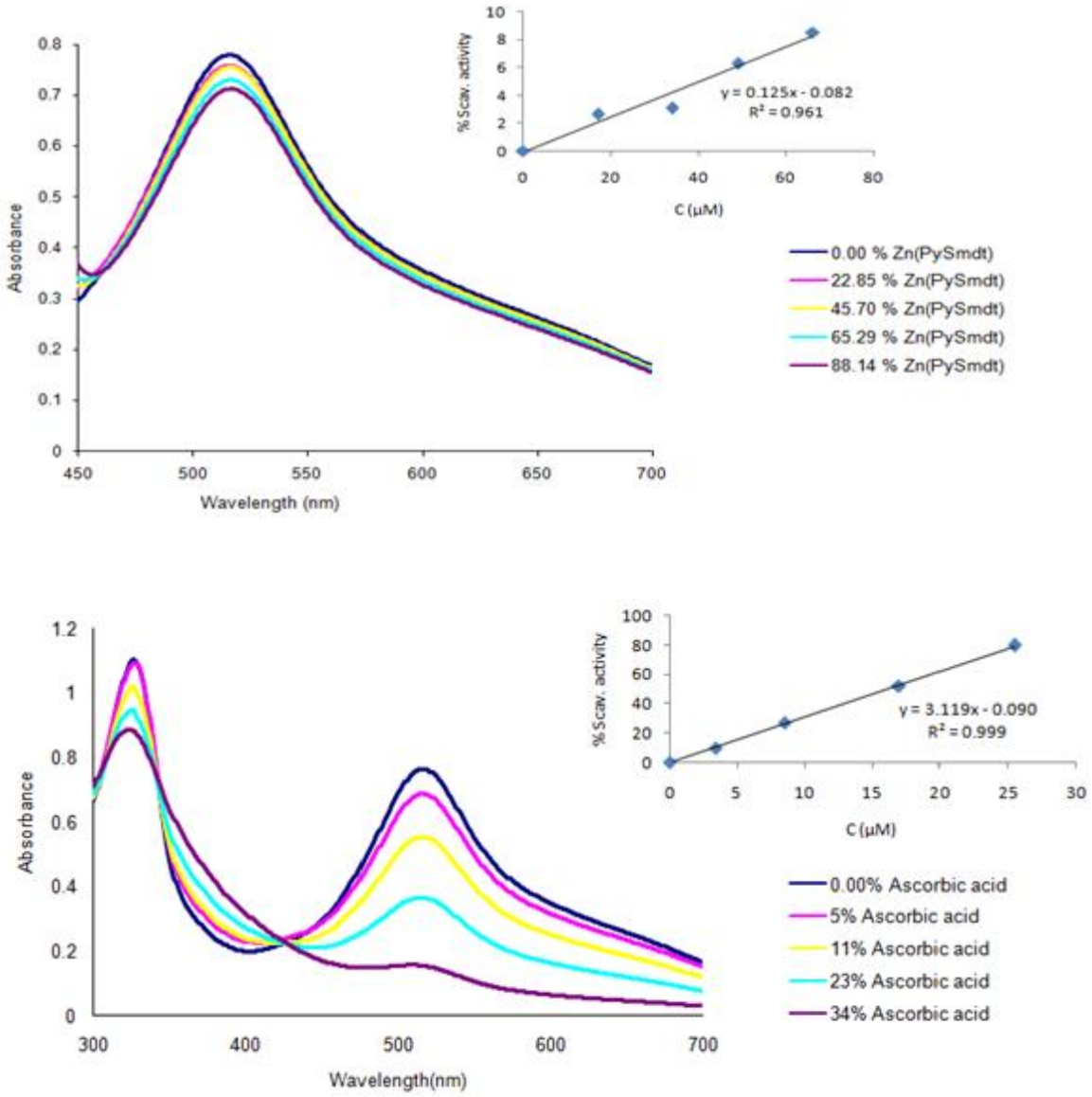

Figure 26 UV-Vis absorption spectra measured for solutions containing DPPH (67-75 μM in MeOH) and different % (n(compound) / n(DPPH)) of compounds. Inset: Linear regression of % scavenging activity vs. [compounds] for the DPPH assay, from which the IC_{50} values were obtained

Table 11: IC_{50} values and molar ratio of compound to DPPH obtained from the DPPH assays for the synthesized S-methyl dithiocarbazate derived Schiff base ligands, their zinc(II) complexes and ascorbic acid

Compound	IC_{50} (μM)	n(comp) / n(DPPH)
SalSmdt	43.1	0.59
$Mp(Smdt)_2$	42.1	0.58
VanSmdt	42.4	1.51
PySmdt	38.4	1.37
$Zn[(SalSmdt)(H_2O)]$	na	na
$Zn_2[(Mp(Smdt)_2)(CH_3COO)]$	na	na
$Zn[(VanSmdt)(H_2O)]$	na	na
$Zn[(PySmdt))(CH_3COO)]$	400.7	5.33
Ascorbic acid	16.1	0.21

'na'-no antioxidant activity

From the results it can be concluded that, the presence of phenol substituents on the aromatic ring enabled the ligands to have free radical scavenging activity. This is the reason why a considerable increase in the percent of scavenging activity was found with increasing concentration of the S-methyl dithiocarbazate derived Schiff base ligands. But in the complexes, this phenol group is unavailable since it is coordinated to zinc ion. Because of this reason, the zinc complexes, except $Zn[(PySmdt))(CH_3COO)]$ did not show any free radical scavenging activity. All the IC_{50} values of the compounds, which showed scavenging activity, are greater than the IC_{50} value of the control (ascorbic acid). Hardly any differences are found among the ligands with different substituents in the aromatic moiety.

3.2.4. Phosphatase activity studies

The phosphatase activity of the zinc complexes of the S-methyl dithiocarbazate Schiff bases was also evaluated using the disodium salt of (4-nitrophenyl) phosphate hexahydrate (PNPP) as monophosphate ester substrate, following the procedure described in the experimental section. None of the compounds showed an increase in UV-visible absorption between 400-430 nm, which in turn indicates that they do not have any phosphatase activity. As an example, the spectra measured for $Zn_2[Mp(smdt)_2]$ are shown in **Figure 27.**

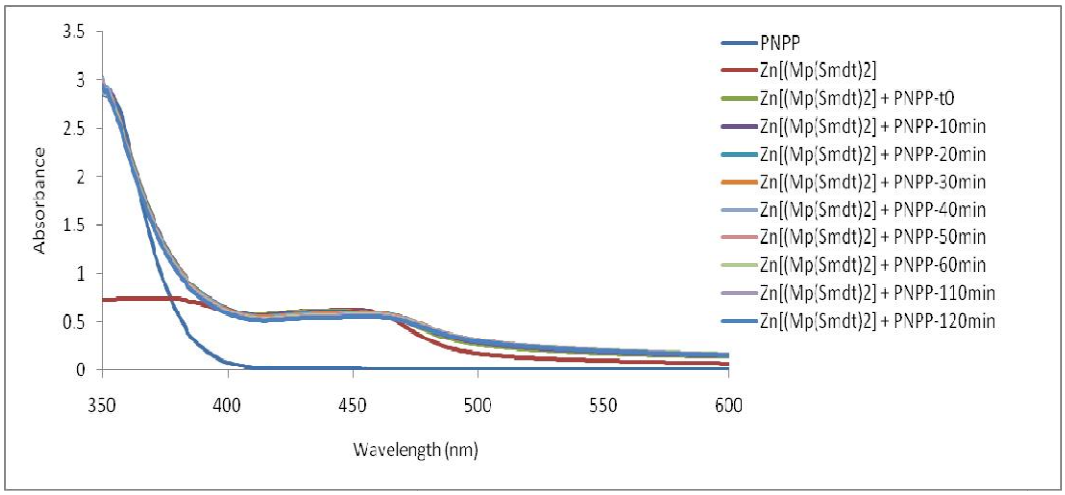

Figure 27 Wavelength scan for the hydrolysis of PNPP in the absence and presence of $Zn_2[(Mp(Smdt)_2)(CH_3COO)]$ in PBS recorded at 25 ^oC at an interval f 10 minutes for 120 minutes. [PNPP] = 0.5 mM, [Complex] =0.05 mM.

3.3. Cytotoxicity studies

The cytotoxicity of the Schiff bases was evaluated on human PC-3, MCF-7 and CACO-2 cancer cells. The evaluation was also done for 5-fluorouracil (5-FU, the positive control) for comparative purposes. The antiproliferative effects of the Schiff bases were determined by the MTT assay at incubation period of 48 h for all cell lines. The IC_{50} values were calculated by sigmoidal fitting considering 95 % confidence interval and are presented in **Table 12.** The data shown are representative of at least two independent experiments.

Table 12: Estimated IC_{50} values (μM) for all compounds in PC-3, MCF-7 and CACO-2 cells.

Compound	PC-3		MCF-7		CACO-2	
	IC_{50}	R^2	IC_{50}	R^2	IC_{50}	R^2
SalSmdt	4.41	0.99	-	-	-	-
$Mp(Smdt)_2$	9.73	0.98	14.94	1	12.58	1
VanSmdt	28.99	0.99	-	-	22.12	0.99
PySmdt	>100	-	-	-	-	-
5-FU	3.30	1	4.93	0.99	0.82	0.99

The cytotoxicity effect of Zn(II)(Rphen) complexes was also evaluated on human A2780 ovarian cancer cell line using MTT assay at different incubation periods and compared with that of their corresponding ligands. The cytotoxicity of the compounds is presented in **Table 13.**

Table 13: Estimated IC_{50} values (μM) for Zn(II)(Rphen) complexes compared to IC_{50} values of their corresponding ligands on A2780 cell line

Compound	3h	24h	48h
$Zn(phen)_2$	>100	103±59.5	2.40±1.3
$Zn(Mephen)_2$	121±68.2	22.9±16.5	0.19±0.08
$Zn(aminophen)_2$	61.6±23.6	33.4±16.7	0.75±0.13
phen	>100	134±62	5.84±2.3
Mephen	37.4±8.1	14.0±5.1	1.42±0.41
aminophen	>100	40.6±29.4	1.84±0.56

As it can be seen from the above tables, all the Schiff bases, with the exception of PySmdt (IC_{50} > 100 μM) have shown cytotoxicity effect on the tested cell lines with IC_{50} values ranging from 4.41 to 28.99 μM after 48 h. The salicylaldehyde Schiff base, SalSmdt shows an IC_{50} value on the μM range against the PC-3 cell line, comparable with the one obtained for the positive control, 5-fluorouracil. The antiproliferative studies with the Zn-complexes are currently ongoing.

Similarly, $Zn(Rphen)_2$ complexes have shown cytotoxicity effect on the human ovarian carcinoma cell line, A2780, with the IC_{50} values ranging from 0.19 to 2.4 μM after 48 h. The phenanthroline ligands have also shown cytotoxicity effect on the same cell line with IC_{50} values ranging from 1.42 to 5.84 μM. However, taking into consideration that each metal complex contains two ligands coordinated to the metal ion, and that the ligands itself are cytotoxic, for a synergistic effect to take place the IC_{50} value of the complexes should be at least half of the respective ligand. This is what happens at longer time intervals (48h).

In general, the cytotoxicity effect of both the Schiff bases and the zinc(II) complexes with phenanthroline ligands on tested cancer cells is promising and can be used as basis for further studies.

4. Conclusion

In the current work four new S-methyl dithiocarbazate Schiff base derived ligands were synthesized: SalSmdt, $Mp(Smdt)_2$, VanSmdt and PySmdt; and four corresponding Zn(II) complexes: $Zn[(SalSmdt)(H_2O)]\bullet 0.5H_2O$, $Zn_2[(Mp(Smdt)_2)(CH_3COO)]$, $Zn[(VanSmdt)(H_2O)]$ and $Zn[(PySmdt)(CH_3COO)]\bullet 1.5H_2O$. Three zinc(II) complexes: $Zn[(phen)_2(NO_3)_2]\bullet 2H_2O$, $Zn[(aminophen)_2(NO_3)_2]\bullet 1.5H_2O$ and $Zn[(Mephen)_2(NO_3)_2]\bullet 3.5H_2O$ were also developed by reaction of $Zn(NO_3)_2\bullet 4H_2O$ with commercially available phenanthroline derived ligands.

All compounds were successfully characterized by the usual elemental and spectroscopic techniques. The characterization suggests that the Schiff base ligands coordinate the metal ion through the phenolate-O, the imine-N and sulfur atom in the thiol form (except in $Zn[(PySmdt)(CH_3COO)]$ for which a thione form is proposed). The Zn(II) ion has coordination number four, with the ligands tridentate and a water molecule or an acetate ion occupying the 4^{th} coordination position. On the other hand, characterization showed that the phenanthroline derivative ligands coordinate the metal ion through the two nitrogen atoms of the aromatic ring. Characterization with ^{1}H and ^{13}C NMR proved that in solution there is formation species of different stoichiometries, which correspond to 1:1, 1:2 and 1: 3 Zn:L molar ratios.

The stability of the compounds in buffered aqueous media (5 % DMSO and 95 % PBS) was evaluated and all are stable at least for three hours. The antioxidant potential of the compounds was tested using the DPPH assay. All S-methyl Schiff bases showed moderate antioxidant activity but the Zn(II) complexes, with the exception of $Zn[(PySmdt)(CH_3COO)]$, are inactive. The Zn(II) phenanthroline complexes were tested for their DNA binding ability. The results indicated that there is interaction between the complexes and ctDNA. The cytotoxicity effect against tumor cells was also evaluated. The Schiff bases have shown promising results with IC_{50} values ranging from 4.41 to 28.99 μM on cell lines (PC-3, MCF-7 and CACO-2) after 48 h. The IC_{50} values of Zn(II) phenanthroline complexes on A2780 cell line ranged from 0.19 to 2.4 μM after 48 h, which indicate that the cytotoxicity effect is slightly greater than that of the ligands, at least for longer times. Cytotoxicity study of zinc(II)-Schiff base complexes is still ongoing.

In general, both families of compounds show potential to proceed further for biological studies to allow their development as metallodrugs, particularly the phenanthroline Zn(II) compounds.

References

1. Sartaj T., Ahmad A., Farukh A., Mohd. A., Vivek B. Synthesis and characterization of copper(II) and zinc (II) - based potential. *Eur. J. Med. Chem* **2012,** *58,* 308-316.

2. Chandraleka S., Ramya K., Chandramohan G., Dhanasekaran D., Priyadharshini A., Panneerselvam A. Antimicrobial mechanism of copper (II) 1,10 phenanthroline and 2,2' bipyridyl complex on bacterial and fungal pathogens. *J. Saudi. Chem. Soc.* **2011,** *doi: 10.1016/j.jscs.2011.11.020*.

3. Katja D.M. and Chris O. Metallodrugs in medicinal inorganic chemistry. *Chem. Rev.* **2014,** *114,* 4540 −4563.

4. Muthusamy S. and Natarajan R. Pharmacological activity of a few transition metal complexes: A short review. *J. Chem. Bio.Ther.* **2016,** *1* (2), 1-17.

5. Mariya D.M., Iyyam P.S., Subramanian S., Pradeepa S., Damodar K.S. Synthesis, spectroscopic characterization and DNA interaction of schiff base Cu(II), Ni(II) and Zn(II) complexes. *Int. J. Inorg. Bioinorg. Chem.* **2014,** *4* (4), 61 - 67.

6. Chung H.L., Sheng L., Hai J.Z. and Dik L. M. Metal complexes as potential modulators of inflammatory and autoimmune responses. *Chem. Sci.* **2015,** *6,* 871–884.

7. Rezvania A.R., Saravania H. and Hadadzadeh H. Synthesis, crystal structure, electrochemical and fluorescence studies of a novel Zn(II)-fluorophore, 1,10-phenanthroline-5,6-dione (phen-dione). *J. Iran. Chem. Soc.* **2010,** *7* (4), 825-833.

8. Wang L., Liang N. and Jia Y. Syntheses, structures, fluorescent properties and natural bond orbital analyses of metal–organic complexes based on 5,6-substituted 1,10-phenanthroline derivatives. *Polyhedron* **2013,** *59,* 115–123.

9. Peter G. S. and Gokhan Y. 1,10-Phenanthroline: A versatile ligand. *Chem. Soc. Rev.* **1994,** 327-334.

10. Cungen Z. and Christoph J. Six-coordinated zinc complexes: [Zn(H2O)4(phen)](NO3)2·H2O and [ZnNO3(H2O)(bipy)(Him)]NO3 (phen = 1,10-phenanthroline, bipy = 2,20-bipyridine,and Him = imidazole). *J. Chem. Crystallogr.* **2002,** *31* (1), 29-35.

11. Cungen Z., Kaibei Y., Dan W. and Chengxue Z. Tetraaqua(1,10-phenanthroline)zinc(H)sulfate dihydrate. *Acta Crystallogr. Sect. C* **1999,** 1815-1817.

12. Rajkumar M.A. and Natarajan R. A therapeutic journey of mixed ligand complexes containing 1,10-phenanthroline derivatives : A review. *Int. J. Curr. Pharm. Res.* **2016,** *8* (3), 1-6.

13. Taghreed H. A., Faiza H. G. and Aliea S. K. Synthesis, characterization, and antibacterial activity of Mn (II), Fe(II), Co(II), Ni(II), Cu(II), Zn(II), Cd(II), and Hg (II) mixed- ligand complexes containing furan-2-carboxylic acid and (1,10-phenanthroline). *Adv. Phys. Theor. Appl.* **2014,** *29,* 5-13.

14. Rajkumar M. and Natarajan R. Enthused research on DNA-binding and DNA-cleavage aptitude of mixed ligand metal complexes. *Spectrochim. Acta A* **2013,** *112,* 198-205.

15. Natarajan R., Rajkumar M., and Liviu M. Bio-sensitive activities of coordination compounds containing 1,10-phenanthroline as co-ligand: Synthesis, structural elucidation and DNA binding properties of metal(II) complexes. *Spectrochim. Acta A* **2014,** *131,* 355-364.

16. Mesut G., Cihan A. and Belgin E. Synthesis, characterization and antibacterial activity of 2-p-tolyl-1H-imidazo[4,5-f][1,10]phenanthroline and its Co(II), Ni(II) and Cu(II) complexes. *Bull. Chem. Soc. Eth.* **2013,** *27* (2), 213-220.

17. Kabeer A. S. and Azeem A. Synthesis, characterization and antibacterial activity of imidazole derivatives of 1,10-phenanthroline and their complexes. *Int. J. Adv. Res. Chem. Sci.* **2014,** *1* (8), 40-44.

18. Sudeshna R., Katharine D. H., Palanisamy U. M., Martin L., Anthony L. S., Reedijk J. and Gilles P.V. W. Phenanthroline derivativ es with improved selectivity as DNA-targeting anticancer or antimicrobial drugs. *ChemMedChem* **2008,** *3,* 1427 – 1434.

19. Alka P. and Anil K. A review: An overview on synthesis of some Schiff bases and there metal complexes with antimicrobial activity. *Chem. Process Eng. Res.* **2015,** *35,* 84-86.

20. Muhammad A. A., Karamat M. and Abdul W. Synthesis, characterization and biological activity of Schiff bases. *International conference on chemistry and chemical process*, Singapore, 2011; pp 1-7.

21. Cleiton M. S., Daniel L. S., Luzia V. M., Rosemeire B. A., Maria A. R., Cleide V.B. and Angelo F. Schiff bases: A short review of their antimicrobial activities. *J. Adv. Res.* **2011,** *2,* 1-8.

22. Xavier A. and Srividhya N. Synthesis and study of Schiff base Ligands. *IOSR J. Appl. Chem.* **2014,** *7* (11), 6-15.

23. Navneet K., Prasad A.V., Pratima S. Synthesis and antibacterial evaluation of some new Schiff bases. *Int. J. Pharm. Sci. Rev. Res.* **2013,** *23* (2), 231-236.

24. Ahmed M. A., and Ibrahim M.A. M. A review on versatile applications of transition metal complexes incorporating Schiff bases. *BENI-SUEF Uni. J. Basic. Appl. Sci.* **2015,** *4,* 119-133.

25. Enis N.M.Y., Thahira S. A. R., Edward R. T. T., Abhimanyu V., Karen A. C., Mohamed I. M. T., and Haslina A. Synthesis, characterization and biological evaluation of transition

metal complexes derived from N, S bidentate ligands. *Int. J. Mol. Sci.* **2015,** *16,* 11034-11054.

26. Anu K., Suman B., Sunil K., Neha S.and Vipin S. Schiff bases: A versatile pharmacophore. *J. Catal.* **2013,** 1-13.

27. Begum M. S. , Howlader M.B.H., Sheikh M. C., Miyataked R. and Zangrando E. Crystal structure of S-hexyl (E)-3-(2-hydroxy-benzylidene)dithiocarbazate. *Acta Cryst.* **2016,** *E72,* 290–292.

28. Kudrat Z. M. and Islam M. S. Synthesis, characterization, and antimicrobial activity of complexes of Cu(II), Ni(II), Zn(II), Pb(II), Co(II), Mn(II),and U(VI) containing bidentate Schiff base of [S-Methyl-3-(4-methoxybenzylidine)dithiocarbazate]. *Russ. J. Gen. Chem.* **2015,** *85* (4), 979–983.

29. Akbar A. M., Mirza A.H., Fatriah H. B. , Malai H. S.A. and Paul V. B.. Synthesis, characterization and X-ray crystallographic structural study of copper(II) and nickel(II) complexes of the 2-quinoline carboxaldehyde Schiff base of S-methyldithiocarbazate (Hqaldsme). *Polyhedron* **2006,** *25,* 3245–3252.

30. Ming X. L., Li Z. Z., Chun L. C., Jing Y. N., Bian S. J. Synthesis, crystal structures, and biological evaluation of Cu(II) and Zn(II) complexes of 2-benzoylpyridine Schiff bases derived from S-methyl- and S-phenyldithiocarbazates. *J. Inorg. Biochem.* **2012,** *106,* 117-125.

31. Mohd A. M., Ibrahim M. T. M, Karen A. C., Fiona N.-F. and David J. W. Synthesis, characterization and antibacterial activity of Schiff base derived from S-methyldithiocarbazate and methylisatin. *J. Chem. Crystallogr.* **2012,** *42,* 173–179.

32. Tarafder M.T.H., Kar B. C., Karen A. C. , Ali A.M., Yamin B.M. and Fun H. K. Synthesis and characterization of Cu(II), Ni(II) and Zn(II) metal complexes of bidentate NS isomeric Schiff bases derived from S-methyldithiocarbazate (SMDTC): bioactivity of the bidentate NS isomeric Schiff bases, some of their Cu(II), Ni(II) and Zn(II). *Polyhedron* **2002,** *21,* 2683 - 2690.

33. Singh H. L. and Varshney A.K. Synthetic , structural , and biochemical studies of organotin(IV) With Schiff bases having nitrogen and sulphur donor ligands. *Bioinorg. Chem. Appl.* **2006,** 1-7.

34. Yutaka Y. and Hiroyuki Y. Zinc complexes developed as metallopharmaceutics for treating diabetes mellitus based on the bio-medicinal inorganic chemistry. *Curr. Top. Med. Chem.* **2012,** *12,* 210-218.

35. Alketa T., George P., Catherine P. R. and Dimitris P. K. Zinc complexes of the antibacterial drug oxolinic acid : Structure and DNA-binding properties. *J. Inorg. Biochem.* **2009,** *103,* 898–905.

36. Hamideh S. and Niloufar A. T. Synthesis and characterization of new four-coordinated Zinc(II) complex containing phenanthroline derivatives. *Iran. J. Org. Chem.* **2011,** *3* (2), 611-614.

37. Davar M. B. and Mehrnaz G. Spectral characterization of novel ternary zinc(II) complexes containing 1,10-phenanthroline and Schiff bases derived from amino acids and salicylaldehyde-5-sulfonates. *Spectrochim. Acta A* **2007,** *67,* 944 – 949.

38. Massimo D. V., Carla B., Pierluigi O., Luigi M., Bruno B. and Paolo Z. Clioquinol, a drug for alzheimer's disease specifically interfering with brain metal metabolism: Structural characterization of its zinc(II) and copper(II) complexes. *Inorg. Chem.* **2004,** *43* (13), 3795-3797.

39. Li Z.Q., Hu, C. W., Wu F.J., Zhang Y. H., Gong Y. and Gan M. Y. Synthesis, characterization and activity against staphylococcus of metal(II)- gatifloxacin complexes. *Chinese J. Chem.* **2007,** *25,* 1809—1814.

40. Jean A., Georges M., Nour E. G., Didier D., Bernard F., Francois B., Emma D., Mehrez S., Yanling L., Yves J. and John R.J. S. Crystal structures and physico-chemical properties of Zn(II) and Co(II)tetraaqua(3-nitro-4-hydroxybenzoato) complexes: Their anticonvulsant activities as well as related (5-nitrosalicylato)–metal complexes. *Polyhedron* **2008,** *27,* 537–546.

41. Qianli Q., Changge Z., Yanfu L., Chunlei M., Jianquan H., Song L. and Xiuying C. Synthesis, crystal structure and characterizations of new 3,4,7,8-tetrachloro-1,10-phenanthroline Zn(II) complex. Chinese scientific papers online. HYPERLINK "http://www.paper.edu.cn" http://www.paper.edu.cn (accessed April 20, 2017).

42. Gehad G. M. and Zeinab H. A. E. Mixed ligand complexes of bis(phenylimine) Schiff base ligands incorporating pyridinium moiety synthesis, characterization and antibacterial activity. *Spectrochim. Acta A* **2005,** *61,* 1059–1068.

43. Ariane A., Jean C. D., Jean B. and Bernard M. The ligand 1,10-phenanthroline-2,9-dicarbaldehyde dioxime can act both as a tridentate and as a tetradentate ligand to synthesis, characterization and crystal structures of its transition metal complexes. *Eur. J. Inorg. Chem.* **2000,** 1985-1996.

44. Ruma D. G., Satyajit D., Avishek G., Kaushik B., Paramita C., Avijit S., Mitali C., Ashis N., Kiran P. and Soumitra K. C. An in vitro and in vivo study of a novel zinc complex, zinc N-(2-hydroxyacetophenone)glycinate to overcome multidrug resistance in cancer. *Dalton Trans.* **2011,** *40,* 10873–10884.

45. Nadiah A. and Uwaisulqarni O. Synthesis and characterization of Co(II), Cu(II), Cd(II), Zn(II) and Ni(Ii) complexes of Schiff base ligand derived from S-benzyldithiocarbazate (Sbdtc) and acetophenone with their biological activity studies. *IOSR J. Eng.* **2013,** *3* (8), 38-50.

46. Prafulla M. S., Jahanvi P. and Yogini P. Meal complexes: Current trends and future potential. *Int. J. Pharm. Chem. Bio. Sci.* **2012,** *2* (3), 251-265.

47. Hijazi A. A., Hadeel F., Mohanad D. and Emilia R. Synthesis, charcterization, and biological activity of new mixed-ligand complexes of Zinc(II) naproxen with nitrogen based ligands. *Eur. J. Med. Chem.* **2015,** *89,* 67 - 76.

48. Nahid S. and Somaye M. Synthesis characterization and DNA interaction studies of a new Zn(II) complex containing different dinitrogen aromatic ligands. *Bioinorg. Chem. Appl.* **2012,** 1-8.

49. Yan G., Wu R., Chang Y. and Kang D. Pharmacokinetics and bio-distribution of new Gd-complexes of DTPA-bis (amide) (L3) in a rat model. *J. Korean. Soc. Magn. Reson. Med.* **2013,** *17* (4), 259-266.

50. Zhang D., Luo G., Ding X. and Lu C. Review: Preclinical experimental models of drug metabolism and disposition in drug discovery and development. *Acta Pharm. Sin. B* **2012,** *2* (6), 549-561.

51. Leuner C. and Dressman J. Improving drug solubility for oral delivery using solid dispersions. *Eur. J. Pharm. Biopharm.* **2000,** *50,* 47-60.

52. Mohammad M. D., Urvashi S., Hammad A., Nikhat M., Shaeel A. A.T. and Athar A. H. Synthesis, electrocatalytic behavior and biological evaluation of trimetallic macrocyclic complex with two different bridging ligands. *Can. Chem. Trans.* **2015,** *3* (2), 184-194.

53. Waseem A. W., Zeid A. O., Imran A., Kishwar S. and Ming F. H. Copper(II), nickel(II), and ruthenium(III) complexes of an oxopyrrolidine-based heterocyclic ligand as anticancer agents. *J. Coord. Chem.* **2014,** *67* (12), 2110–2130.

54. Nevin T., Ercan B., Naki C. and Kenan B. Investigation of synthesis, structural characterization, antioxidant activities and thermal properties of Zn(II), Fe(II) and Mn(II) complexes with thiophene-carboxylate ligand. *J. Chem. Biochem.* **2015,** *3* (2), 13-29.

55. Ikechukwu P. E. and Peter A. A. Synthesis, characterization and biological studies of Metal(II) Complexes of (3E)-3-[(2-{(E)-[1-(2,4-Dihydroxyphenyl) ethylidene]amino}ethyl)imino]-1-phenylbutan-1-one Schiff Base. *Mol.* **2015,** 20, 9788-9802.

56. Floyd B., Jeffrey T., Jason W., Jacob D., Nikolay G., Antonio G. S. and Navindra P. S.. Synthesis and structure of [(η6- p-cymene)Ru(2-anthracen-9-ylmethylene-N-ethylhydrazinecarbothioamide)Cl]Cl; biological evaluation, topoisomerase II inhibition and reaction with DNA and human serum albumin. *Metallomics* **2011,** *3* (5), 491–502.

57. Wozniak K. and Blasiak J. Review: Recognition and repair of DNA-cisplatin adducts. *Acta Biochem. Pol.* **2002,** *49* (3), 583-596.

58. Maria D. A. M., Iyyam P. S., Joel C., Biju B. R., Subramanian S., and Damodar K. S. Design, synthesis, characterization and DNA interaction of new Schiff base metal complexes. *J. Chem. Pharm. Res.* **2015,** *7* (11), 105-116.

59. Yong L., Zheng Y.Y. and Ming F.W. Synthesis, characterization, DNA binding Properties, fluorescence studies and antioxidant activity of transition metal complexes with hesperetin-2-hydroxy benzoyl hydrazone. *J. Fluoresc.* **2010,** *20,* 891–905.

60. Sutapa S., Samiran M., Parimal K. and Manas K.r S. Synthesis, characterization and structural studies of mono- and polynuclear complexes of zinc(II) with 1,10-phenanthroline, 2,2'-bipyridine and 4,4'-bipyridine. *Polyhedron* **1997,** *16* (14), 2475- 2481.

61. Alexander J. P., Thomas M. M. and David M. B. Phenanthroline complexes of the d10 metals nickel(0), zinc(ll) and silver(I) comparison to copper(I) species. *Poyhedron* **1997,** *16* (16), 2711-2719.

62. Huilu W., Xingcai H., Jingkun Y., Fan K., Guisheng C., Beibei J. and Yang Y. Synthesis, crystal structure and DNA binding properties of f a nickel (II) complex with 2, 6-bis(2-benzimidazolyl)pyridine. *Z. Naturforsch* **2010,** *65b,* 1334 – 1340.

63. Ning N., Da Q. Z., Heng L., Nan J., Jin Y. W. and Hai Y. L. DNA binding, photonuclease activity and human serum albumin interaction of a water soluble free base carboxyl corrole. *Mol.* **2016,** *21* (54), 1-14.

64. Russ A. W., Melissa M. and Ulrich J. K. Fluorescence resonance energy transfer and complex formation between thiazole orange and various dye DNA conjugates: Implications in signaling nucleic acid hybridization. *J. Fluoresc.* **2006,** *16,* 555–567.

65. Sunita M., Anupama B., Ushaiah B., Gyana K. C. Synthesis, characterization, DNA binding and cleavage studies of mixed-ligand copper (II) complexes. *Arab. J. Chem.* **2015,** *xxx,* xxx – xxxx.

66. Ponnusamy S., Ramaswamy N., Nanjan N., Krishnaswamy V. and Raju N. Catechol oxidase, phosphatase like activity, DNA / BSA binding studies of Ru(II) complexes of S-allyldithiocarbazate: Synthesis and spectral studies. *J. Braz. Chem. Soc.* **2017,** *0* (0), 1-16.

67. Ikechukwu P. E. and Peter A. A. Synthesis, characterization, antioxidant, and antibacterial Studies of Some Metal(II) Complexes of Tetradentate Schiff Base L igand: (4E)-4-[(2-{(E)-[1-(2,4-Dihydroxyphenyl)ethylidene]amino}ethyl)imino]pentan-2-one. *Bioinorg. Chem. Appl.* **2015,** 1-9.

68. Balamurugan V., Shankar S. and Chandramohan S. Synthesis , characterization and antioxidant activity of a novel Cu(II) complex of Schif base derived from N,N'-bis(benzoin)-1,4- butane diimine. *Int. J. Bio. Chem.* **2014,** *8* (2), 85-90.

69. Sanyal R., Chakraborty P., Zangrando E. and Das D. Phosphatase models: Synthesis, structure and catalytic activity of zinc complexes derived from a phenolic Mannich-base

ligand. *Polyhedron* **2015,** *97,* 55-65.

70. Ria S., Averi G., Totan G., Tapan K.M., Ennio Z. and Debasis D. Influence of the coordination environment of Zinc(II) complexes of designed Mannich ligands on phosphatase activity: A combined experimental and theoretical study. *Inorg. Chem.* **2014,** *53,* 85−96.

71. Gianluca A., Andrea L., Yoosaf K. and Nicola A. 1,10-Phenanthrolines: Versatile building blocks for luminescent molecules, materials and metal complexes. *Chem. Soc. Rev.* **2009,** *38,* 1690–1700.

72. Davar M. B. and Fatemeh B. Synthesis, characterization and fluorescence spectra of mononuclearZn(II), Cd(II) and Hg(II) complexes with 1,10-phenanthroline-5,6-dione ligand. *J. Coord. Chem.* **2007,** *60* (3), 347–353.

73. Wenyong G., Zhenghe P., Daocong L., Yunhong Z. Synthesis and structural characterization of zinc(II) and cadmium(II) complexes with 2-oxo-1,3-dithiole-4,5-dithiolate and 1,10-phenanthroline. *Polyhedron* **2004,** *23,* 1701–1707.

74. Yan H., Chaofan Z., Yu Z. and Hailiang Z. Synthesis and luminescent properties of novel Cu (II), Zn (II) polymeric complexes based on 1,10-phenanthroline and biphenyl groups. *J. Chem. Sci.* **2009,** *121* (4), 407–412.

75. Shawnt T., Charles J. R., Andrew R., Elma F. and Jack F. E. Synthesis, characterization, and stability of iron (III) complex ions possessing phenanthroline based ligands. *J. Inorg. Chem.* **2013,** *3,* 7-13.

76. Natalia N. S., Marion D. M., Gisela M. V., Anthony M. D. and Mathias O. S. Stability and spectral properties of europium and zinc phenanthroline complexes as luminescent probes in high content cell-imaging analysis. *J. Inorg. Biochem.* **2011,** *105,* 1589–1595.

77. Elham S. A. Synthesis and characterization of mononuclear and binuclear metal complexes of a new fluorescent dye derived from 2-hydroxy-1-naphthaldehyde and 7-amino-4-methylcoumarin. *JKAU: Sci.* **2010,** *22* (2), 101-116.

78. Somnath R., Tarak N. M., Anil K. B., Sachindranath P. , Samik G., Arijit H., Ray J. B., Allen D. H., Matthias Z. and Susanta K. K. Metal complexes of pyrimidine derived ligands – Syntheses,characterization and X-ray crystal structures of Ni(II), Co(III) and Fe(III) complexes of Schiff base ligands derived from S-methyl/S-benzyl dithiocarbazate and 2-S-methylmercapto-6-methylpyrimidin. *Polyhedron* **2007,** *26,* 2603–2611.

Appendices

In the following appendices several data is included, namely:

A – NMR spectra

B – ESI-MS spectra

C – FTIR spectra

D – RP-HPLC chromatograms.

A. NMR spectra

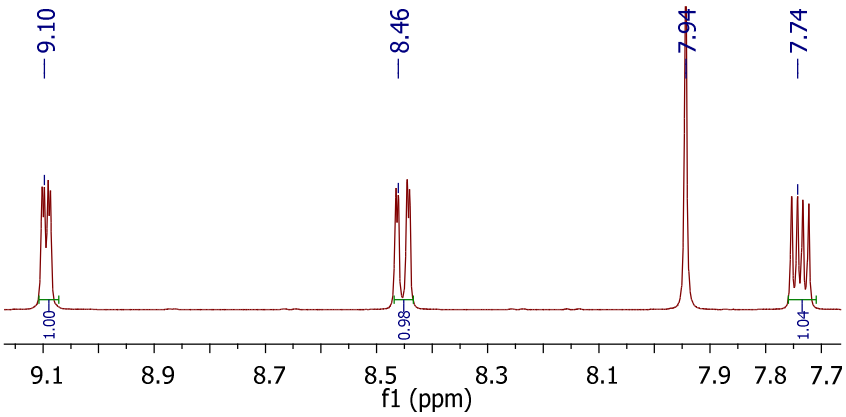

Figure A 1 ^{1}H NMR spectrum of phen in DMSO-d_6 at room temperature

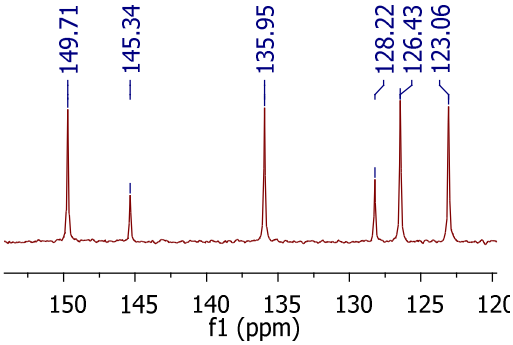

Figure A 2 ^{13}C NMR spectrum of phen in DMSO-d_6 at room temperature

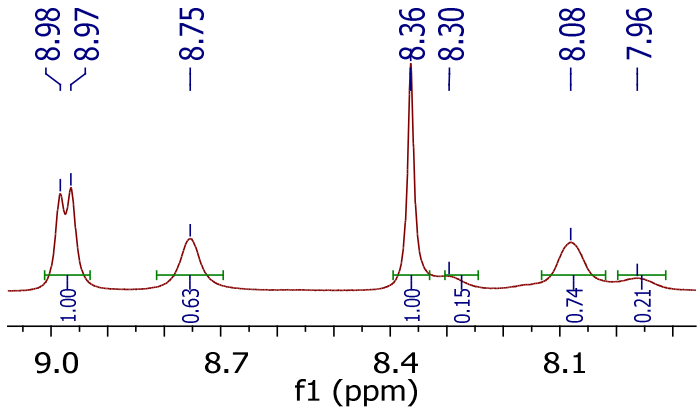

Figure A 3 ^{1}H NMR spectrum of $Zn[(phen)_2(NO_3)_2]\bullet 2H_2O$ in DMSO-d_6 at room temperature

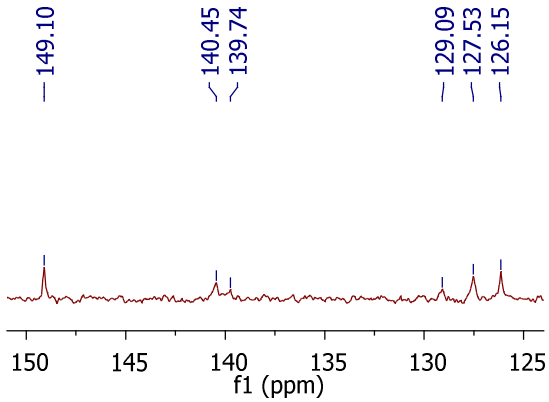

Figure A 4 ^{13}C NMR spectrum of $Zn[(phen)_2(NO_3)_2]\bullet 2H_2O$ in DMSO-d_6 at room temperature

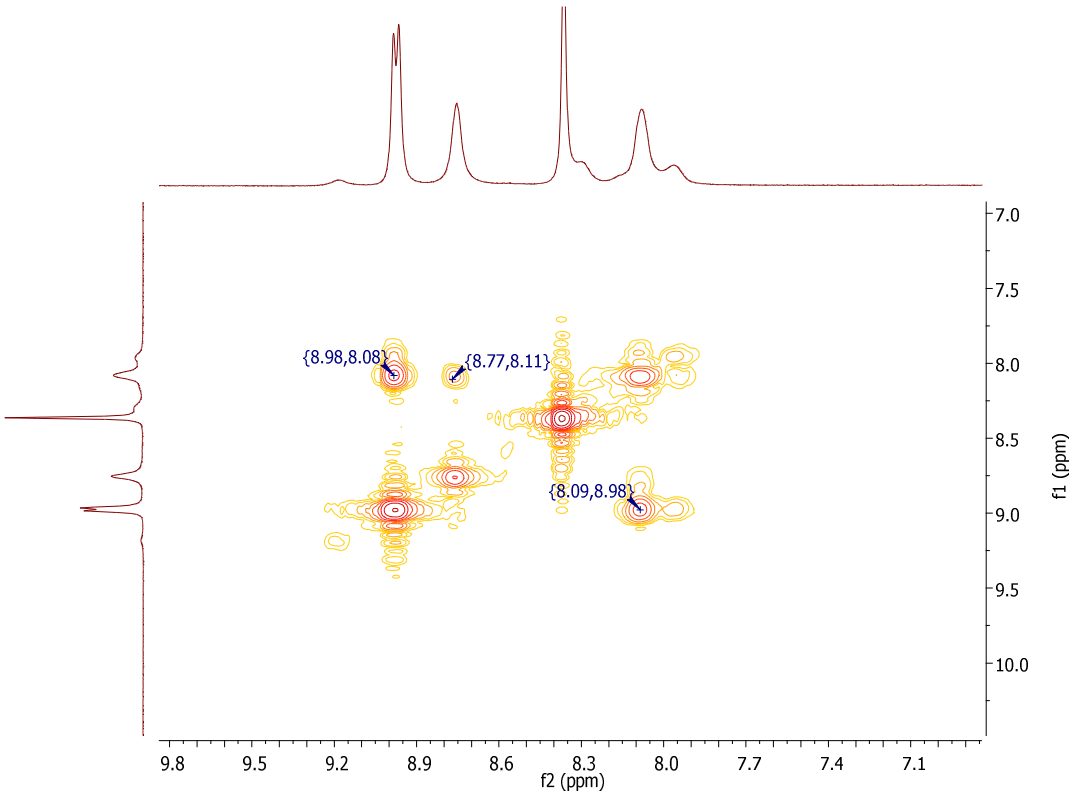

Figure A 5 COSY NMR spectrum of $Zn[(phen)_2(NO_3)_2]\bullet 2H_2O$ in DMSO-d_6 at room temperature

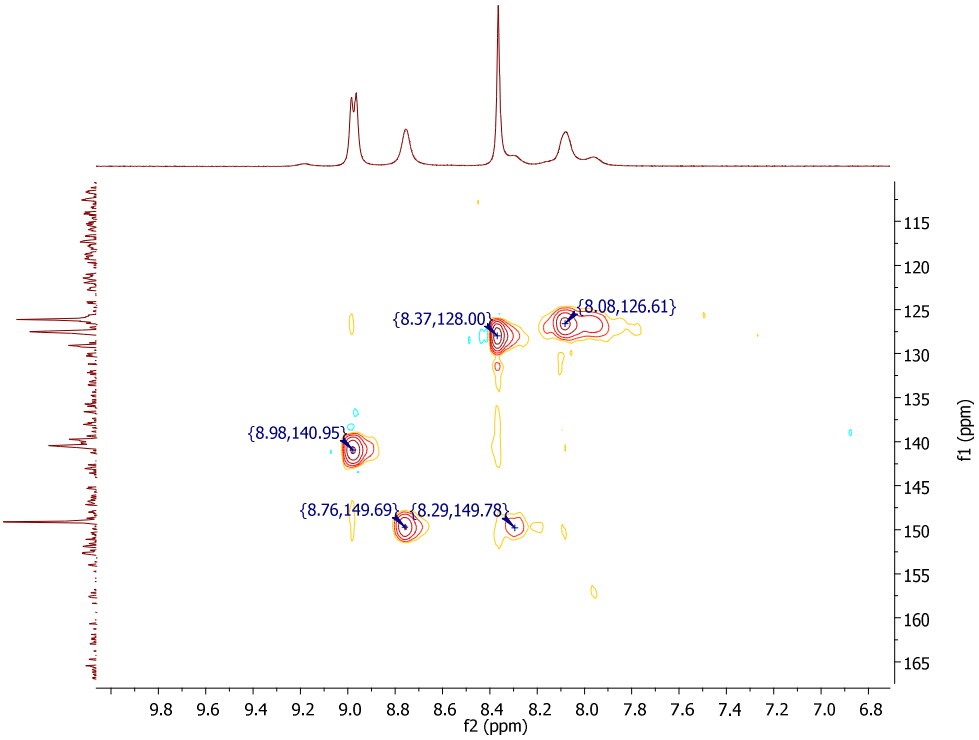

Figure A 6 HSQC NMR spectrum of $Zn[(phen)_2(NO_3)_2]\bullet 2H_2O$ in DMSO-d_6 at room temperature

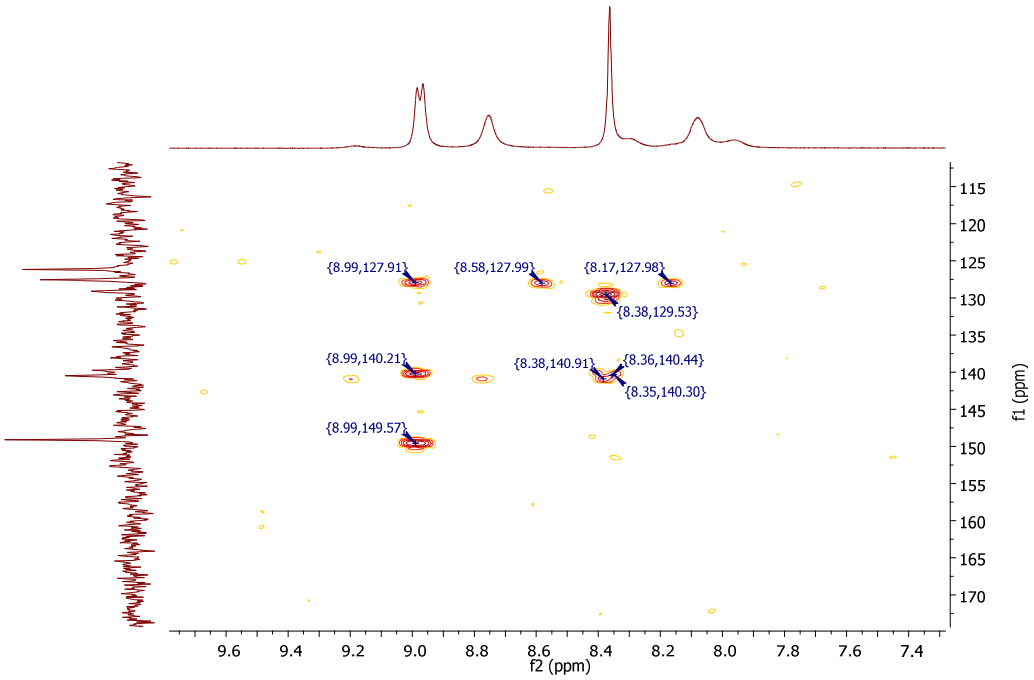

Figure A 7 HMBC NMR spectrum of $Zn[(phen)_2(NO_3)_2]\bullet 2H_2O$ in DMSO-d_6 at room temperature

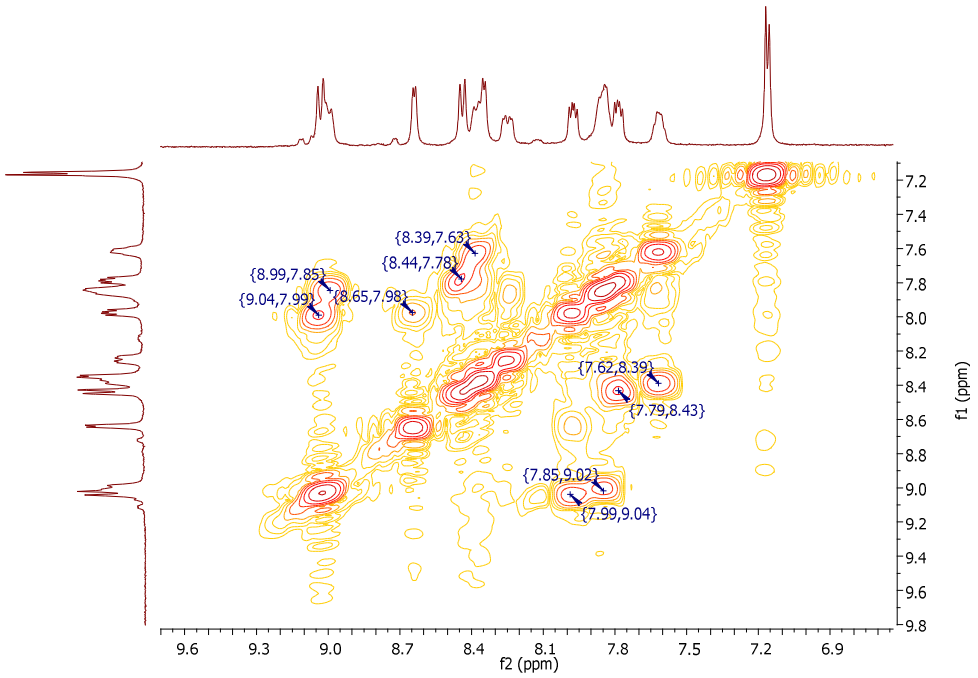

Figure A 8 COSY NMR spectrum of Zn[(aminophen)$_2$(NO$_3$)$_2$]•1.5H$_2$O in CD$_3$OD at room temperature

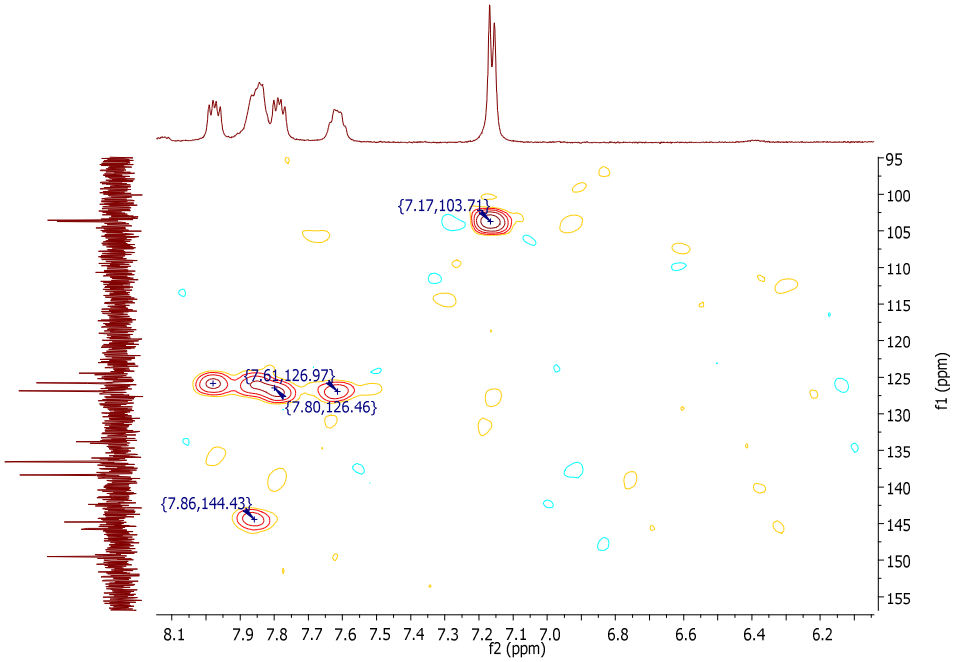

Figure A 9 HSQC NMR spectrum of Zn[(aminophen)$_2$(NO$_3$)$_2$]•1.5H$_2$O in CD$_3$OD at room temperature

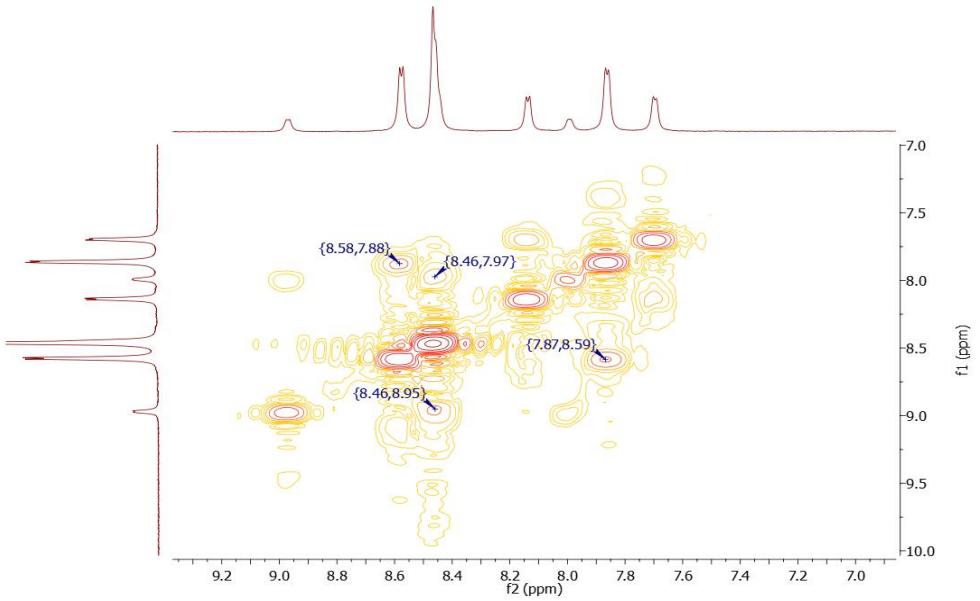

Figure A 10 COSY NMR spectrum of $Zn[(Mephen)_2(NO_3)_2]\bullet 3.5H_2O$ in CD_3OD at room temperature

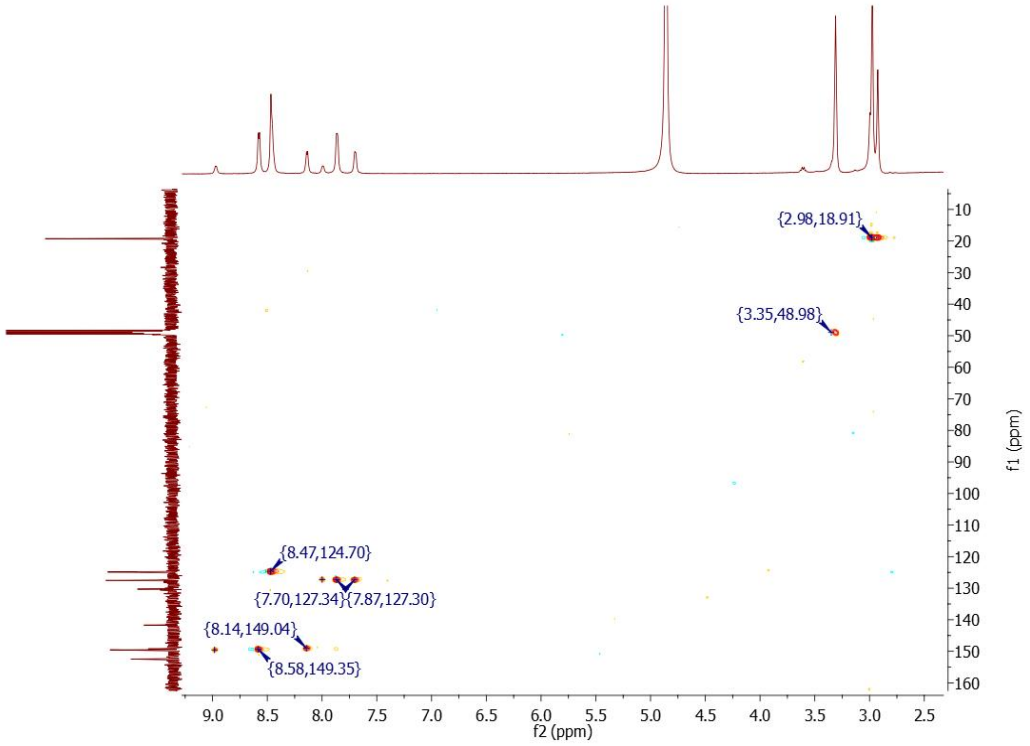

Figure A 11 HSQC NMR spectrum of $Zn[(Mephen)_2(NO_3)_2]\bullet 3.5H_2O$ in CD_3OD at room temperature

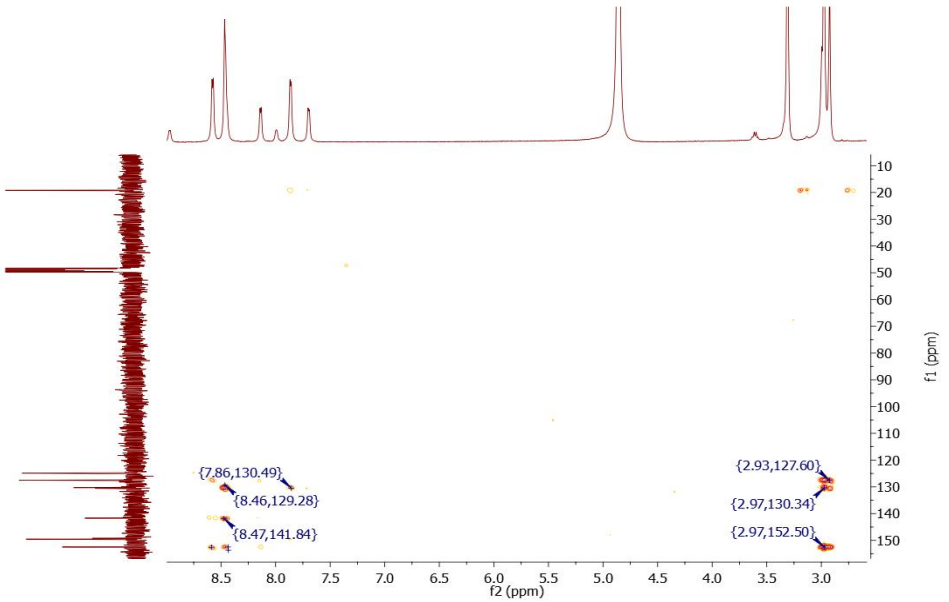

Figure A 12 HMBC NMR spectrum of $Zn[(Mephen)_2(NO_3)_2]\bullet 3.5H_2O$ in CD_3OD at room temperature

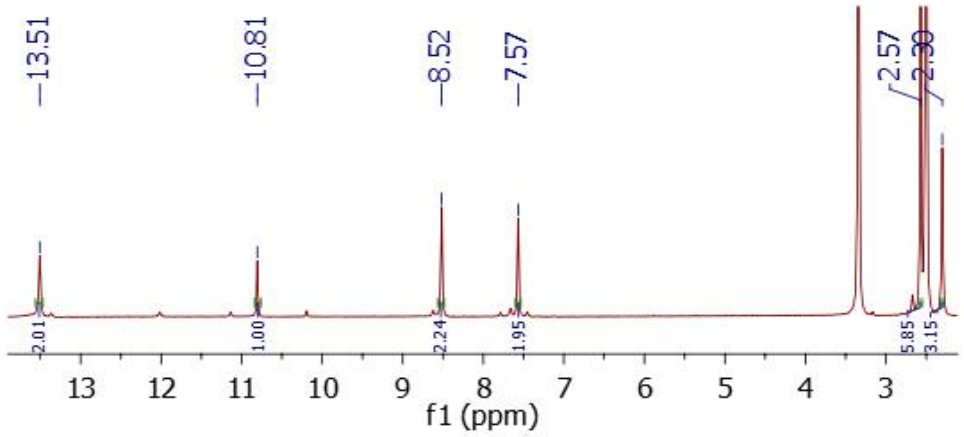

Figure A 13 ^{1}H NMR spectrum of $Mp(Smdt)_2$ in DMSO-d_6 at room temperature

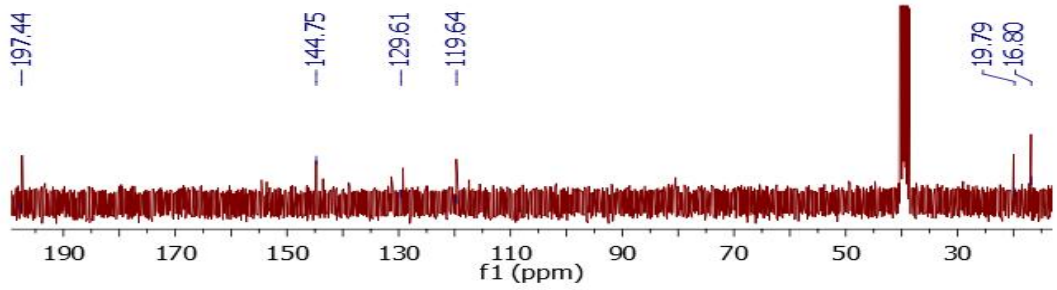

Figure A 14 ^{13}C NMR spectrum of $Mp(Smdt)_2$ in DMSO-d_6 at room temperature

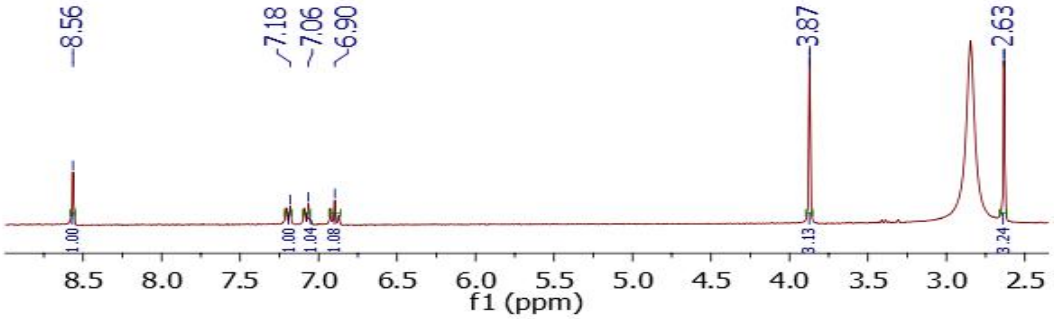

Figure A 15 ^{1}H NMR spectrum of VanSmdt in acetone-d_6 at room temperature

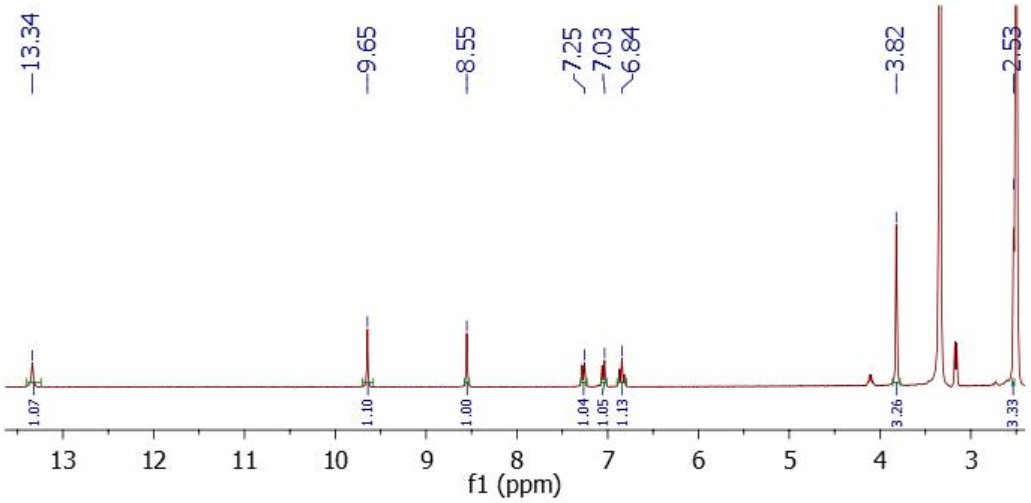

Figure A 16 ^{1}H NMR spectrum of VanSmdt in DMSO-d_6 at room temperature

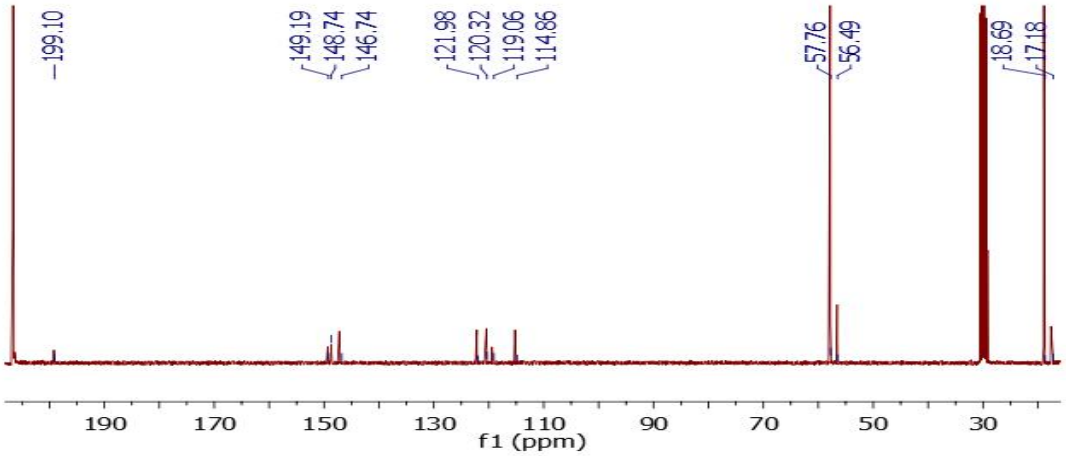

Figure A 17 ^{13}C NMR spectrum of VanSmdt in acetone-d_6 at room temperature

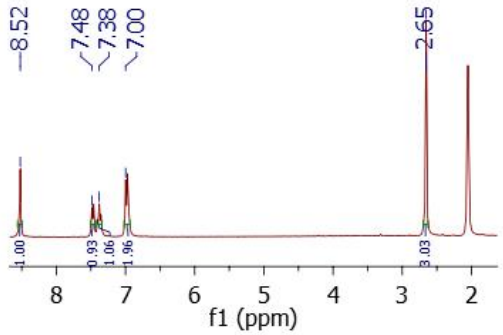

Figure A 18 ^{1}H NMR spectrum of SalSmdt in acetone-d_6 at room temperature

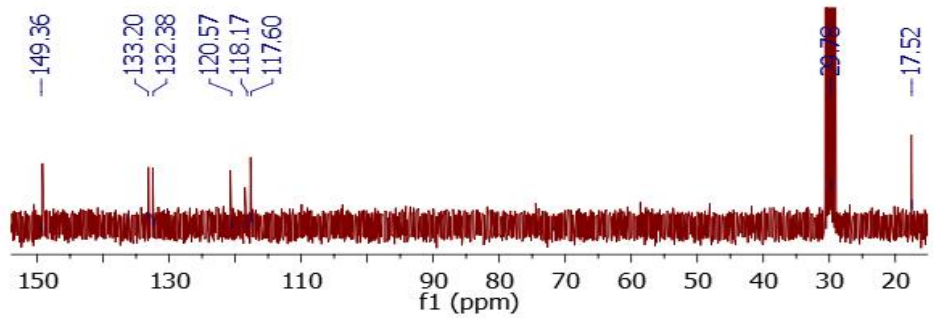

Figure A 19 ^{13}C NMR spectrum of SalSmdt in acetone-d_6 at room temperature

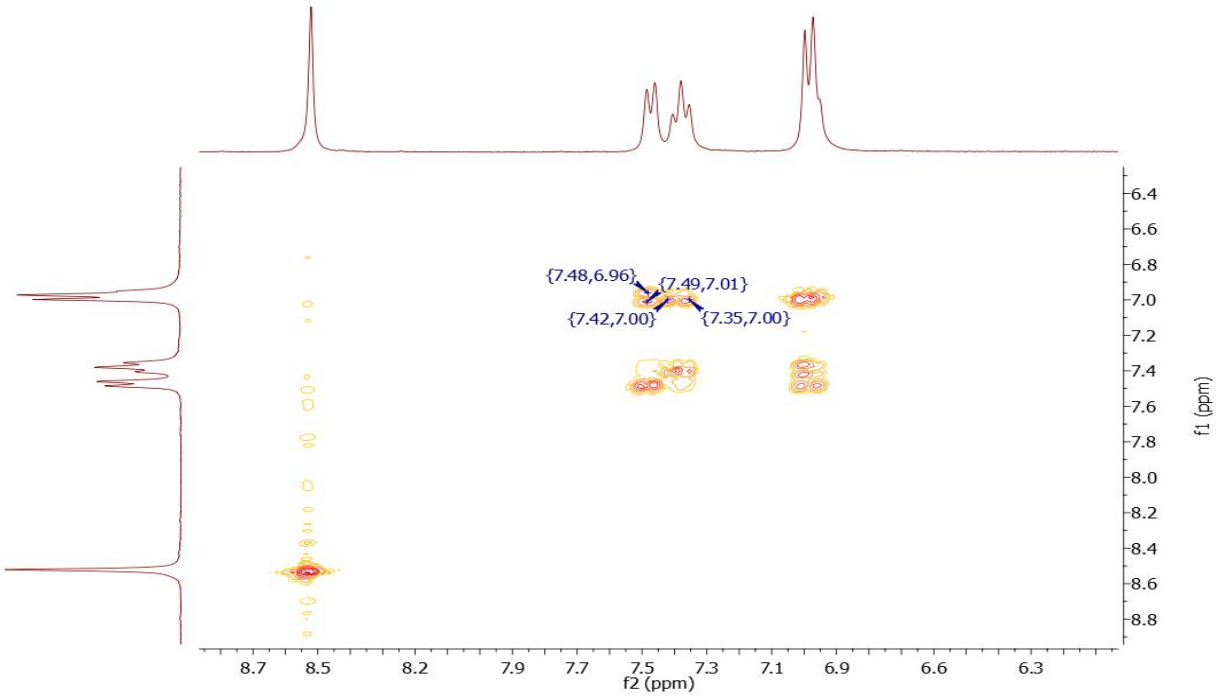

Figure A 20 COSY NMR spectrum of SalSmdt in acetone-d_6 at room temperature

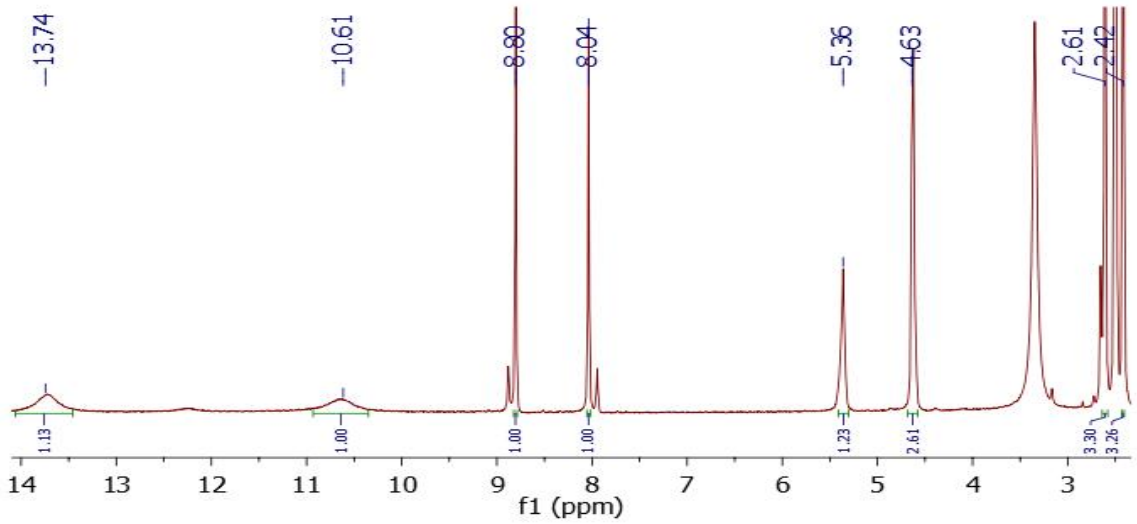

Figure A 21 ^{1}H NMR spectrum of PySmdt in DMSO-d_6 at room temperature

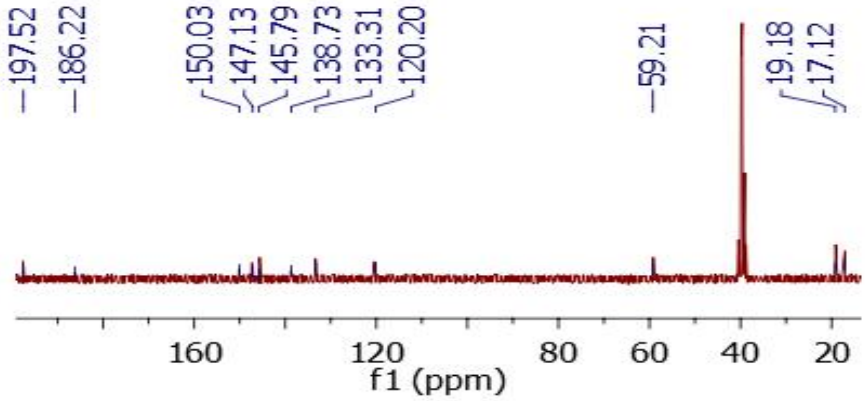

Figure A 22 ^{13}C NMR spectrum of PySmdt in DMSO-d_6 at room temperature

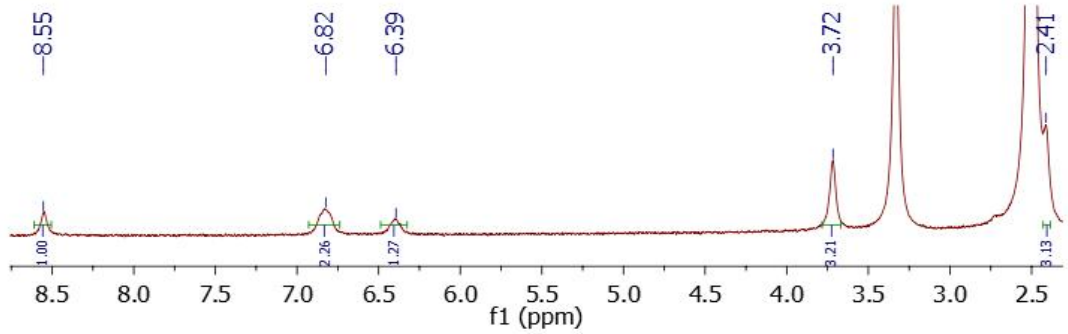

Figure A 23 ^{1}H NMR spectrum of Zn[(VanSmdt) (H_2O)] in DMSO-d_6 at room temperature

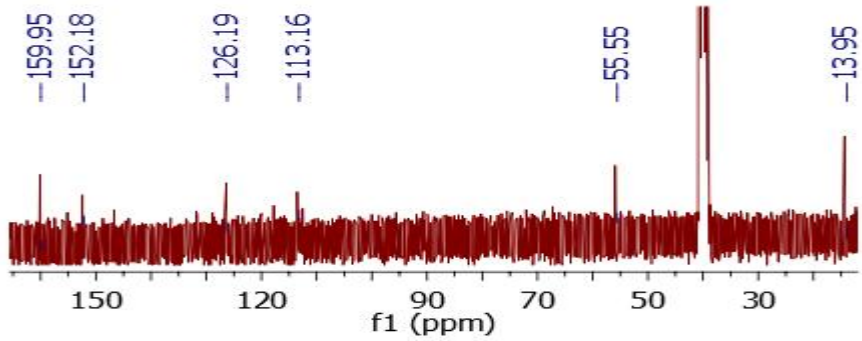

Figure A 24 ^{13}C NMR spectrum of Zn[(VanSmdt) (H_2O)] in DMSO-d_6 at room temperature

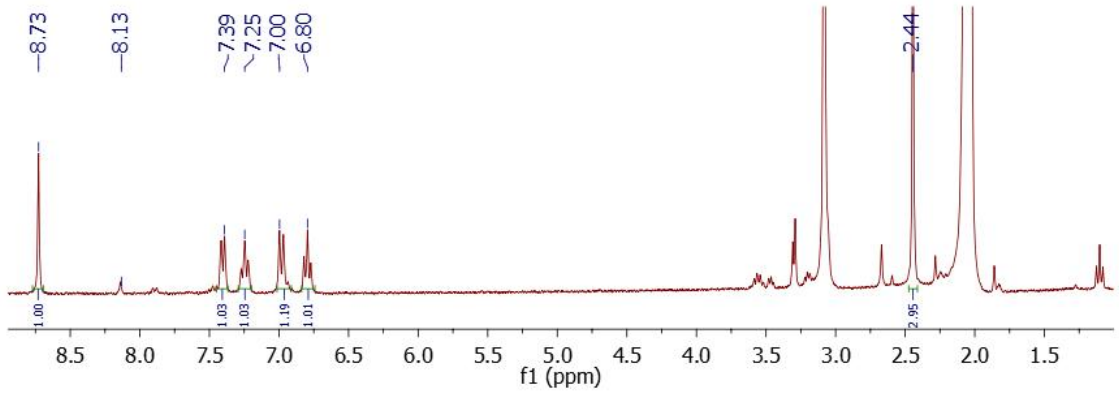

Figure A 25 ^{1}H NMR spectrum of Zn[(SalSmdt)(H_2O)]•0.5H_2O in acetone-d6 at room temperature

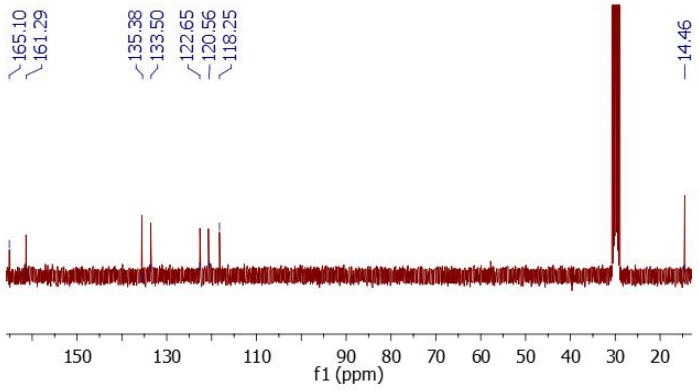

Figure A 26 ^{13}C NMR spectrum of Zn[(SalSmdt)(H_2O)]•0.5H_2O in acetone-d6 at room temperature

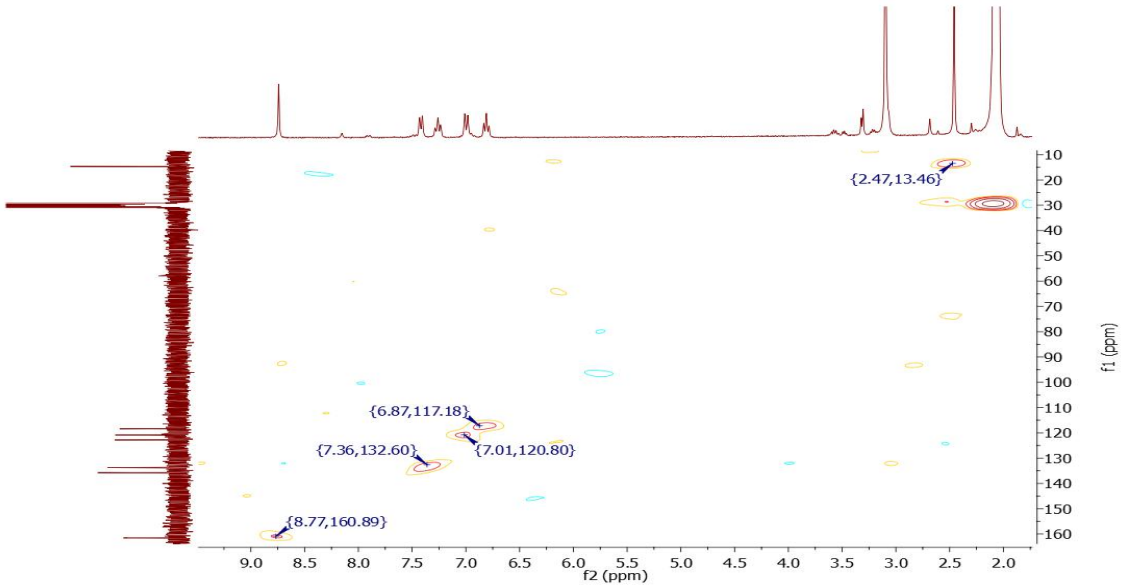

Figure A 27 HSQC NMR spectrum of Zn[(SalSmdt)(H_2O)]•0.5H_2O in acetone-d_6 at room temperature

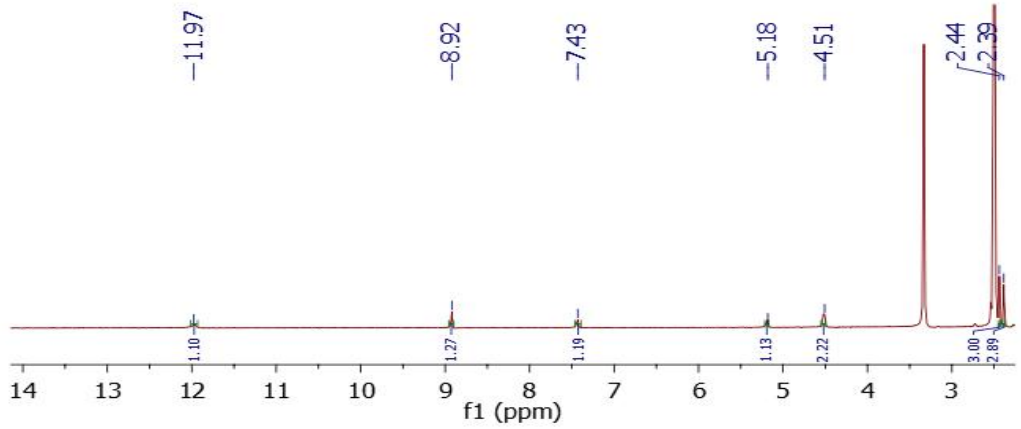

Figure A 28 ^{1}H NMR spectrum of Zn[(PySmdt)(CH_3COO)]•1.5H_2O in DMSO-d_6 at room temperature

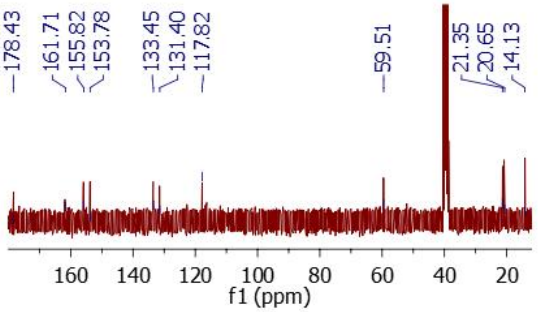

Figure A 29 ^{13}C NMR spectrum of Zn[(PySmdt)(CH_3COO)]•1.5H_2O in DMSO-d_6 at room temperature

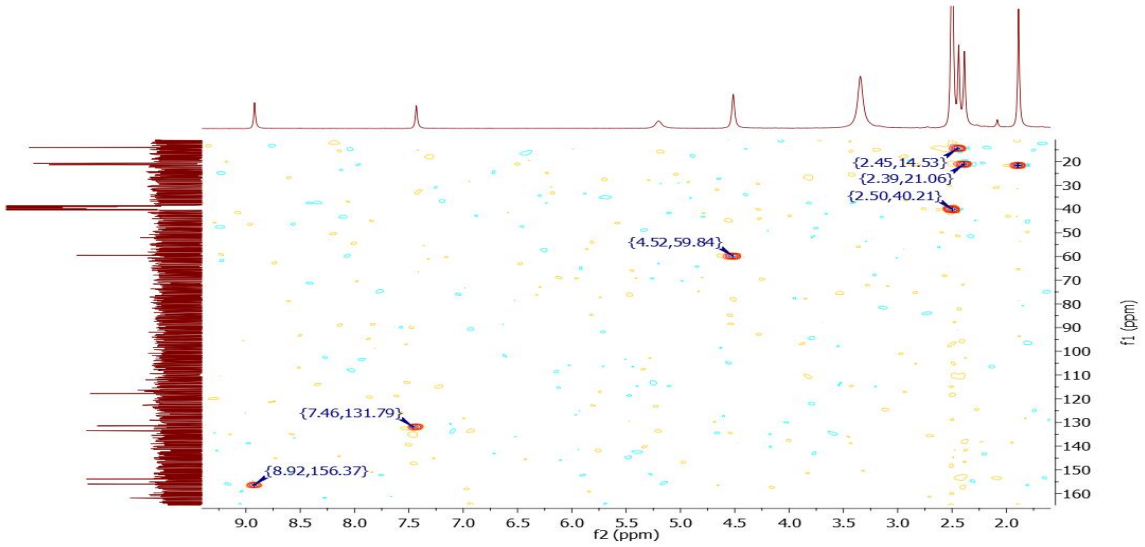

Figure A 30 HSQC NMR spectrum of Zn[(PySmdt)(CH_3COO)]•1.5H_2O in DMSO-d_6 at room temperature

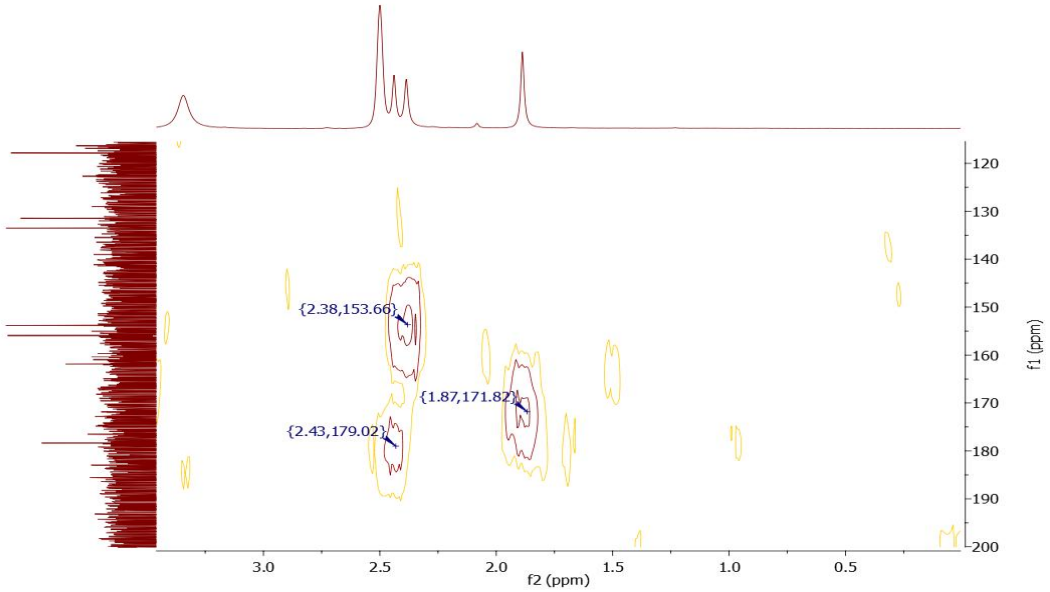

Figure A 31 HMBC NMR spectrum of Zn[(PySmdt)(CH_3COO)]•1.5H_2O in DMSO-d_6 at room temperature

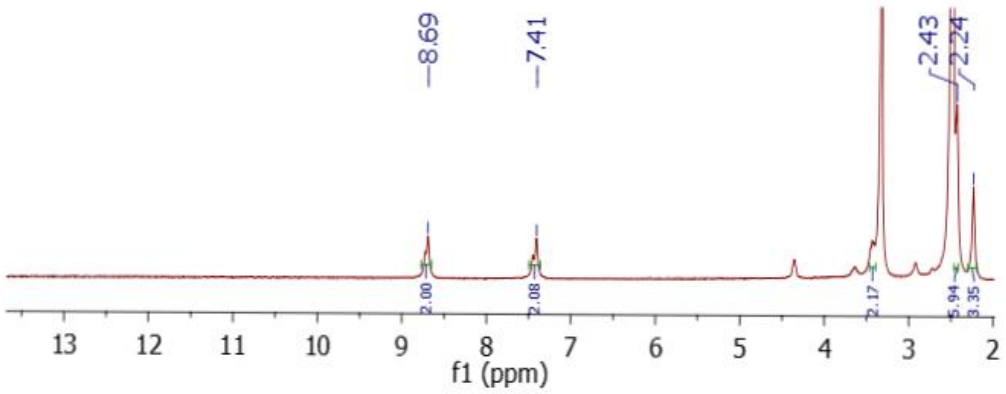

Figure A 32 ^{1}H NMR spectrum of $Zn_2[(Mp(Smdt)_2)(CH_3COO)]$ in DMSO-d_6 at room temperature

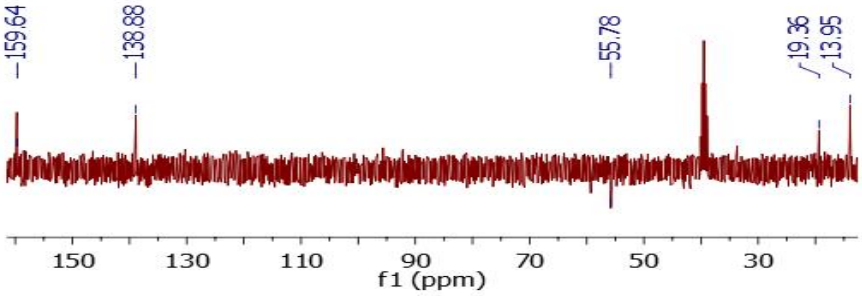

Figure A 33 DEPT NMR spectrum of $Zn_2[(Mp(Smdt)_2)(CH_3COO)]$ in DMSO-d_6 at room temperature

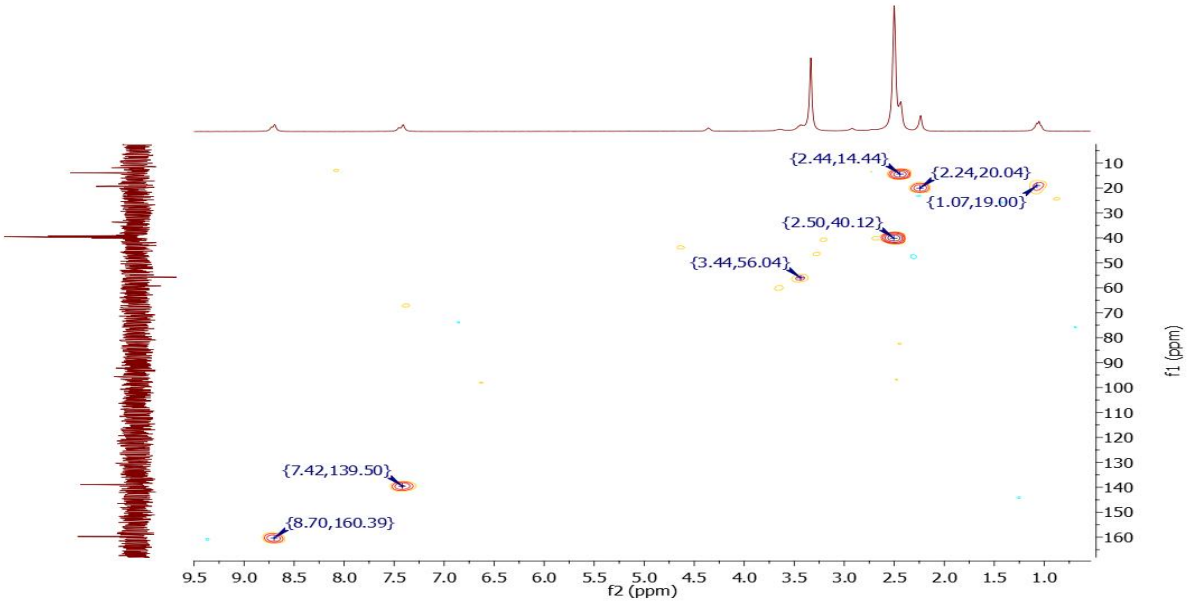

Figure A 34 HSQC NMR spectrum of $Zn_2[(Mp(Smdt)_2)(CH_3COO)]$ in DMSO-d_6 at room temperature

B. ESI-MS spectra

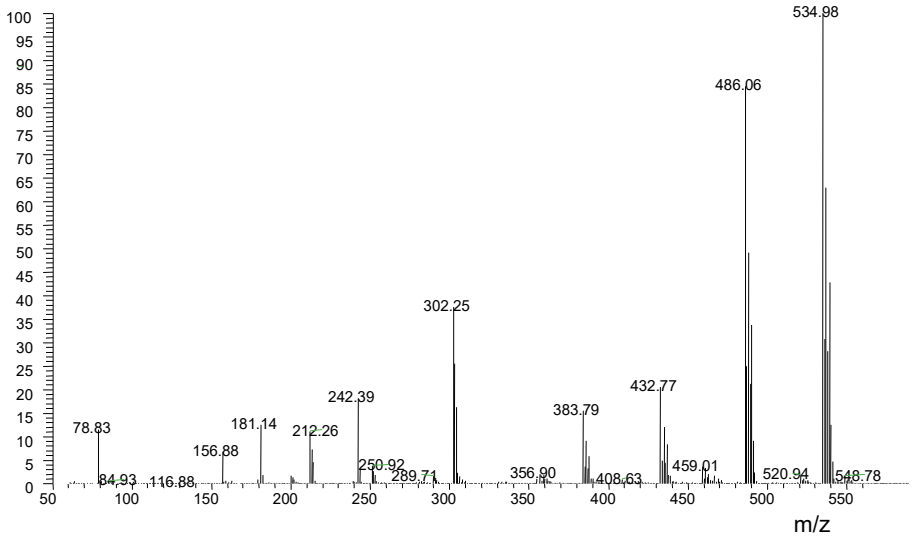

Figure B 1 ESI(+)-MS spectrum of $Zn[(phen)_2(NO_3)_2]\bullet 2H_2O$

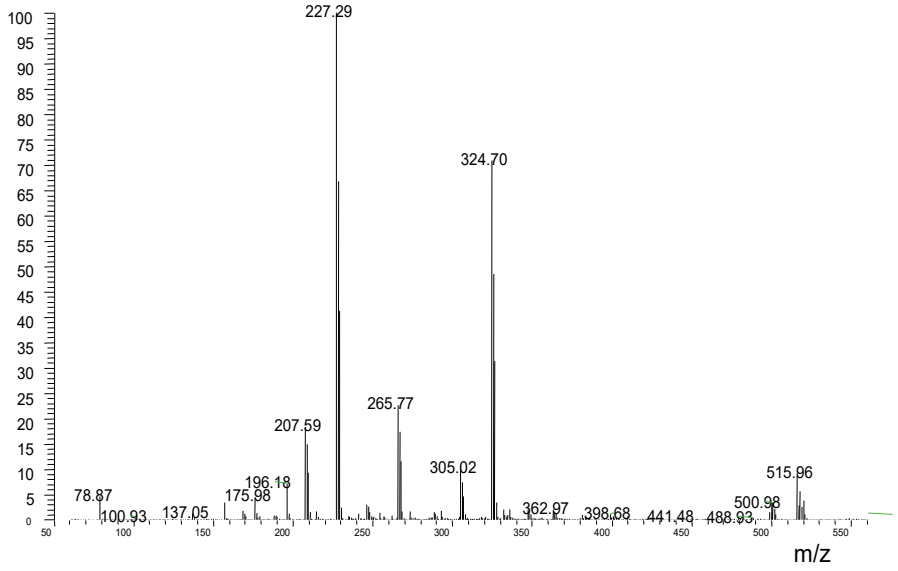

Figure B 2 ESI(+)-MS spectrum of $Zn[(aminophen)_2(NO_3)_2]\bullet 1.5H_2O$

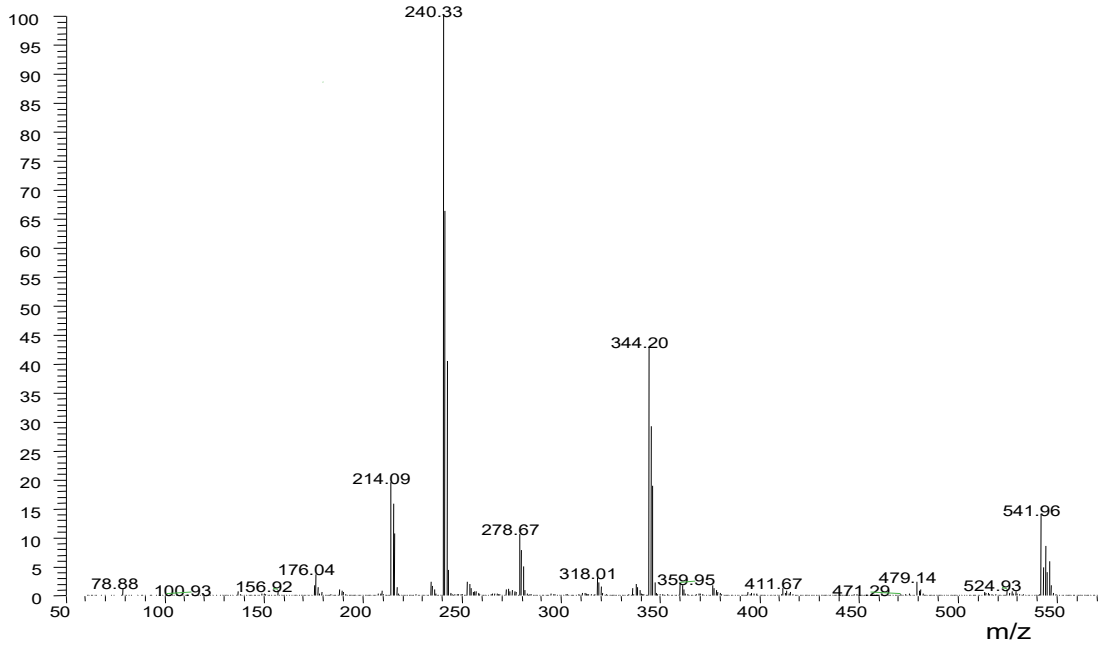

Figure B 3 ESI(+)-MS spectrum of $Zn[(Mephen)_2(NO_3)_2]\bullet 3.5H_2O$

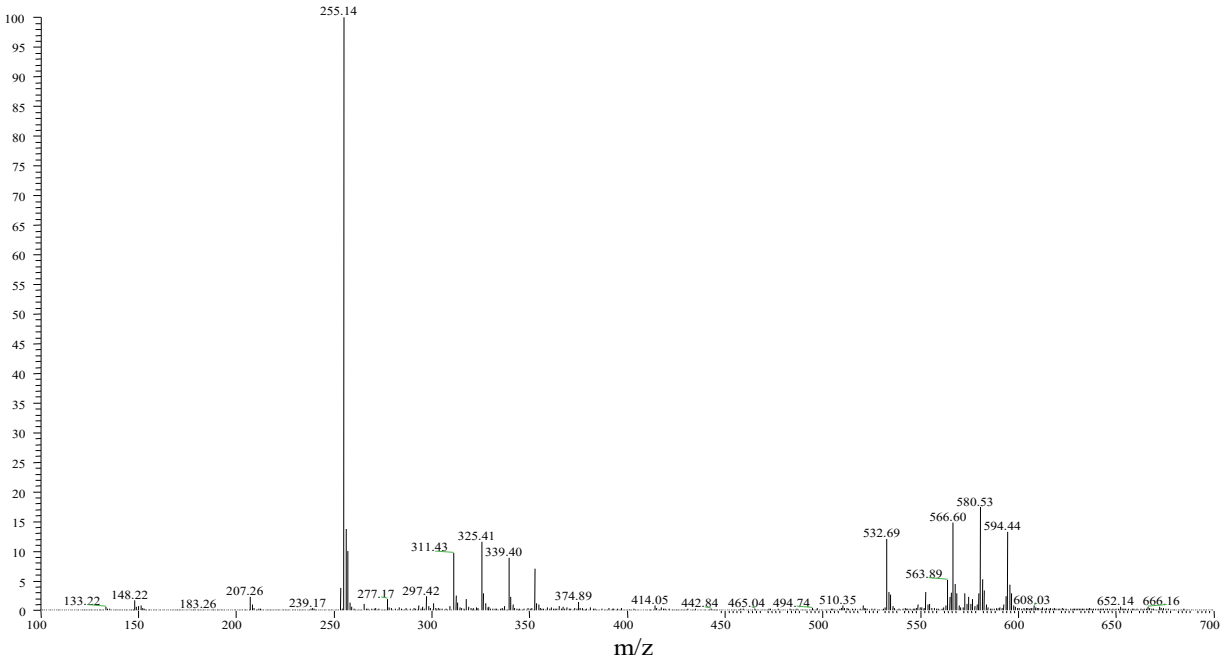

Figure B 4 ESI(-)-MS spectrum of VanSmdt

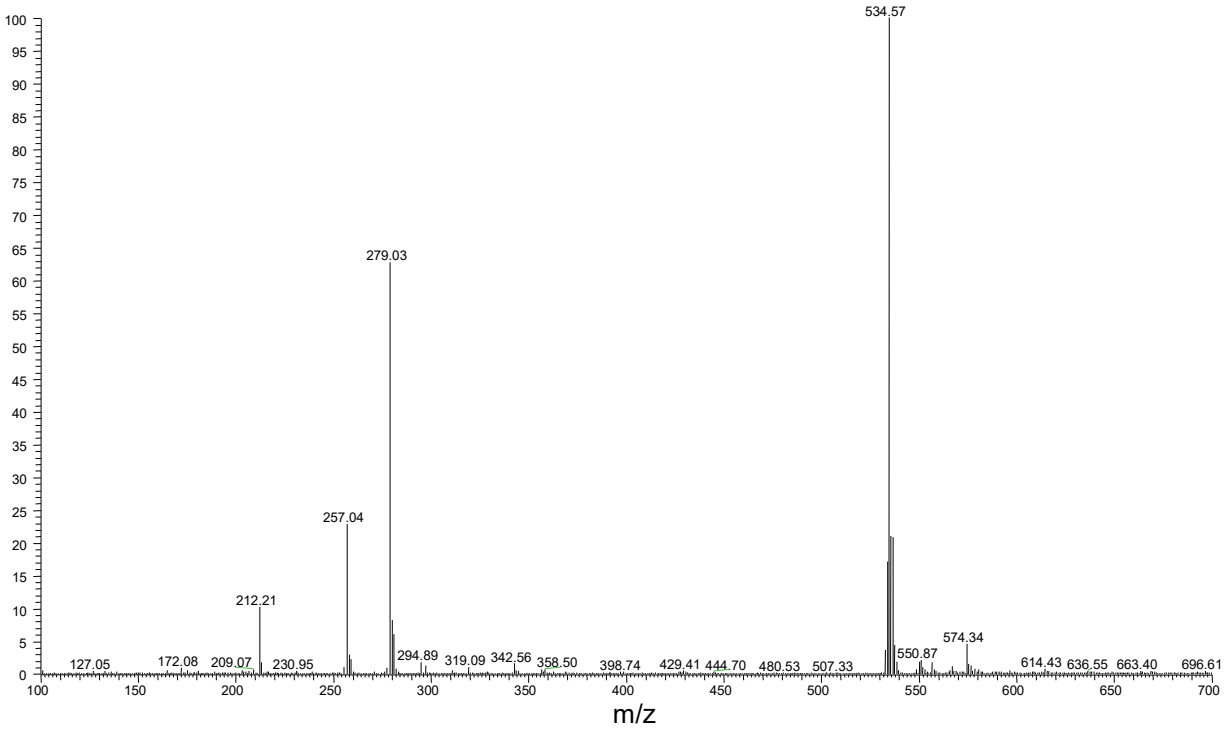

Figure B 5 ESI(+)-MS spectrum of VanSmdt

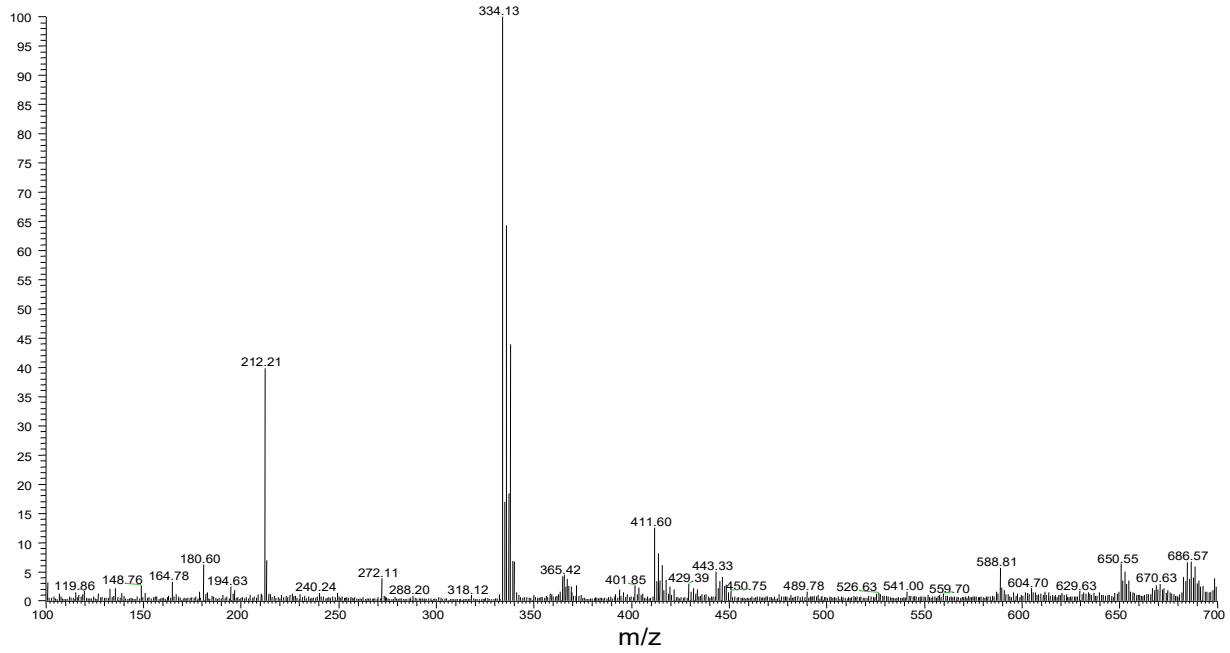

Figure B 6 ESI(+)-MS spectrum of $Zn[(PySmdt)(CH_3COO)]\bullet 1.5H_2O$

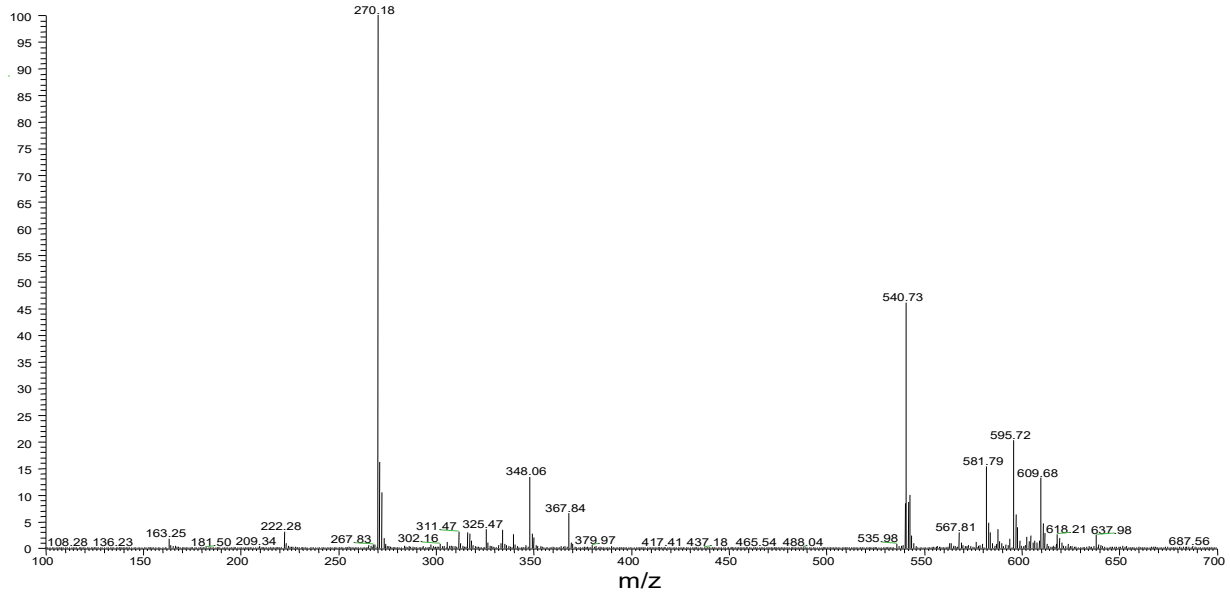

Figure B 7 ESI(-)-MS spectrum of PySmdt

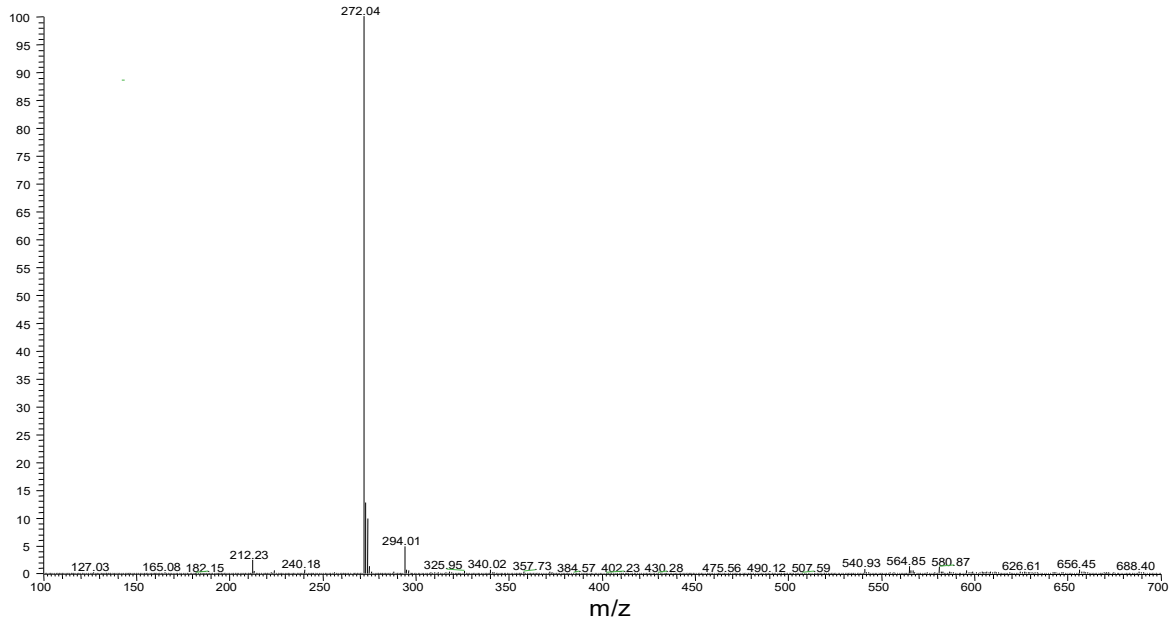

Figure B 8 ESI(+)-MS spectrum of PySmdt

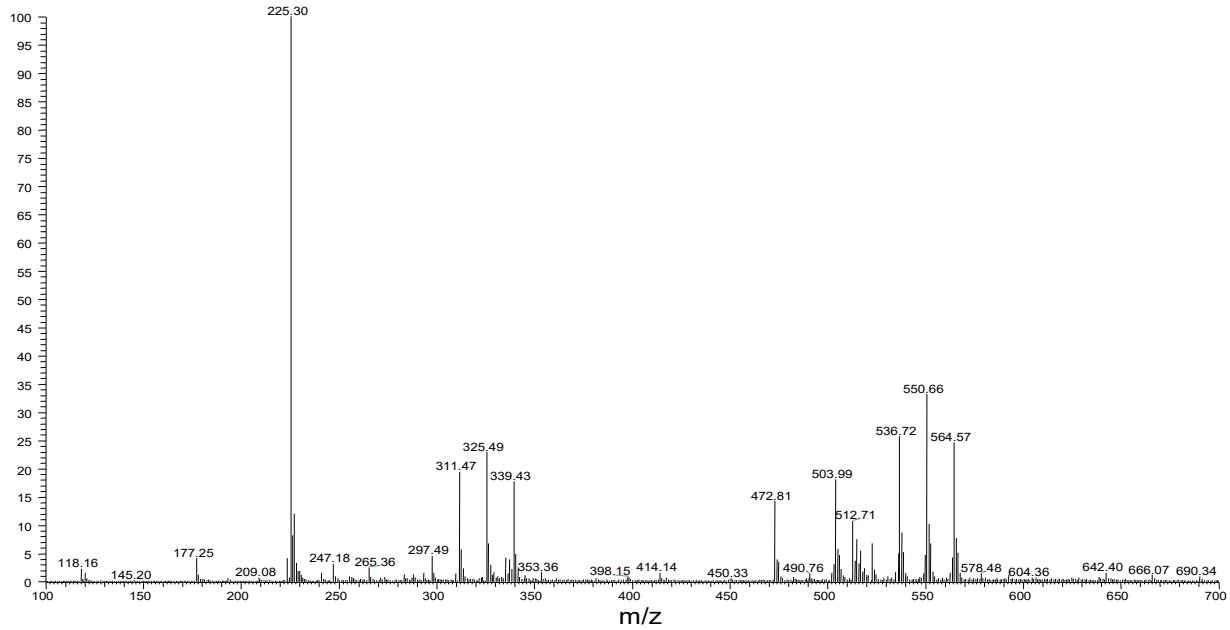

Figure B 9 ESI(-)-MS spectrum of SalSmdt

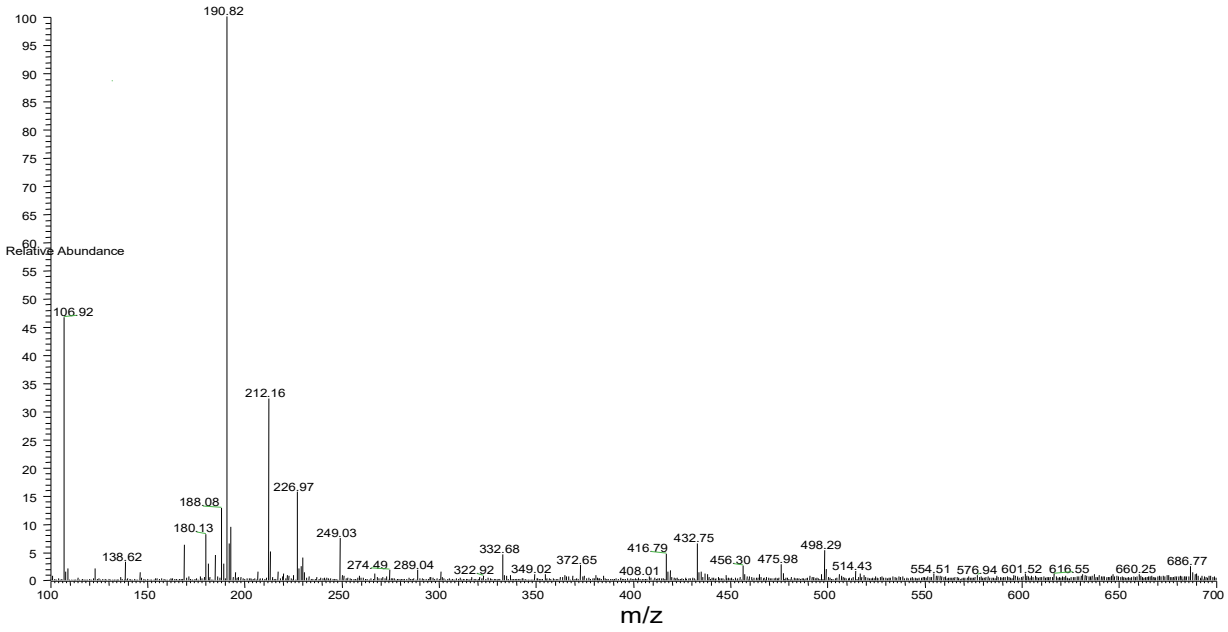

Figure B 10 ESI(+)-MS spectrum of SalSmdt

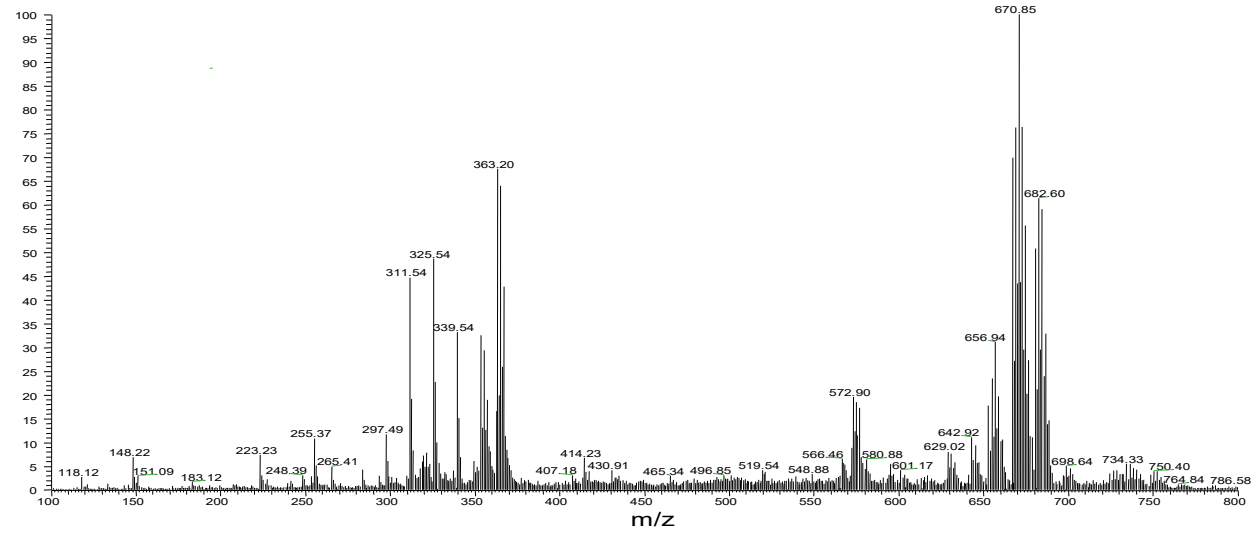

Figure B 11 ESI(-)-MS spectrum of Zn[(VanSmdt)(H_2O)]

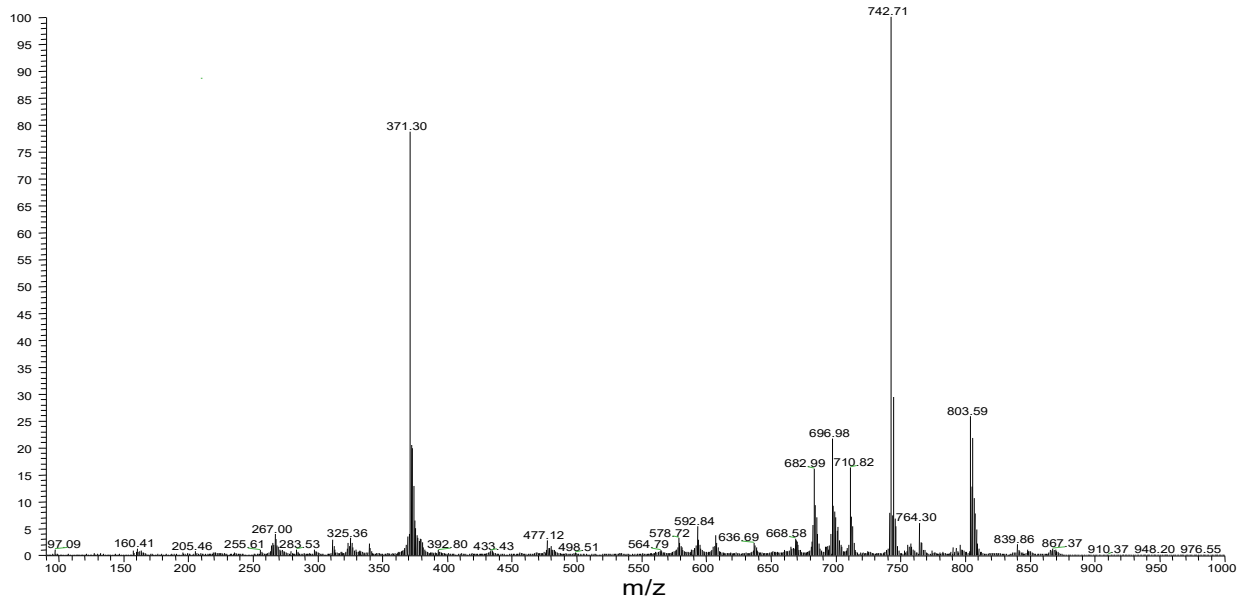

Figure B 12 ESI(-)-MS spectrum of $Mp(Smdt)_2$

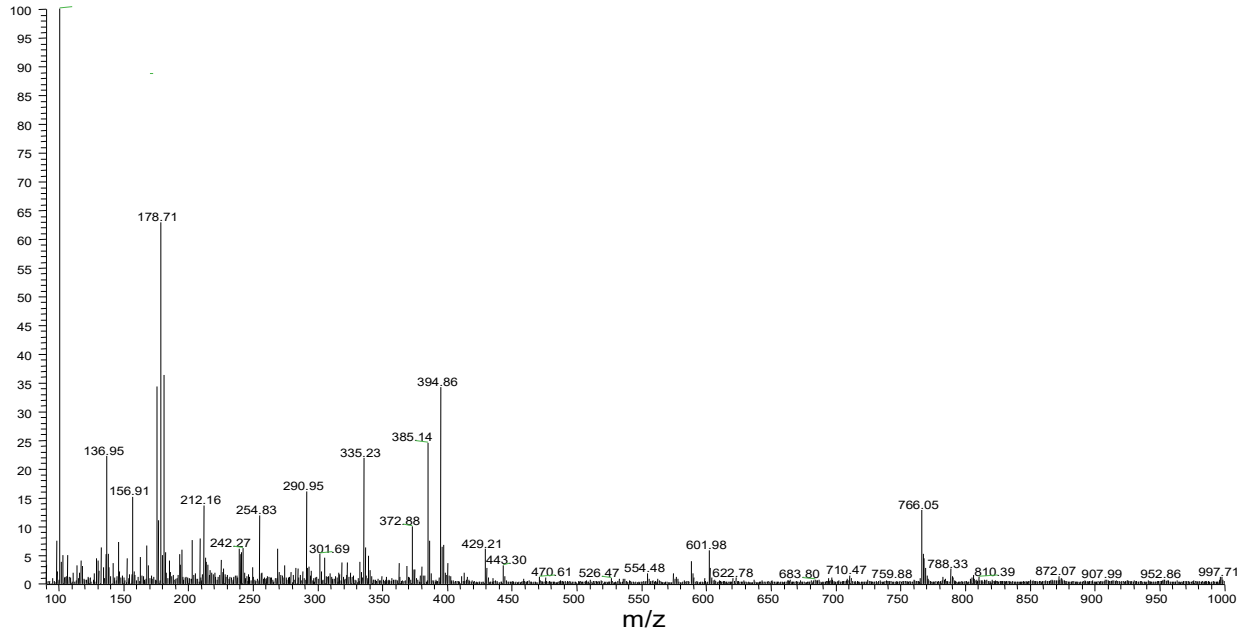

Figure B 13 ESI(+)-MS spectrum of $Mp(Smdt)_2$

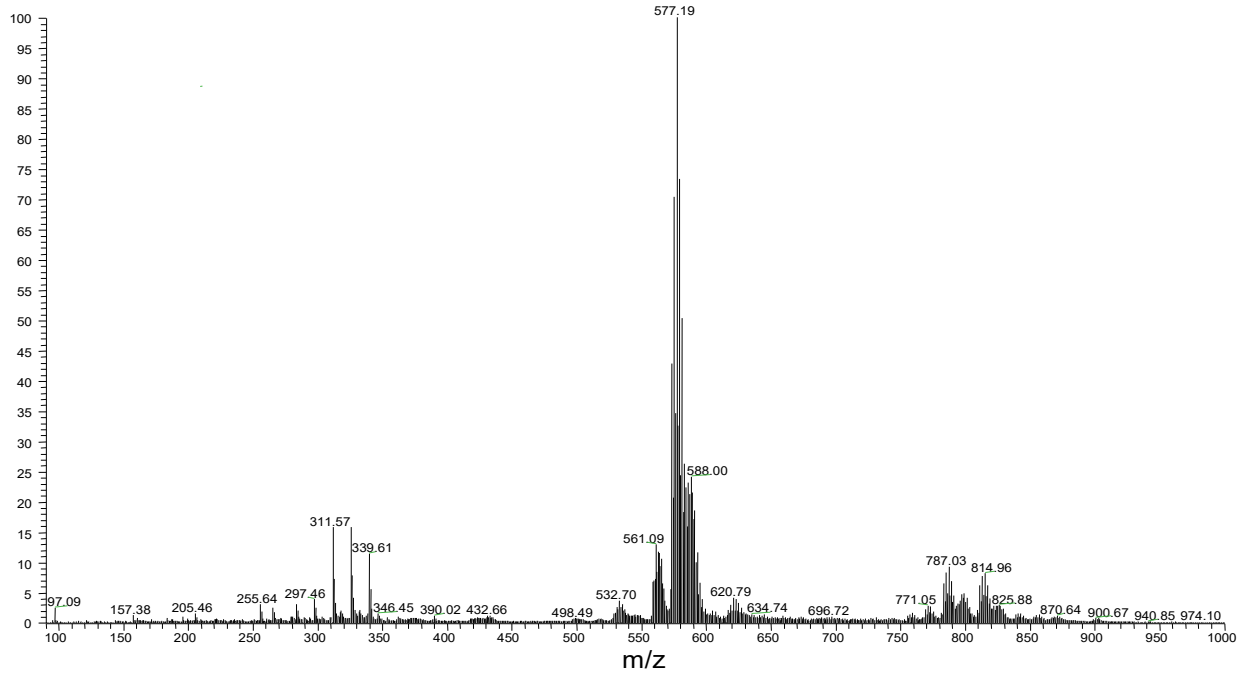

Figure B 14 ESI(-)-MS spectrum of $Zn_2[(Mp(Smdt)_2)(CH_3COO)]$

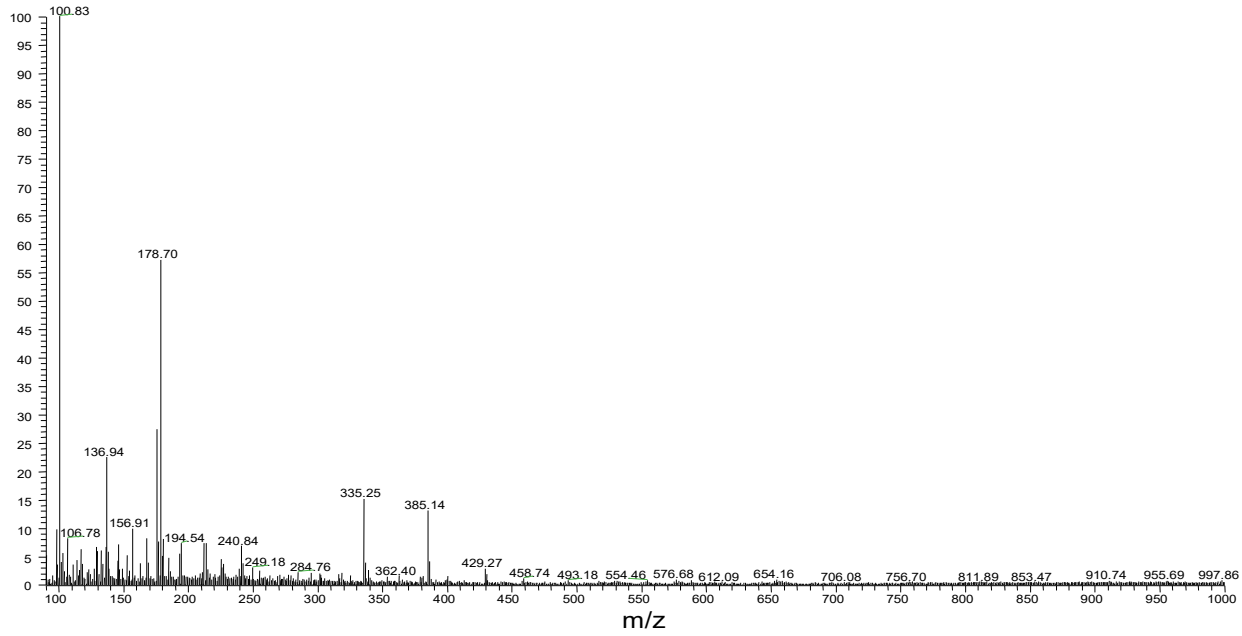

Figure B 15 ESI(+)-MS spectrum of $Zn_2[(Mp(Smdt)_2)(CH_3COO)]$

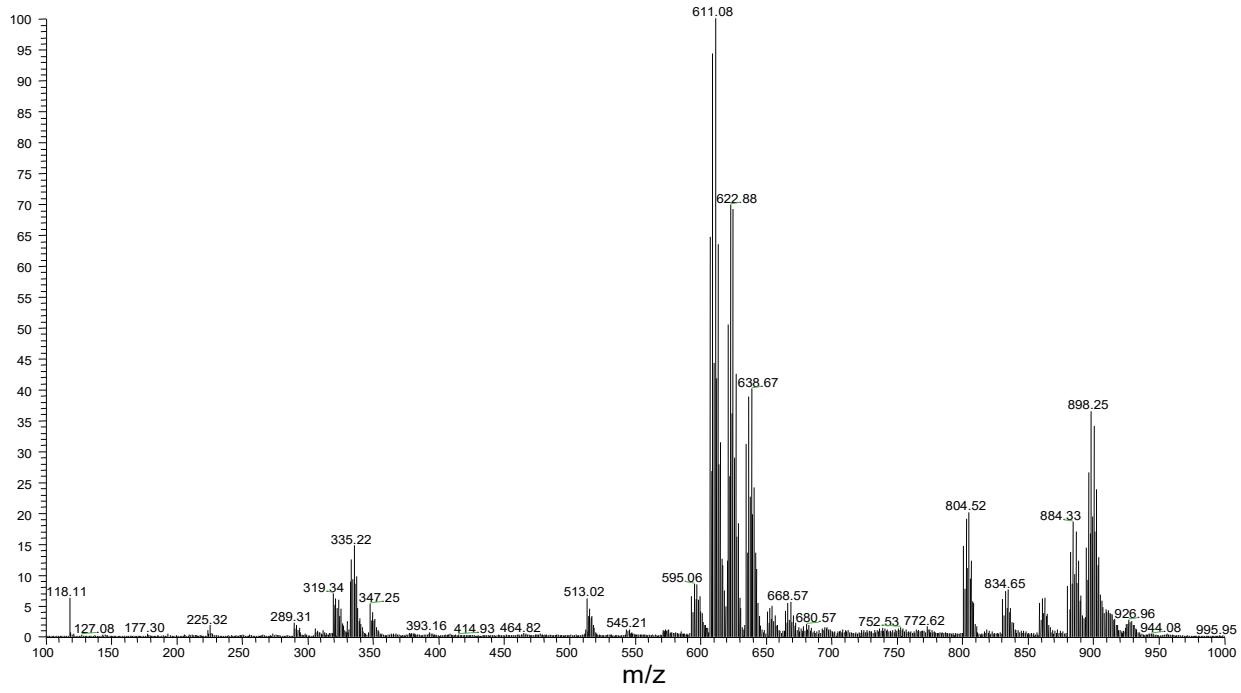

Figure B 16 ESI(-)-MS spectrum of Zn[(SalSmdt)(H_2O)]•0.5H_2O

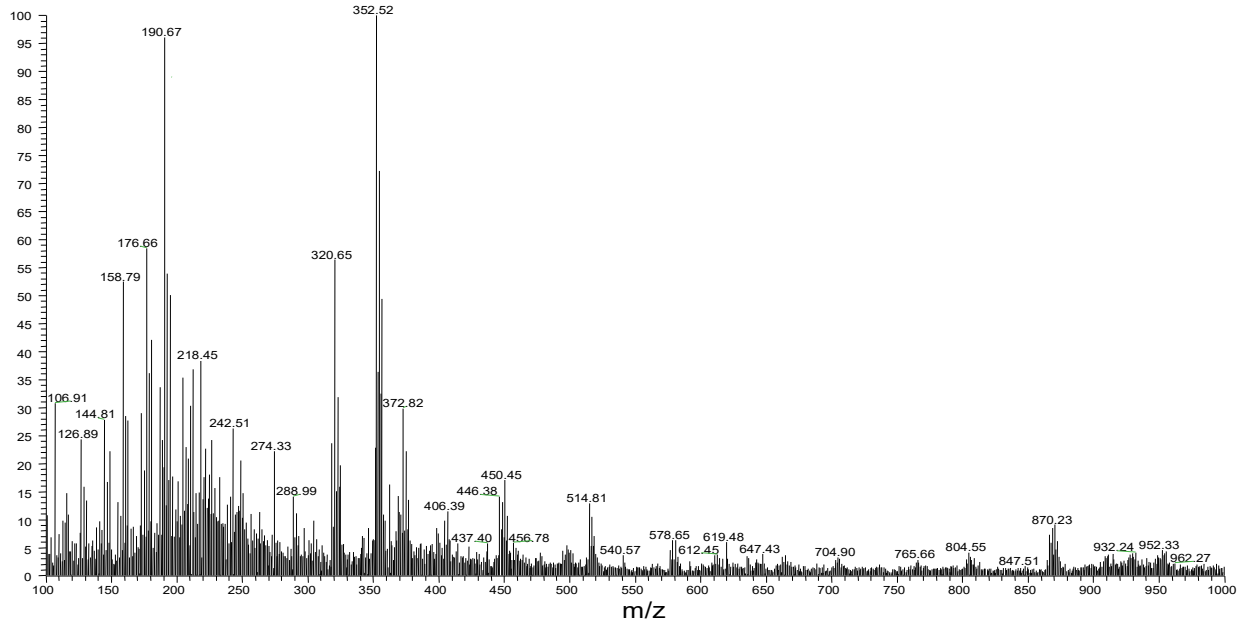

Figure B 17 ESI(+)-MS spectrum of Zn[(SalSmdt)(H_2O)]•0.5H_2O

C. FTIR Spectra

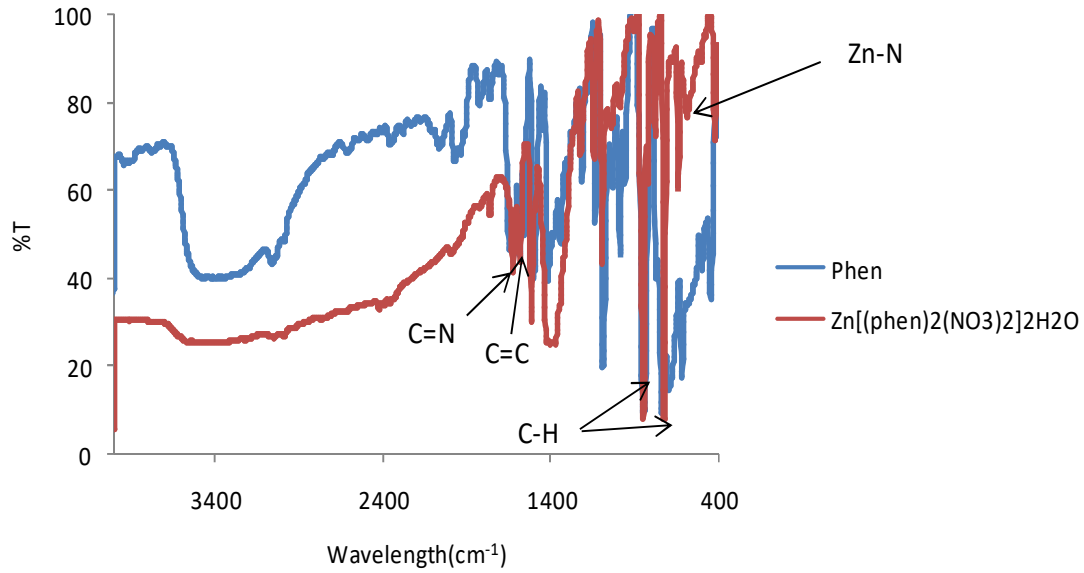

Figure C 1 FTIR spectra of phen and $Zn[(phen)_2(NO_3)_2]\bullet 2H_2O$

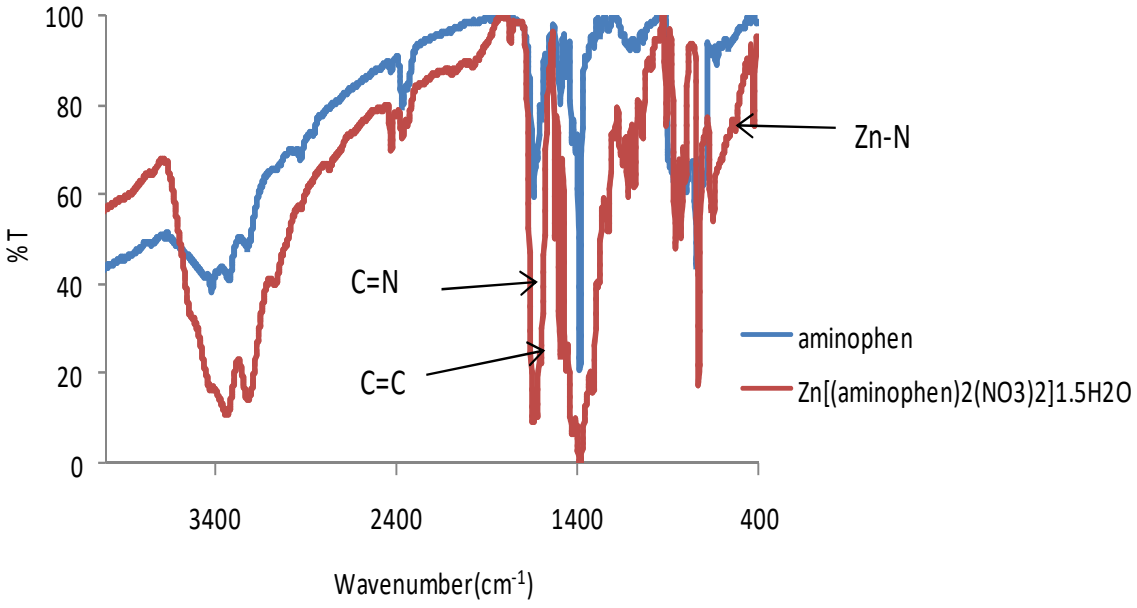

Figure C 2 FTIR spectra of aminophen and $Zn[(aminophen)_2(NO_3)_2]\bullet 1.5H_2O$

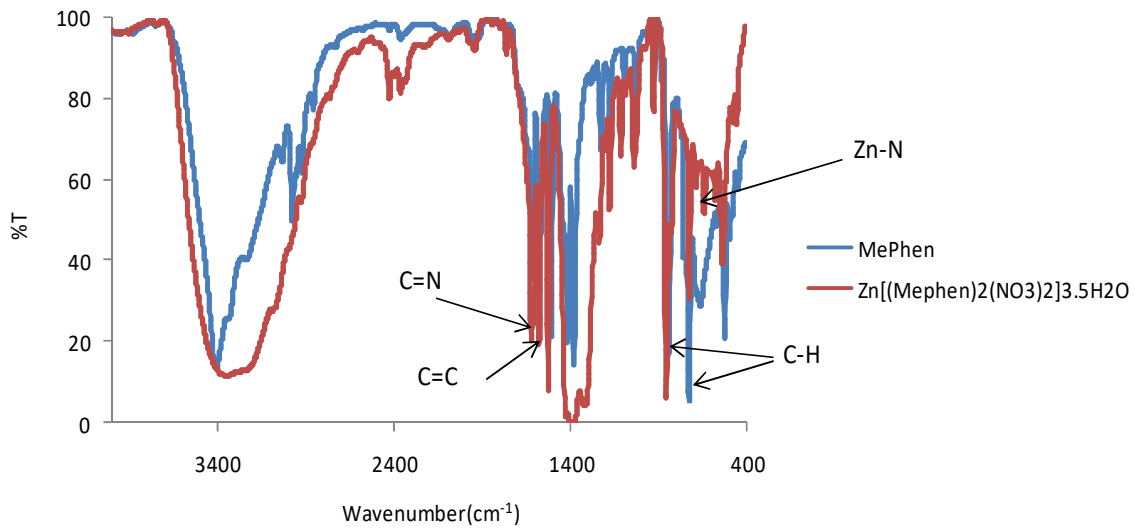

Figure C 3 FTIR spectra of Mephen and $Zn[(Mephen)_2(NO_3)_2]\bullet 3.5H_2O$

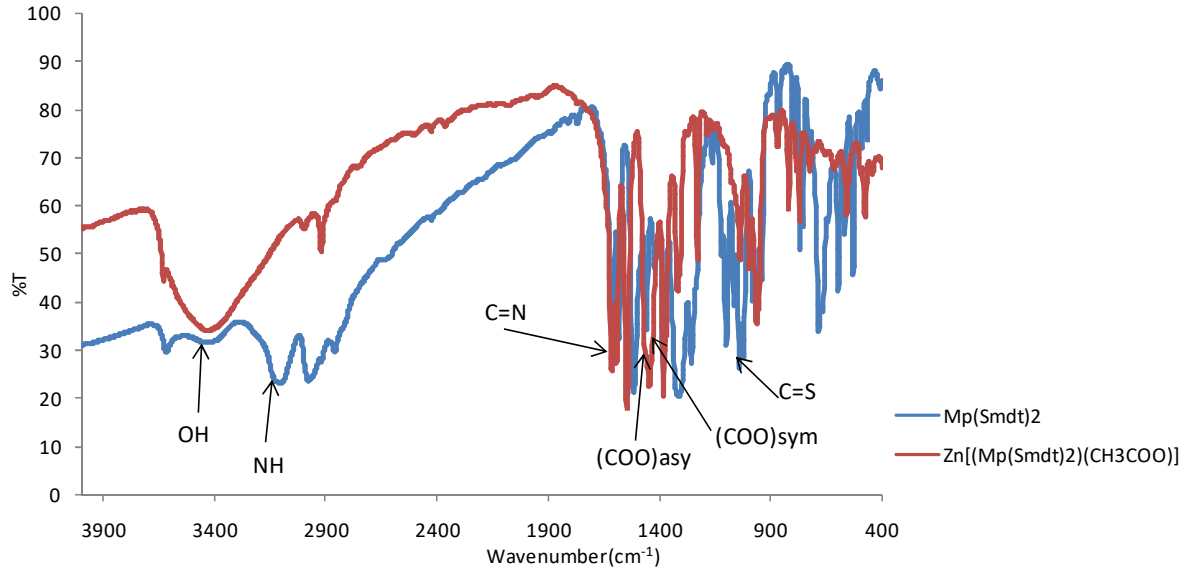

Figure C 4 FTIR spectra of $Mp(Smdt)_2$ and $Zn[(Mp(Smdt)_2(CH_3COO)]$

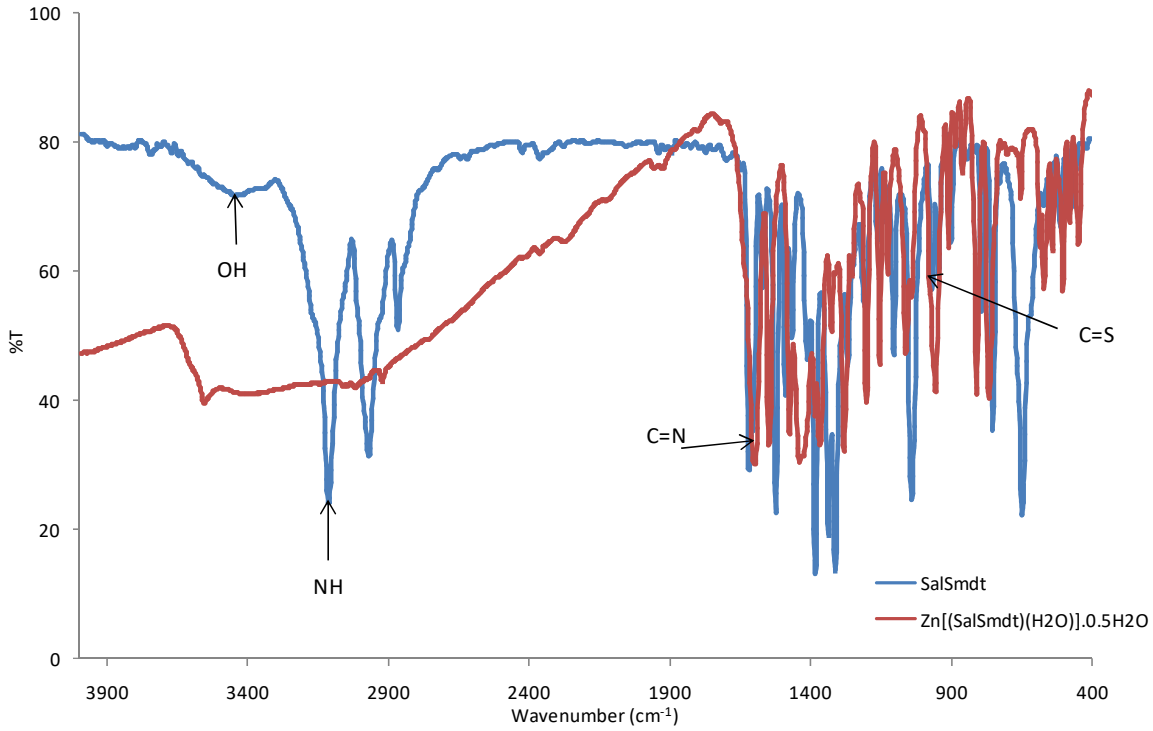

Figure C 5 FTIR spectra of SalSmdt and Zn[(SalSmdt)(H_2O)]•0.5H_2O

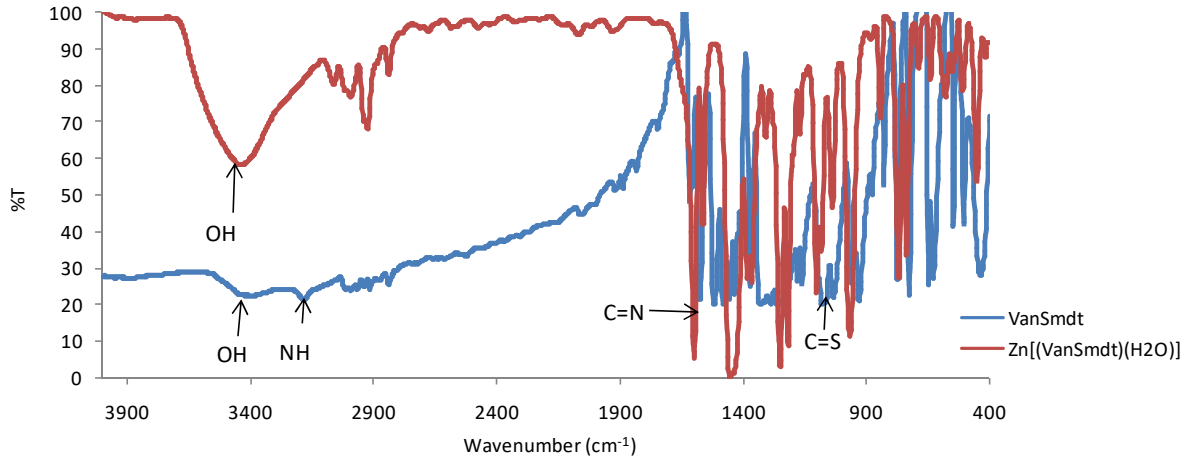

Figure C 6 FTIR spectra of VanSmdt and Zn[(VanSmdt)(H_2O)]

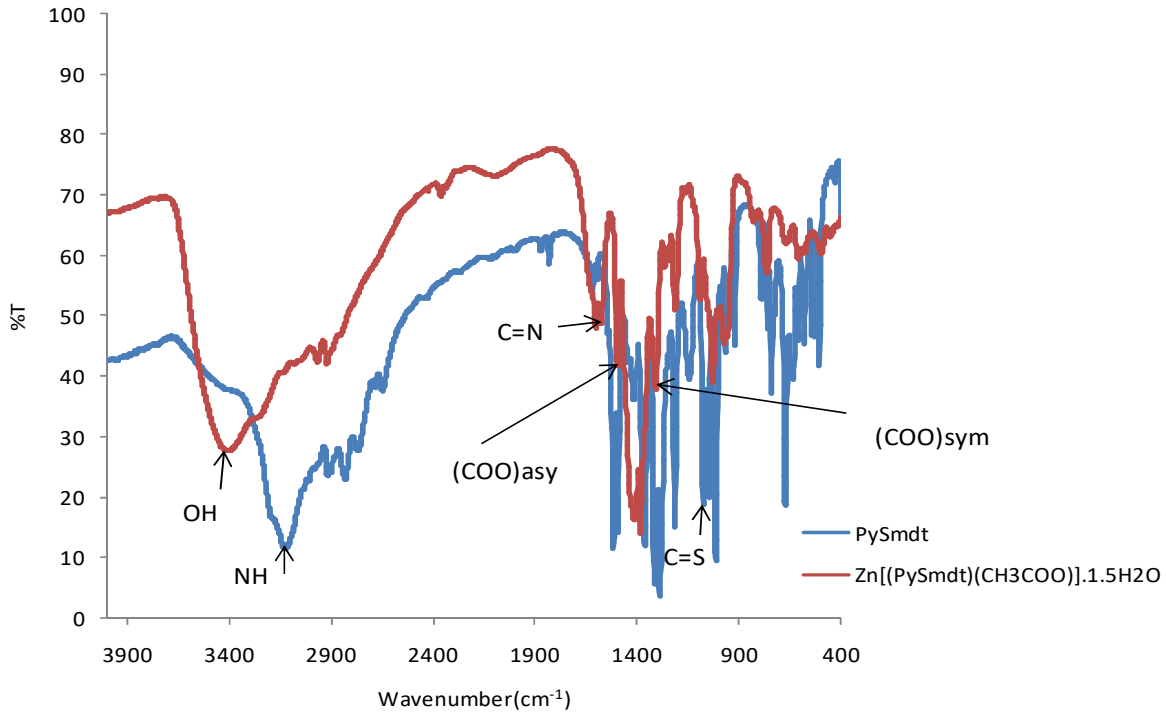

Figure C 7 FTIR spectra of PySmdt and $Zn[(PySmdt)(CH_3COO)]\bullet 1.5H_2O$

D. RP-HPLC chromatogram

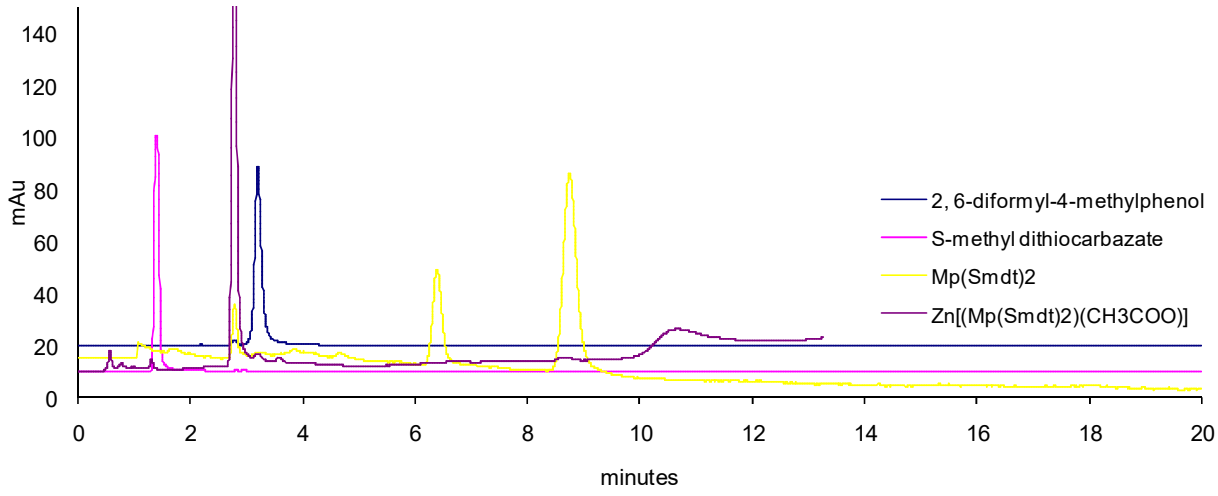

Figure D 1 RP-HPLC chromatograms of 2,6-diformyl-4-methylphenol, Smdt , $Mp(Smdt)_2$ and $Zn_2[(Mp(Smdt)_2)(CH_3COO)]$, eluted with 50% CH_3CN: 50% H_2O at a flow rate of 1 ml / min.

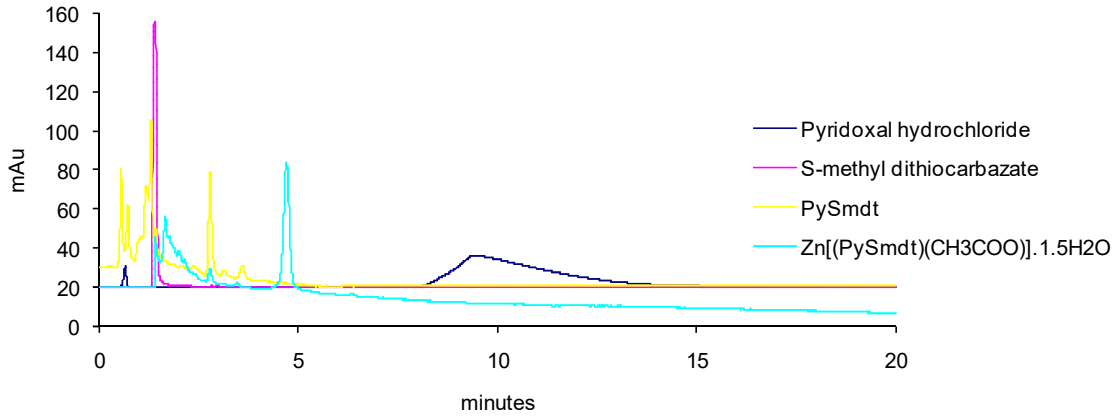

Figure D 2 RP-HPLC chromatograms of Pyridoxal hydrochloride, Smdt , PySmdt and Zn[(PySmdt)(CH_3COO)]•1.5H_2O, eluted with 50% CH_3CN: 50% H_2O at a flow rate of 1 ml / min.